An Investigation into the Feasibility of the use of an Electrostatic Technique for the Measurement of Mass Flow Rate of Pneumatically Conveyed Solids

by

Evan D. Hole

Dissertation submitted in compliance with the requirements for
Masters Degree in Technology
Department of Electrical Engineering (Light Current), Technikon Natal

This Dissertation represents my own work

E. D. Hole

APPROVED FOR FINAL SUBMISSION

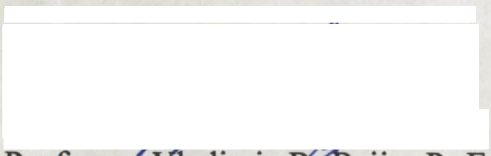

Professor Vladimir B. Bajic, Pr.Eng., D.Eng.Sc. (EE)
Supervisor

13/08/97
Date

Durban, August, 1997

I would like to dedicate this dissertation to my family.

ACKNOWLEDGEMENTS

I would like to thank the following people for their help.

Professor V Bajic	Technikon Natal
Mr D Hellinger	Technikon Natal
Mr R Lings	Eskom T-R-I
Mr R Barnard	Eskom T-R-I
Mr S Marantos	Eskom T-R-I
Mr J van Tonder	Eskom T-R-I
Mr J Geustyn	Eskom T-R-I
Mr M van Staden	Eskom T-R-I
Mr G Hasse	Eskom T-R-I
Mr J Jansen van Rensburg	Eskom T-R-I
Mr S Ramdhani	Eskom T-R-I
Mr S Bisnath	Eskom T-R-I
Mr H van Rensburg	Eskom T-R-I
Mr W Conradie	Eskom T-R-I
Mr D Blanchard	Eskom Hendrina
Mr J Dicks	Eskom Hendrina
Mr A McLean	Eskom Hendrina
Mr F Scheepers	Eskom Kendal
Mr J Stiekema	Eskom Kendal
Mr C du Randt	Eskom Lethabo
Mr M Vermeulen	Eskom Matimba
Mr L Marais	Eskom Matimba

SUMMARY

This report details the findings of work carried out over the course of 1994 and 1995 to determine if it is feasible to use an electrostatic technique for the measurement of mass flow rate of pneumatically conveyed solids. This includes results from tests done on a flow rig and at various power stations.

A survey carried out in 1991 highlighted the electrostatic (tribo-electric) method as being the most likely technique from which a successful measuring device could be developed. There were various reasons for this but the primary ones were cost, ruggedness and ease of maintenance.

In 1992 and 1993 the concept of using electron transfer, as a means of mass flow rate measurement of pneumatically conveyed solids, was tested at Lethabo and Kendal power stations, which are Eskom [1]utilities, and on a flow rig. Problems such as roping were detected and methods to overcome them developed.

Attempts to match measurements made at this early stage to actual mass flow rate proved inconsistent and this led to the tests, done on the flow rig and at two different power stations, discussed in this report.

The results of these tests show that the electrostatic method is suitable from the point of view of ruggedness and maintenance. Problems with probe wear can be overcome and the required test equipment is relatively inexpensive given the potential cost savings.

The accuracy of the method is hindered by the inability to measure the particle size on-line. Changing particle size has been shown to cause innaccuracies in mass flow rate measurement of up to 15%. This is because a fixed particle size is assumed for flow rate calculation.

Even though the accuracy of the technique in its present form is not very good there are advantages to be gained from the use of the test equipment. The velocity of the pulverised fuel can be measured accurately (±2%) and a good representation of the distribution of pulverised fuel across the pipes of a mill can be obtained. With this information things such as blocked pipes and inefficient combustion due to poor

[1] Eskom is the South African power utility which controls all the power stations referred to in this text.

distribution could be eliminated.

In short although in this study the accuracy of the electrostatic technique as a means for the measurement of mass flow rate of pneumatically conveyed solids has not been proven it is feasible to use the technique to improve the combustion process.

TABLE OF CONTENTS PAGE

TABLE OF CONTENTS cont PAGE

LIST OF TABLES PAGE

LIST OF FIGURES PAGE

LIST OF FIGURES cont: 0 PAGE

LIST OF ACRONYMS

T-R-I	Eskom technology group's Test, Research and Investigation department.
PF	Pulverised fuel (in this case coal dust).
ROI	Return on investment.
CGP	Collapsible grating probe.
Mech Tech	The mechanical technology group of T-R-I.
CAER	Cold accelerated erosion rig.
DAT	Data Acquisition Tape

1 INTRODUCTION

In the boiler plant area of Eskom power stations, the main producer of electricity in South Africa, the instrumentation and transducers used in the measurement and control process are subject to harsh conditions. Temperatures are higher than normal ambient temperature, there is a high level of noise, the quantity of dust is excessive and vibration levels are high. It would be desirable to perform more direct measurements in and around the boiler rather than use assumed transfer functions in the control philosophy.

Marantos (1991) pinpointed the mass flow rate measurement of pulverised fuel (PF), between the mill and the boiler, as one direct measurement which could enhance the control of a power station boiler.

The aim of this project is to continue the work which began in 1992 and continued through 1993 (Marantos 1993a; Marantos 1993b). The work involves the investigation of a method for the on-line measurement of mass flow rate of pneumatically conveyed solids.

1.1 Reasons for the need for a technique to measure the mass flow rate of PF

The following factors were identified as being of importance in a combustion control environment. With the techniques presently used (iso-kinetic sampling) the problems may go undetected or detection may be too late for any corrective action to be taken.

(I) The distribution of PF in the pipes is non-uniform. This results in different quantities of PF entering the boiler at the different burners. In turn there are thus areas of the boiler which are burning rich, and other areas which are burning lean. If the flow in each pipe were measurable it is possible that corrective action could be taken.

(ii) The total flow of PF into the boiler is inferred from the quantity of coal which is entering the mill. This is not an accurate means of measuring PF flow since there is a time difference between the coal entering the mill and the PF leaving it. Since the quantity of PF entering the boiler is inferred, the true air/fuel ratio within the boiler is not accurately known. This may lead to an inefficient boiler flame.

(iii) Since no on-line measurement is made a blockage in a PF pipe may go

undetected for an indefinite period of time. This would again lead to an inefficient boiler flame.

Some of the advantages of an on-line, real time flow rate measurement device are:

(I) The possible reduction in excess air if the PF distribution could be equalised.

(ii) The device can be used to make critical measurements of mass flow rate and particle velocity when performing accelerated erosion tests.

(iii) The device would remove the need for the iso-kinetic sampling process which is time consuming and inaccurate.

(iv) The control of the mills, burner and entire boiler could be enhanced. This would result in both immediate cost savings and extended plant life.

The details of these advantages are discussed in depth in Appendix G.

1.2 The use of Iso-kinetic sampling for the measurement of PF flow

Iso-kinetic sampling is the method presently used to measure the flow rate of PF. This method makes use of a probe inserted into the pipe once a plug has been removed. The probe is then held at various points of the cross-section of the pipe for a fixed period of time. The total mass of the extracted sample is measured and the flow rate in the pipe calculated using the time over which the sample was extracted.

1.2.1 Disadvantages of Iso-kinetic sampling

(I) It is *not* on-line and thus a problem may go undetected for long periods of time. Iso-kinetic sampling is carried out either on a regular basis (maximum weekly) or when it is suspected that there is a problem with the PF distribution. If the sampling is done on a regular basis it is done when the unit is operating under stable load conditions. Since it is changing load conditions which normally lead to problems, it is not ideal to test under stable load conditions.

(ii) The equipment required is cumbersome and the conditions around the boiler, where the temperature is high and the light is often poor, are not conducive to accurate measurement since these conditions lead to human error. Further, since the method requires a probe to be inserted in the pipe a plug must be

removed and hot PF escapes at high velocity.

(iii) Application of the method is time consuming. To test all six mills on a single unit will take two people a full day (du Randt 1994). Between the first mill tested and the last one, conditions may have changed. This may invalidate any comparison made between the mills.

(iv) The method is labour intensive and thus becomes costly.

1.3 Alternative means to measure PF flow

In 1992 an investigation was done to determine the best technique for the measurement of flow rate of PF (Marantos 1992). Various factors were taken into account when selecting the technique to be pursued. The resultant instrument would have to have the following characteristics:

(I) It must be robust to withstand the conditions at the measurement point.
(ii) It would have to be inexpensive to build, install and maintain. The maintenance should be simple and easy to carry out.
(iii) It would have to be an on-line, real time device.

1.4 Electrostatic mass flow rate measurement

The technique selected was the electrostatic technique since it appeared to fill the necessary criteria. The details of the method are discussed in the Background (Section 2, pp 6) but basically it relies on the fact that electron transfer occurs when particles travelling in a gas strike an insulated object. The quantity of charge transfer gives an indication of the number of particles in the gas and thus of the mass flow rate of particles. This technique appears to be well suited to the power station environment.

This report will detail various levels of physical construction of the required measurement devices (probes) and it will be shown that all of them are simple and relatively inexpensive. They have no moving parts once they have been inserted and hence are unlikely to break. Fitting the measurement devices to the PF pipes does not require major structural changes to the plant pipe work and the entire boiler does not have to be shut done for probe insertion. If this device were fitted on a permanent basis probe replacement, which is inevitable given the probe wear, would be simple. This is an important factor since shutting down and lighting up a boiler is very expensive.

The projected required computer processing power needed for the data processing is available. At no great cost the device can process the probe current data and supply measurement on an almost real time basis i.e. the available data will have a few second delay (±20) and since the process is relatively slow changing this is quite acceptable. A single 486 IBM compatible computer is adequate for this task. Although computers are reducing in price, at the time the decision was made to pursue the electrostatic technique the computer power required for a technique such as flow imaging was prohibitively expensive.

The fact that this device is intrusive, i.e. in the direct flow of PF, means that problems caused by roping are easy to overcome by designing and using a probe that covers the cross-sectional area of the pipe.

Hence, given the conditions prevalent at a power station the electrostatic technique appears to be the most viable.

1.5 Research Objective

The objectives of this research was to establish the feasibility of the use of the electrostatic technique for PF flow measurement. This took a three part format:

(I) Use a flow rig to measure the effects of particle size, temperature, relative humidity, particle velocity and mass flow on the charge transfer which occurs when solid particles strike an insulated probe and use these results to:
   (a) Verify the relationships described by Equation 13.
   (b) Assess the effect on probe current of factors which are not described in Equation 13.

$$M = I \frac{\overline{D}_p}{K_m} \overline{u}^{\beta} \qquad (13)$$

where
- M is the mass flow rate.
- I is the probe current.
- $\overline{D}_p$ is the average particle size.
- $\overline{u}$ is the average air velocity.
- β is the material constant.
- K_m is the probe constant.

The factors described above were determined as being important since particle size and mass flow rate are included in Equation (13) and in previous tests, where only weather conditions varied, the measured probe current varied. The possibility existed that these changing weather conditions (relative humidity and temperature) were responsible for the varying probe currents.

Particle shape was also considered. However the problem is to find particles of different shape while maintaining a similar average particle size. The material would also have to have the same chemical make-up.

Although the effects of these parameters could not be measured they will not cause errors in the other results since they will both be constants for the test series.

The problem of particle shape may not be so important however since the particle shape of PF is set by the type of mill and the coal quality. Since the mill is specific to a station (some have vertical spindle mills while others have tube mills) the particle shape should not change over a short period. The same unfortunately does not hold true for chemical composition since the coal quality can change thereby changing the chemical makeup of the coal.

(ii) Tests to compare electrostatic measurement techniques to iso-kinetic sampling results were carried out at Hendrina power station during the course of 1994 and Kendal and Hendrina power stations in 1995. Test methods and results are included here since they became a substantial part of the project.

The results from the Hendrina tests done, in both 1994 and 1995, were statistically analysed in order to determine:

(a) The accuracy of the electrostatic mass flow measurement using iso-kinetic sampling as a reference.

(b) Determine the error incurred due to varying particle size when calculating the mass flow rate.

(iii) While performing the tests described in (ii), measure the temperature and relative humidity in the PF pipes to determine the error incurred in the resultant measurement caused by changes in these two parameters.

2 BACKGROUND

In this section the following topics are discussed:

(I) The various flow techniques which have been investigated in the past.
(ii) Details of the charge transfer process which occurs when pneumatically conveyed solids strike an insulated object.
(iii) The probe development which has occurred over the three years since the inception of this research by T-R-I.
(iv) The method of particle velocity calculation using a cross correlation technique.

2.1 Flow measurement techniques

Work on the measurement of mass flow rate of two phase flow has been going on for some years and various different techniques have been investigated (Masuda *et al* 1976-1977, Cheng *et al* 1970, Cole *et al* 1969-1970, Parkinson 1969). All the techniques have some advantages and some disadvantages. Up till now no particular method has been singled out as being better than another. Each would appear to be suited to some applications and not others and most are still in the development stage.

Coulthard *et al* (1991: 15-8) discuss a number of different techniques. Figure 2.1-1 shows a graphic summary of the methods discussed and the approximate year in which investigation began. Following is a brief explanation of each technique. In some cases a reference is given in which the technique is discussed in more detail than that given by Coulthard *et al* (1991: 15-8).

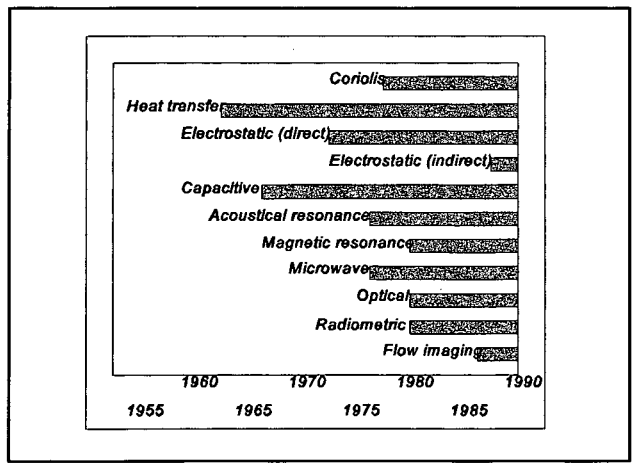

Figure 2.1-1 History of two phase mass flow measurement

2.1.1 Coriolis mass flow meters

Coriolis mass flow meters are not ideal in this application since impacting particles on the required U-tube set up incorrect resonant frequencies. Also the impacting particles cause erosive wear on the tubes. These meters are better suited to liquid flow.

2.1.2 Heat tramsfer flow meters

Heat transfer mass flow meters measure the temperature of the fluid material at two points in the pipe which are axially apart. The pipe is heated downstream of the first measurement point, and upstream of the second. The temperature difference of the two measurement points is proportional to mass flow. This method is more applicable for dense phase flow and the effect of the solid distribution in the flow is unknown.

2.1.3 Direct electrostatic mass flow meters

This method (Izakov *et al* 1979, Ighodaro *et al* 1991) uses two chambers. In the first chamber the charging takes place and in the second chamber measurement takes place. The quantity of charge measured in the second chamber is proportional to the mass flow rate.

2.1.4 Indirect electrostatic mass flow meters

Indirect mass flow meters (Satori, Marantos 1993) use the tribo-electric effect as the operating mechanism. Collisions between two objects result in the transfer of electrons and the resultant creation of a charge. The size of the charge is proportional to the number of collisions which occur. Thus by measuring the charge on a probe placed in a pipe it may be possible to determine the number of particles in that particular cross-sectional area of the pipe. Thus it is necessary to determine the velocity of the particles. This is done by placing two sensors in the pipe axially and using a cross correlation technique for velocity measurement. Factors such as particle size, particle velocity, temperature and humidity affect the charge magnitude.

2.1.5 Capacitive mass flow meters

Capacitive mass flow meters (Xie *et al* 1989, Beck *et al* 1990) also measure the solid density of particles in the pipe. The solid acts as the di-electric for the two capacitive plates. Again the velocity must also be determined and is done by using a similar

method as the indirect electrostatic mass flow meter. Capacitive mass flow meters have proved successful on pipes with a diameter of less than 100mm. In larger diameter pipes however, they have been found to be inaccurate. Charge build up on the capacitive plates and solid build up can cause problems.

2.1.6 Acoustical resonance flow meters

Acoustical resonance flow meters (Vetter *et al* 1987) measure the velocity of propagation of a specific frequency through a medium. The denser the medium the slower the velocity of propagation. These measurements are affected by the particle size of the medium.

2.1.7 Microwave flow meters

Microwave flow meters require a metal cavity to be formed in series with the pipeline. One method is to measure the backscatter wave versus the incident radiation. Solids moving through the cavity scatter microwave radiation with a Doppler shifted frequency spectrum, determined by the velocity distribution of the solids, and the direction of the propagation of the microwave radiation inside the cavity. Another method uses the cavity as a resonant circuit. The resonant frequency of the cavity changes by changing the amount of material in the cavity. This incorporated with velocity measurement of the solids will give the mass flow rate. Drawback to the microwave method is the electrical characteristics of the material, moisture content and temperature.

2.1.8 Optical mass flow meters

Optical mass flow meters use a technique based upon the Mie theory. This theory predicts that light intensity should be exponentially related to solids concentrations in the light beam. This method has only been tested on light solid concentrations and errors are introduced due to particle size and distribution. The light windows can also become contaminated with solid build-up.

2.1.9 Flow imaging mass flow meters

Flow imaging mass flow meters are not on-line systems and as yet there are no known industrial applications. Tomography (Huang *et al* 1989, Dickin *et al* 1993) is used to find material distributions in a cross section of the pipe. This technique is therefore valuable in identifying flow patterns, such as roping. The sensors measure the particle

distributions in two dimensions. This information is sent to the computer which recreates the two dimensional picture of the solid pattern in the pipe. The response time of the method is slow and the resolution is low. Thus only an average flow rate can be determined.

As discussed in the introduction the electro-static technique was selected for investigation.

2.2 Indirect electro-static mass flow rate measurement

The indirect electrostatic technique works on the principle that electron transfer occurs when two materials collide with each other.

2.2.1 Details of the charge transfer process of colliding bodies

Charge transfer takes place when the distance between the two materials is less than the critical distance d_c (Cole *et al* 1969-1970). The critical distance is assumed to be in the order of the inter-molecular distance of the materials. When the distance between the two materials has exceeded the critical distance, a voltage V_c is set up between the two surfaces which can be compared to a parallel plate capacitor. The charge transfer is thus $q = CV_c$ where $C = \epsilon S/d_c$, where ϵ is the dielectric constant of air. The contact region S of a particle with radius R, is defined as the maximum area over which charge transfer can take place, as is shown in Figure 2.2.1-1 and is seen to be approximately equal to Πa^2 (where Π is the ratio of the circumference of any circle to its diameter).

$$a^2 = 2Rd_c - d_c^2 \approx 2Rd_c \qquad (1)$$

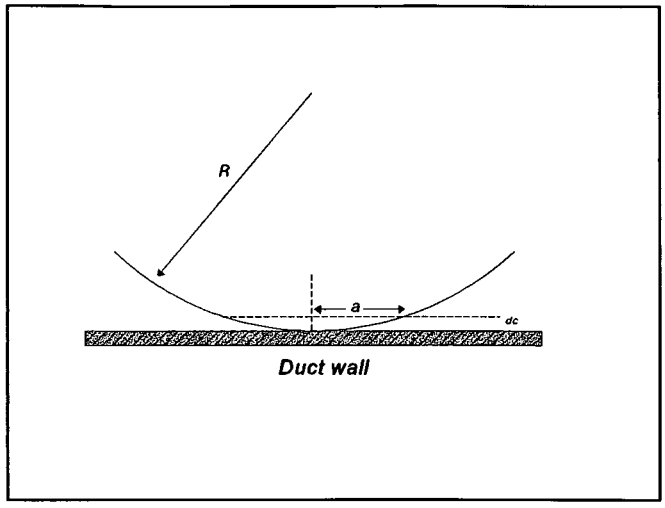

Figure 2.2.1-1 Representation of contact region

It was shown theoretically (Masuda *et al.* 1976-1977) that when using a pipe of length Δx and diameter D, the current generated by the particles coming into contact with a surface can be expressed by:

$$I = \frac{M \in V_c \, \Delta x \Delta t S}{m d_c \, \tau} \cdot \frac{\Delta n}{\Delta x} \qquad (2)$$

Where

	Δt	is the duration of contact,
	M	is the mass flow rate,
	τ	is the relaxation time,
	m	is the mass of the particle.

$\frac{\Delta n}{\Delta x}$ is the number of collisions per unit length of a particle and can be expressed by:

$$\frac{\Delta n}{\Delta x} = m \pi D \xi \qquad (3)$$

Hence ξ is the number of collisions per unit area and unit mass of powder.

The unit area of pipe in which collisions can take place can be defined by:

$$\pi D \Delta x = \Delta A \tag{4}$$

From (2), (3) and (4) one gets

$$= - \frac{\epsilon V_c \Delta t S \xi}{d_c \tau} M \Delta A \tag{5}$$

It was found (Masuda *et al.* 1976-1977) that the relation between the currents generated and the length over which collisions took place was not linear but represented by:

$$I \approx KM \frac{\Delta x}{1 + k\Delta x} \tag{6}$$

Where K is a constant with units A s/m kg.
k ≈ 0.024 cm^{-1}.

Using (6), equation (5) can be modified to become:

$$I = - \frac{\epsilon V_c \Delta t S \xi}{d_c \tau} M \Delta A \eta \tag{7}$$

Where $\eta = 1/(1+k\Delta x)$

It was found experimentally by Masuda *et al* (1976-1977) that the current generated is represented by the following empirical equation

$$I = \alpha \frac{\overline{u}^{\beta}}{\overline{D}_p} M \Delta A \eta \qquad (8)$$

Where α and β are constants dependant on the type of material used. (β varies from 1 to 2 depending on the materials in contact and does not have units) α has units As^2m^2/kg.

$\overline{u}$ is the average air velocity.

$\overline{D}_p$ is the average particle size and

$$\overline{D}_p = \sum_{i=1}^{i=n} D_p / n \qquad (9)$$

Where n is the number of particles in the sample set.

$-\frac{\epsilon V_c \Delta t S \xi}{d_c \tau}$ in equation (7) is represented by $\alpha \frac{\overline{u}^{\beta}}{\overline{D}_p}$ in equation (8), indicating a relationship between the charge generated per particle and the velocity of the particle.

Let

$$K_m = \alpha \Delta A \eta \qquad (10)$$

K_m depends on the physical construction and material characteristics of the charge collecting surface and the flowing material which is coming into contact with this surface. As these variables are assumed constant for a specific sensor and flowing material, K_m is defined as the probe/material constant.

The empirical equation (8) can now be given as follows:

$$I = K_m \frac{\overline{u}^{\beta}}{\overline{D}_p} M \qquad (11)$$

It was shown by Cheng *et al.* (1970: 135-149) using various types of probes as opposed to the pipe wall, as with Cole *et al.* (1969-1970) and Masuda *et al.* (1976-1977), that for a particular probe voltage the relationship between the mass flow rate and the probe current I can be expressed by:

$$I = K_p \rho u \qquad (12)$$

Where K_p is the probe/material constant.
ρ is the dust cloud density.
u is the mass velocity.

Cheng *et al.* (1970: 135-149) simplified the experiment and kept the size of the particles constant during the experiment and thus ignored the effect of particle size from equation (11), or rather incorporated its effects into the probe/material constant (K_p). In equation (12) the velocity is not raised to any power. In a number of graphs represented by Cheng *et al.* (1970: 135-149), the effect of the velocity on the current was dependent on the probe material used and thus the velocity has to appear in a form other than u. It is clear then that equation (12) can be considered as a simplified version of equation (11) and in fact equation (11) represents the process better.

Equation (13) is shown below. This is merely Equation (11) which is rearranged in order that M (mass flow rate) is the subject of the formula. Equation (13) is that which is used for the calculation of mass flow rate over the course of this project.

$$M = I \frac{\overline{D}_p}{K_m} \overline{u}^{\beta} \qquad (13)$$

This equation is limited and fails to take into account some factors which may affect the charge magnitude. Thus the investigation of the factors discussed in the introduction (1.5).

2.3 Direct electrostatic mass flow rate measurement

The direct electrostatic method for flow rate measurement uses the technique of first charging the particles and then measuring the charge on the particles downstream. The mechanics of this technique led to the following theory. If two probes are placed one

after another in a stream of particles, then the charge on the second probe will be dependent on that on the first probe. This means that the relationship between the charge on each probe may be an indication of mass flow rate. Thus, some factors such as current difference and current ratio are studied.

2.4 Probe development

The probes used in the early studies (Marantos 1992) are shown in Figure 2.4-1. The finger probe is merely a mild steel metal rod inserted into the pipe until it nearly touches the opposite wall of the pipe.

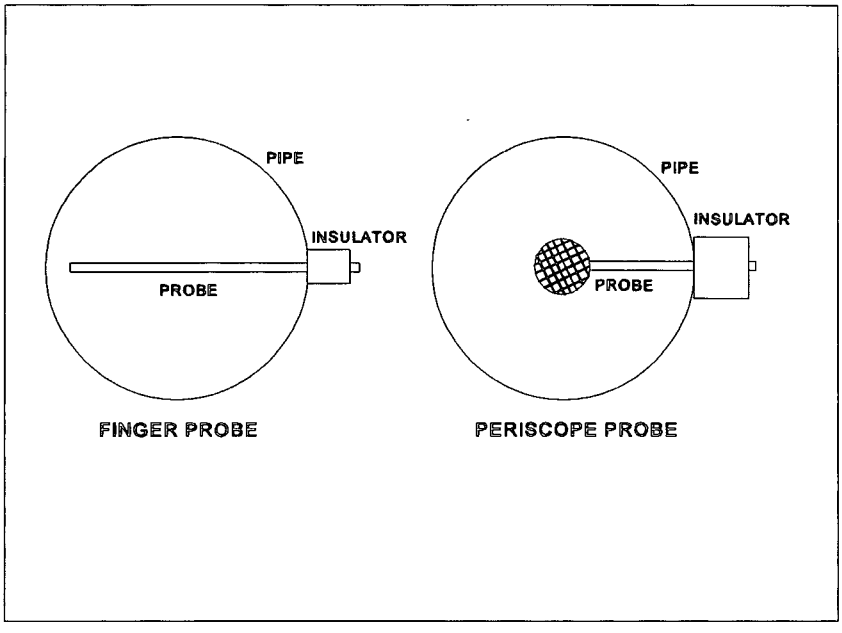

Figure 2.4-1 Early probes

When solid particles move with a stream of air an effect occurs which is termed roping. This is when the solid forms coils in the airflow. The result is that the solid is not evenly distributed across the cross section of the pipe. It is thus possible that the "rope" may miss the finger probe altogether and an error would be recorded when the charge magnitude is measured.

The periscope probe with the enlarged grating on the end was used in an effort to overcome the roping effect (Marantos 1992). However results showed that even this enlarged probe may produce an erroneous reading due to roping.

The probes used during the flow rig tests and those done at Hendrina Power Station in 1994 are shown in Figure 2.4-2. They are called collapsible grating probes. These probes are inserted into the pipe through a 50mm socket when in the closed state. Once in the pipe they are opened and in this manner the entire cross-section of the pipe is covered and a rope cannot miss the probe.

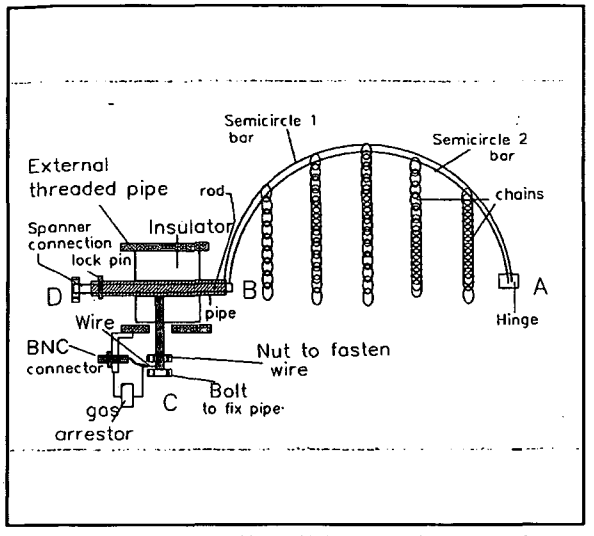

Figure 2.4-2a Collapsible grating probe - closed

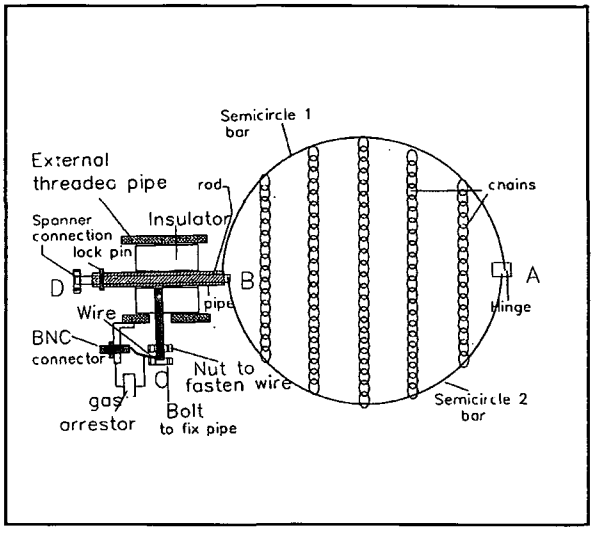

Figure 2.4-2b Collapsible grating probe - open

These probes although overcoming the roping problem turned out to be unsuitable for Hendrina (Marantos 1993a). The reason for this is the erosion rate experienced there. Early tests had shown that probe erosion was minimal and as a result of this it was not an area of concern. However when the probes installed for the Hendrina tests in 1994 were removed approximately one month after the completion of the tests they were worn to a far greater extent than any previous probes had been (Section 4.5).

This was attributed to the fact that the coal at Hendrina is more abrasive and the PF velocity is high. The relationship between velocity and erosion is exponential with the power of the indice being approximately 2. A photographic comparison of the erosion on various probes is shown in Appendix A.

New probes were developed, by the Process Control group of T-R-I, for the 1995 Hendrina test series which are more hardy and also more easily replaceable once the original installation is complete. The new probes are shown in Figure 2.4-3. These new probes have the disadvantage that, once installed, the probes are permanent.

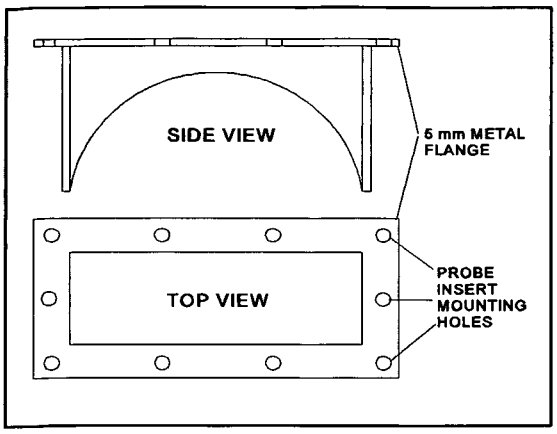

Figure 2.4-3a Probe casing

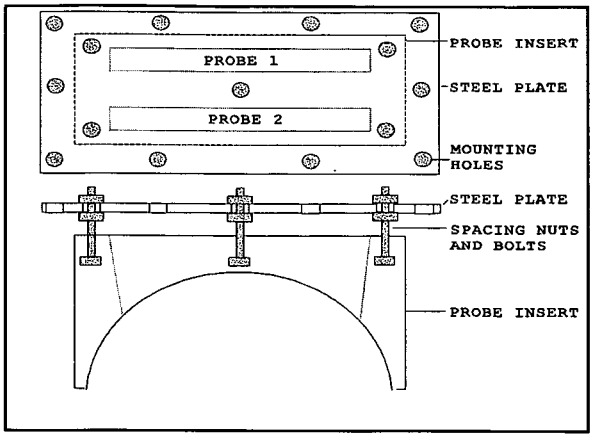

Figure 2.4-3b Probe insert

The figure shows that the probes are made up of three separate parts:

a The probe casings are made of 5mm steel plate and are welded onto the PF pipes which have a corresponding slot cut in them the width of the probe casing and half the diameter of the pipe. The dimensions of the casing are set by the outer diameter of the PF pipe. In the case of Hendrina this is 355mm.

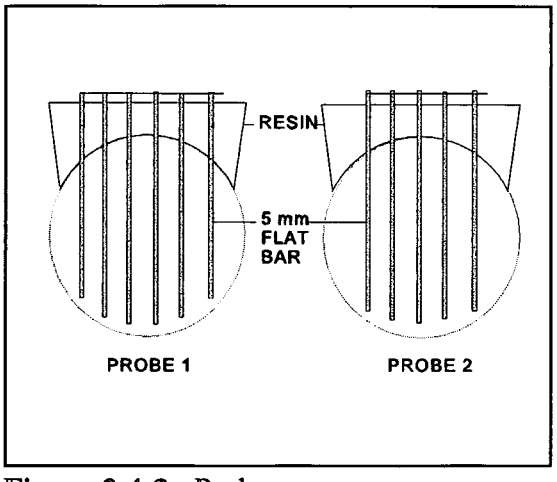

Figure 2.4-3c Probes

b The probe insert is a resin casting. This resin and the mixture was selected after discussions with Scott (1995) and is made up as follows:
For every 1 kg of crystic 199 resin there is:

(I) 0.75 g of resin accelerator
(ii) 0.5 g of resin catalyst

(iii) 1.3 kg of silica powder
(iv) 1.3 kg of aluminium oxide

This specific resin is used because it can handle the temperature of 90°C at which the PF pipes operate. The silica powder and aluminium oxide are included to add bulk to the mixture and to increase the hardness of the final product. These particular powders were chosen for their heat transfer properties i.e. they prevent the mould fracturing during the curing process through good heat dissipation.

The moulds themselves are made from wood which is treated with wax and coated with a release agent. This facilitates the removal of the casting. Once the mould has been poured an insert is pushed into the resin. This insert pushes the mounting bolts and the probe slots into the mould. Once the mould is set the mounting bolts are set tight in the resin and the probe slots are removed so that the probes themselves can be slid into the mould.

c The probes which fit into the slots in the inserts are cast of the same resin mixture as the inserts. The two probes differ from each other in that the front probe has six single probes and the second only five. This configuration is the result of a computer fluid dynamics (CFD) study (Appendix B) which was carried out in an attempt to develop the best probe configuration. The two main factors arising from the study were:

(I) The plan to use 20mm round bar probes had to be abandoned because it would have resulted in an excessive pressure drop in the PF pipes. This in turn would have had an effect on the classifier performance and ultimately on the overall boiler efficiency.
(ii) If the probes had not been staggered (six in front and five behind) the bulk of the PF would not have struck the second row of probes.

2.5 Calculation of particle velocity.

Early tests used a single probe (Marantos 1992) placed in the PF stream. Later two probes were placed one after the other in the particle flow. When observing the resultant waveforms created on the two probes it was seen that their shape was similar. An example of what the waveforms may have looked like is shown in Figure 2.5-1.

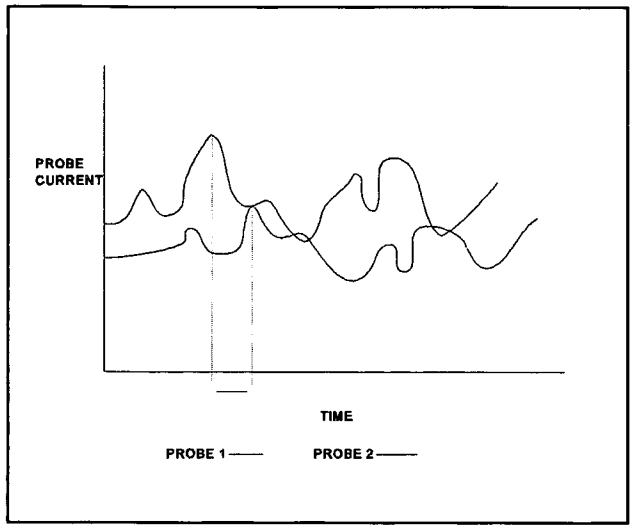

Figure 2.5-1 Particle velocity measurements

The diagram shows that the two waveforms have a similar pattern, but that of probe 2 is shifted by a time factor of t. Since the distance between the probes is known and remains constant, the PF particle velocity can be calculated using Equation (14)

$$v = \frac{S}{t} \qquad (14)$$

where v is the particle velocity.
S is the distance between the probes.
t is the time the particles take between the two probes.

The development of this technique for calculating particle velocity overcame the need for using the air velocity in Equation (13). This is desirable since $\bar{u}$ denotes particle velocity and not air velocity. The particle velocity is different from the air velocity due to the slidage of the particles in the air flow. When the tests were done the Labview analysis applications used a cross correlation technique to calculate the velocity for each data set recorded. This involved the following steps:

(I) Calculate the average voltage on each probe for the data set. Subtract this average from each data point. This amounts to the same as removing the DC component from each of the two signals.

(ii) Subtract each point of the second signal from the corresponding point of the first signal and sum all the results.

(iii) Shift the second signal back by one point and repeat the process.

(iv) The sum mentioned in point (ii) will reach a minimum value whereafter it will begin to increase again. The point at which the minimum is reached is the correlation point.

(v) Since the data logging frequency is known the number of shifts necessary to reach a minimum can be used to calculate the time taken for particles to move from one probe to the next and hence the velocity can be calculated.

3 FLOW RIG, EQUATION VERIFICATION TESTS

This section details the tests as done on the flow rig at T-R-I. This includes the following details:

(I) The flow rig development.
(ii) The measurements made and recorded during the tests.
(iii) The test procedure for each set of tests.
(iv) The measurement system and data analysis procedure.
(v) The test results.

3.1 Flow rig development

Tests were first done on the flow rig in 1992 and the development of the rig to its state at the end of 1993 is discussed in Appendix C.
The flow rig used in 1994 is shown in Figure 3.1-1.

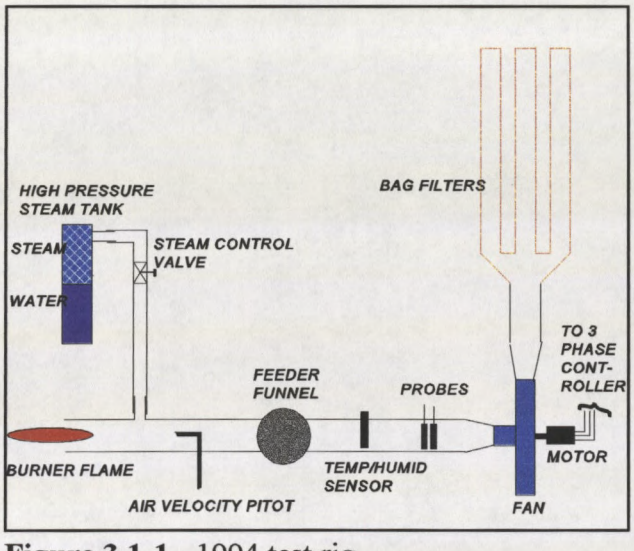

Figure 3.1-1 1994 test rig

3.2 Measurements recorded

As well as the probe currents, the following are recorded during these tests:

(I) The air velocity.
(ii) The temperature and relative humidity.
(iii) The mass flow rate.

3.2.1 Air velocity

Conversion of pressure difference to voltage

Air velocity is generally measured via means of a differential pressure. The problem in this instance is to measure the differential pressure and convert it to a voltage in order that the air velocity can be logged in unison with the probe currents. The problem was overcome using the device shown in Figure 3.2.1-1.

Figure 3.2.1-1a shows how an inclined manometer was made with two metal rods extending the length of the inclined limb. As the velocity of the air increases the total pressure increases and forces the liquid (coloured water) up the inclined limb. When a voltage is applied to the rods the current flow is dependant on the height to which the liquid has risen up the rods. This is because the more liquid there is in contact with the rods, the greater the number of available electrons there are for current flow.

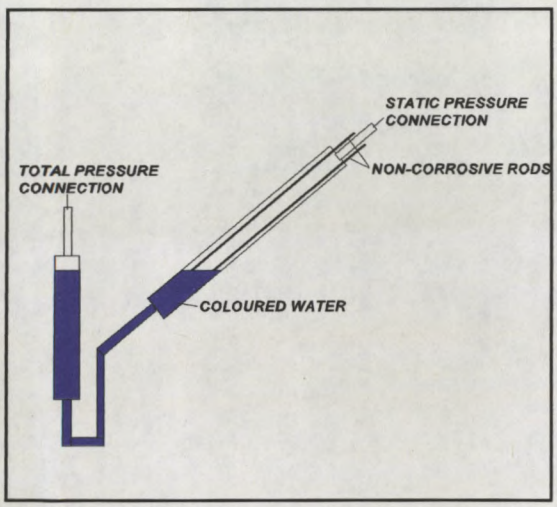

Figure 3.2.1-1a Air velocity manometer

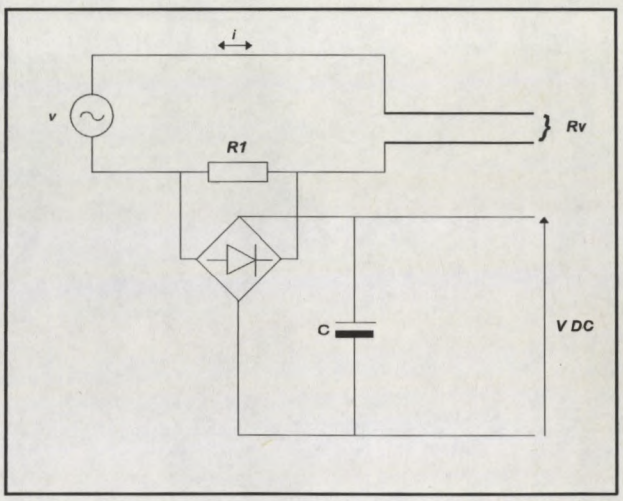

Figure 3.2.1-1b Velocity/Voltage converter cct.

Figure 3.2.1-1b shows the circuit diagram of the air velocity measuring device. It is necessary to apply an alternating voltage to the rods to avoid the movement of electrons in only one direction. Were this to happen, then the characteristics of the liquid would be constantly changing and calibration of the instrument would be impossible. The voltage dropped across R1 increases as the current increases (liquid level rises in the inclined limb). This voltage across R1 is then converted to a DC value and smoothed. The resultant DC voltage is recorded simultaneously with the

probe voltages.

Measuring the air velocity in the flow rig proved to be the most difficult of the required measurements. Ideally the measurement device should be as close as possible to the electrostatic probes. This is so that the measured air velocity is the same as that at the probes. The following means for the measurement were investigated:

Orifice plate

Calculations showed that the pressure drop across the orifice plate with the largest possible diameter that could be used, resulted in a drop in air velocity that was unacceptably high. The amount of settling of the solid particles would be excessive at the resultant maximum velocity.

Reverse Pitot

Experimental results from a reverse Pitot were inconsistent. (Appendix C)

Pitot tube in ash stream

A Pitot tube in the stream of solid particles continually got blocked and the velocity, while actually remaining constant, appeared to be decreasing.

Pitot tube before feeder

A Pitot tube mounted before the feeder in the flow rig proved to be the best possible solution. The problem with this is the calibration of the instrument since there is a hole in the rig where the solid particles are fed into the system. The air velocity before the feeder is different (lower) than the air velocity at the probes. The problem was overcome during the calibration process. The measuring Pitot voltage output was calibrated against the velocity measured at the probes using a second calibration Pitot. This was done when no solid was flowing and thus blockages did not occur in the calibrating Pitot. Table 1 below shows the results from the calibration process.

The resultant curve can be approximated by one from the Richard's family of growth curves (Steyn *et al* 1994). The Richard's family of growth curves includes the modified exponential curve, the Gompertz curve and the logistic curve.

$$y(x) = A*(1 + s * B * (R^{x}))^{\alpha} \qquad (15)$$

where y is a function of x

A, s, B, R & α are constants

Voltage (V)	Velocity (m/s)
1.12	20.8
1.45	24.6
1.86	27.4
2.29	30.3
2.65	31.8
2.9	33.1
3.1	34.1
3.4	35
3.5	36.1
3.65	37.5
3.75	38

Table 3.2.1-1: Air velocity calibration

In this specific case the actual curve is given by Equation (16)

$$v = 62.342\,(1 - 0.87712^{V})^{0.5420015} \qquad (16)$$

where v is the air velocity

V is the measured voltage

3.2.2 Temperature and Relative Humidity

Temperature and relative humidity were measured using a Rotronic CH-8040 probe. This probe has the following operational ranges:

Temperature	-30 to 70 °C
Relative Humidity	0 to 100 % relative humidity

The output for both measurements is a 4 to 20 mA signal. These signals are recorded simultaneously with the probe voltages.

The conversion equations for the two measurements are shown below and are derived from the value of the resistor used for the signal measurement and the operational ranges of the instrument:

$$T(°C) = (\frac{V-0.852}{3.41} * 100) - 30 \qquad (17)$$

$$H(\%) = (\frac{V-0.852}{3.41}) * 100 \qquad (18)$$

where V is the recorded voltage in each case
$T(°C)$ is the temperature in degrees Celsius
$H(\%)$ is the relative humidity in percent

The only difficulty was the blocking of the porous filter which surrounds the sensors. A protective shield, shown in Figure 3.2.2-1, was made to overcome the problem.

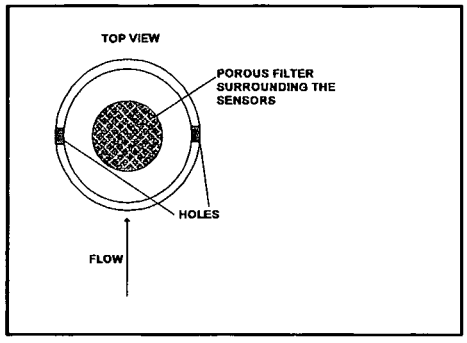

Figure 3.2.2-1 Protective shield for temp/humidity sensor

The shield operates in the following manner:

Particles strike the shield travelling in the direction shown. Their momentum carries them past the holes in the side wall of the shield. Some of the air flow is however deflected into the shield and onto the sensors.

3.2.3 Mass flow rate

Figure 3.1-1 shows the feeder funnel in its simplest form in situ on the rig. In fact the feeder arrangement was more complex and Figure 3.2.3-1 gives a detailed drawing of the arrangement.

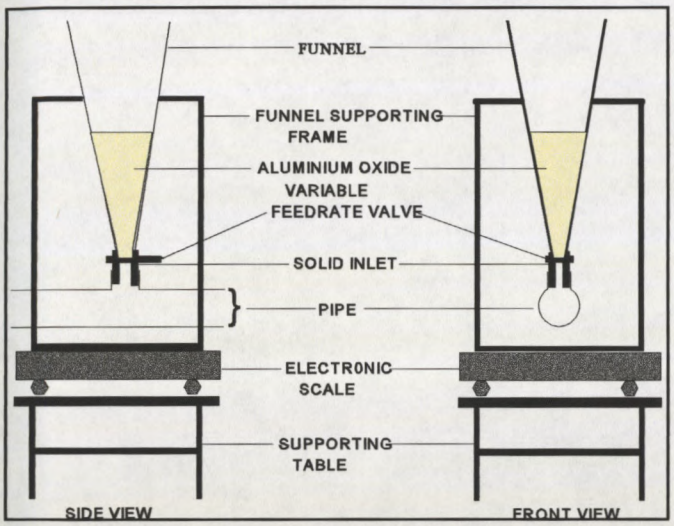

Figure 3.2.3-1 Feeder mechanism

As the figure shows the electronic scale measures the mass of the funnel, its supporting frame and any material in the funnel. During the test the output voltage signal from the load cells of the scale is amplified and recorded simultaneously with the probe voltages. The equation to calculate the mass of material only is shown in Equation (19). The equation was found by plotting the recorded mass against the output voltage when different masses are placed on the scale. The obtained relationship is given by:

$$M = 18.83V - (33.35 + C) \qquad (19)$$

where M is the mass of material,

V is the recorded voltage,

$33.35 + C$ C is the mass of the funnel and frame. The constant, 33.35

is present because the output from the load cell *(V)* is not 0 when M=0,

18.83 is the slope of the straight line.

Figure 3.2.3-2 shows an example of one of the graphs which plots mass against time. The consecutive runs show that the feedrate is almost the same from one run to the next, although each has a different starting mass. In fact the error between Run 1 and Run 3 is 6% and this is the greatest error in the example. Since the slope of the lines is constant (the lines are straight) the feedrate during each run remains constant even though the mass of material in the funnel decreases. In this example the runs show 5 different tests with the same particle size for each test.

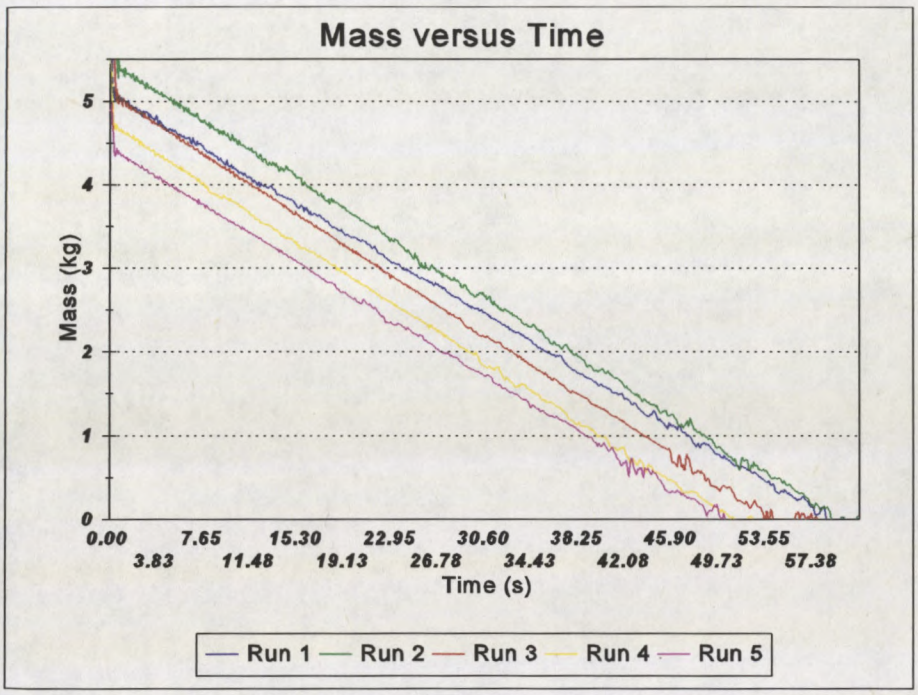

Figure 3.2.3-2 Plot of material mass versus time

3.3 Test procedure

The tests on the flow rig, as described in Section 1.5 (pp 4), were carried out using Aluminium oxide as a test material. The reason for this is that material of a constant particle size is required so that effects of changing particle size are eliminated. Aluminium oxide can be purchased in specific sizes. Although it would have been ideal to use PF, the process of sieving the quantities that were required would have taken too long. Further it is difficult to obtain such large quantities of PF.

Tests were done to measure the effects of the five changing parameters shown below.

3.3.1 Relative humidity and temperature tests

Tests to measure the effect of changing relative humidity on the charge magnitude were carried out by adjusting the relative humidity in the system using the superheater steam outlet valve. The tests were done at three different temperatures of 25, 50 and 75°C. The temperature was controlled by adjusting the regulator on the gas burner. The tests were not done at pre-selected relative humidities, but rather at the relative humidity which resulted from opening the superheater valve a fixed amount. Hence, although the valve positions were the same for the three different temperatures, the resultant relative humidity was not.

3.3.2 Particle velocity tests

The effect of particle velocity on the charge magnitude was measured by varying the air velocity. This is done by adjusting the fan speed with the three phase motor controller (Figure 7). The six test velocities are shown in Table 3.3.2-1.

Test 1	Test 2	Test 3	Test 4	Test 5	Test 6
17.7	19.05	20.1	22.1	23.2	24.6

Table 3.3.2-1: Velocities at which particle velocity tests were done in m/s.

Tests were done at 70°C which was the maximum possible temperature at which we could operate due to constraints of the rig. This was in order that the temperature at which the tests were done, approximates that at which the PF pipes operate (80-90°C).

3.3.3 Mass flow rate tests

The mass flow rate was adjusted by controlling the adjustable feedrate valve (Figure 3.2.3-1) on the feeder mechanism. The mass flow rates are shown in Table 3.3.3-1.

Test 1	Test 2	Test 3	Test 4	Test 5
0.032	0.069	0.077	0.129	0.186

Table 3.3.3-1: Mass flow rates at which mass flow rate tests were done in kg/s.

3.3.4 Particle size tests

Particle size tests were done for three different particle sizes. Figure 3.3.4-1 is a graph showing the distribution curves of the three sets of samples. The legend shows the average particle size of each sample set.

Although the distribution curves do overlap each other, they are distinct enough to represent different particle sizes.

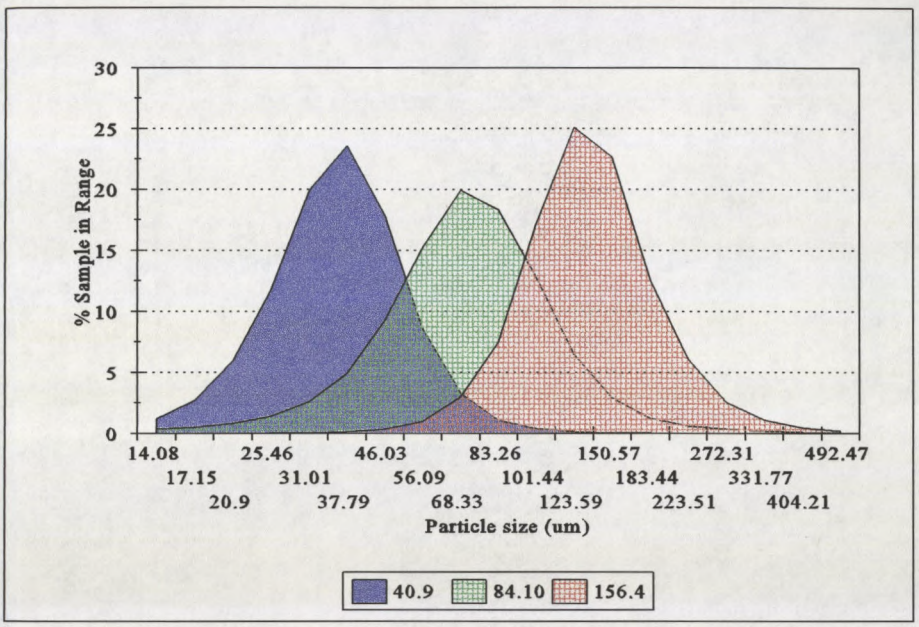

Figure 3.3.4-1 Particle size distribution of Aluminium Oxide used for particle size tests.

3.4 Overall measurement system and data analysis procedure

3.4.1 Measurement system

Figure 3.4.1-1 shows a schematic of the overall measurement system used for recording the different voltages from the two probes, the temperature and humidity sensor, the air velocity Pitot tube and the material mass in the funnel.

The high impedance interface module is used to avoid damage to the analog to digital card. The following equipment was used for the recording process:

CPU	486DX33
A/D Card	Eagle Electronics PC30-HPGL
Software	Eagle Electronics Waveview

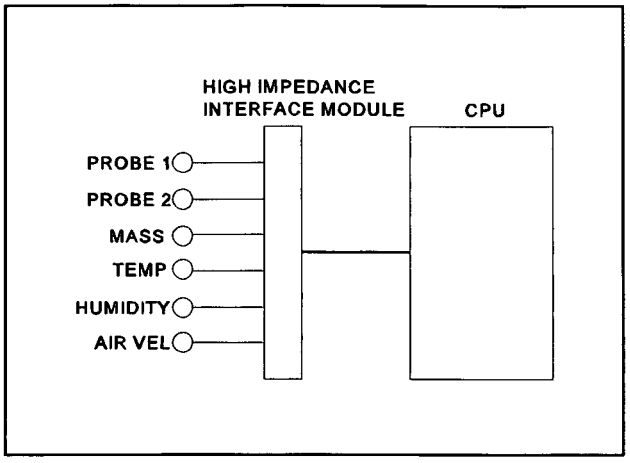

Figure 3.4.1-1 Complete measurement system

The rig tests were done using a PC30-HPGL Analog to Digital input card and Waveview software. This software samples data for the relevant number of channels at approximately 5 kHz per channel. This frequency is limited by the hardware capability. The data is stored in a byte format where each point sampled is represented by 2 bytes.

3.4.2 Data processing procedure

The resultant byte file is run through a Labview application (Figure 3.4.2-1) which reads the data and carries out the following calculations:

(I) A cross correlation procedure to determine the time taken for the particles to move from the first to the second probe. It then divides the distance between the probes by the resultant time. Thus the velocity is calculated. Only one velocity is calculated for each set of data points where a set is 1000 points.

(ii) The average DC probe current, for each probe, for each set of data points.

(iii) The air velocity, temperature, humidity and mass of sample in the funnel using the Equations (16), (17), (18) and (19).

The resultant 7 values are stored to disk in the form of a text file. This text file is

imported into a spreadsheet package where the data can be viewed graphically.

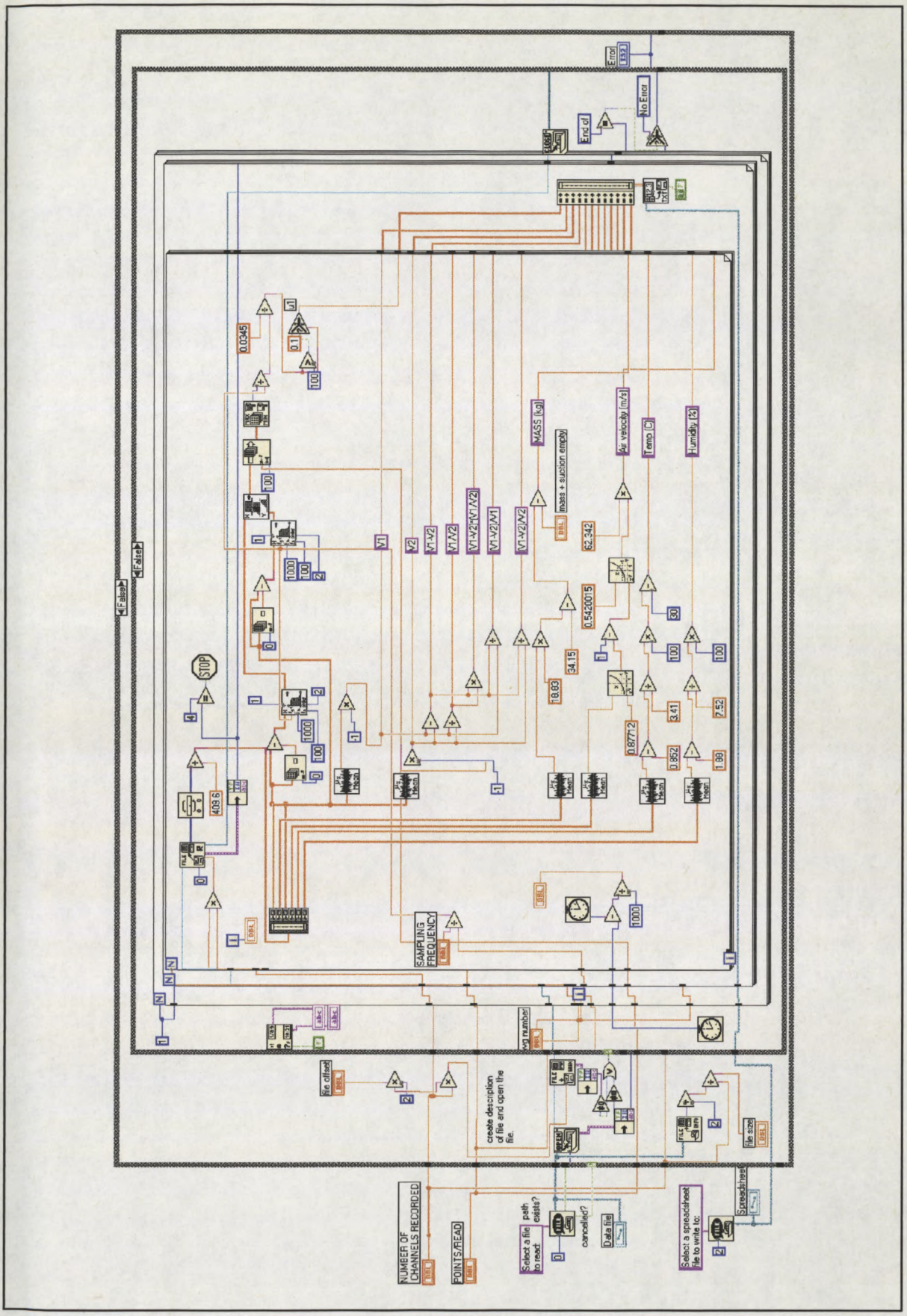

Figure 3.4.2-1: Labview application used for analysis of flow rig tests

3.5 Test results

3.5.1 Relative humidity and temperature tests

Figures 3.5.1-1, 3.5.1-2 and 3.5.1-3 show the graphs representing the results of changing relative humidity at the three different temperatures. I Diff shown on each curve is the current difference between the two probes.

The following results can be seen from the three curves:

25°C Test

Figure 3.5.1-1 shows the following:
At 25°C the current change on probe 1, when the relative humidity changes from 18% to 58%, is 0.094 μA. When the relative humidity changes from 58% to 71% the current change is 0.003 μA. Thus a 40% change of the absolute scale (from 18% to 58%) in relative humidity corresponds to 97% of the total current change. Correcting the probe currents for the changes in mass flow rate and air velocity (these two parameters should have remained constant) then a change in relative humidity from 20% to 50 % corresponds to a change in probe current of 0.097 μA. Thus the current change at the lower end of the relative humidity scale remains the dominant one.

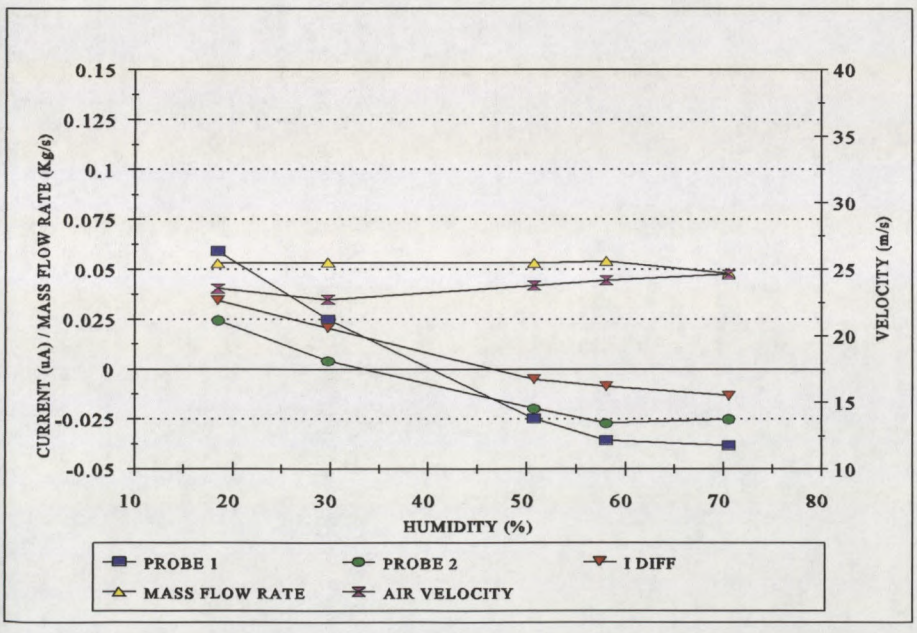

Figure 3.5.1-1 Effects of changing relative humidity at 25 degrees Celsius.

50°C Test

Figure 3.5.1-2 shows the following:
At 50°C the current change on probe 1, when the relative humidity changes from 20% to 40%, is 0.069 μA. When the relative humidity changes from 40% to 60 % it is 0.0438 μA. Thus the first 20% increase in relative humidity results in a 61% change in probe current, while the next 20% relative humidity increase leads to a 39% change in current. In this case the change from 20% to 50% relative humidity corresponds to a change in probe current of 0.075 μA.

70°C Test

Figure 3.5.1-3 shows the following:
At 70°C the current change on probe 1 is 0.074μA when the relative humidity changes from 12% to 35%. When the relative humidity changes from 35% to 50% the current change is 0.018 μA. The first increase from 12% to 35% represents a 97% decrease in probe current while the following relative humidity increase from 35% to 50% only results in a decrease of 3% in the probe currents. A similar change from 20% to 50% in relative humidity corresponds to a change in probe current of 0.05 μA.

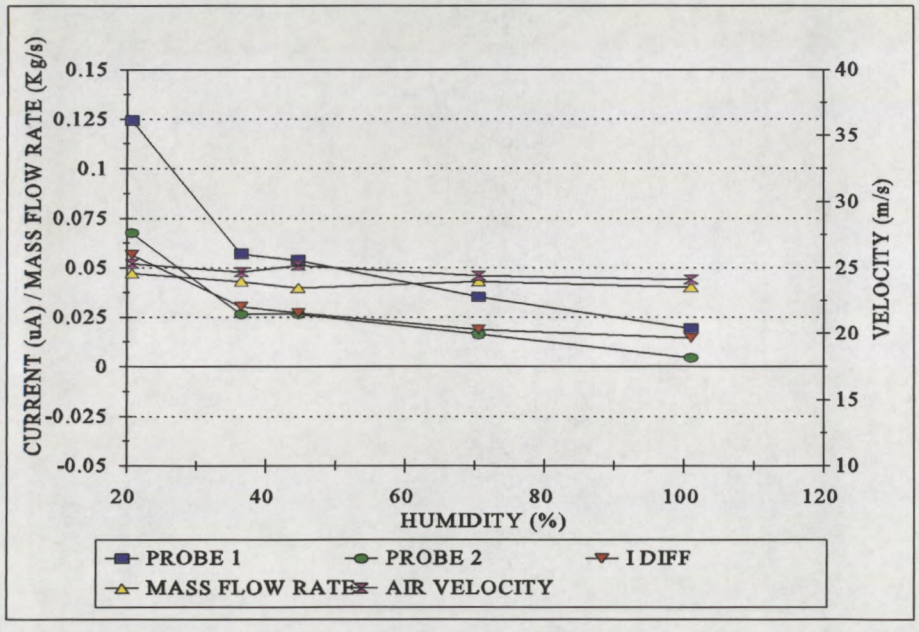

Figure 3.5.1-2 Effects of changing relative humidity at 50 degrees Celsius.

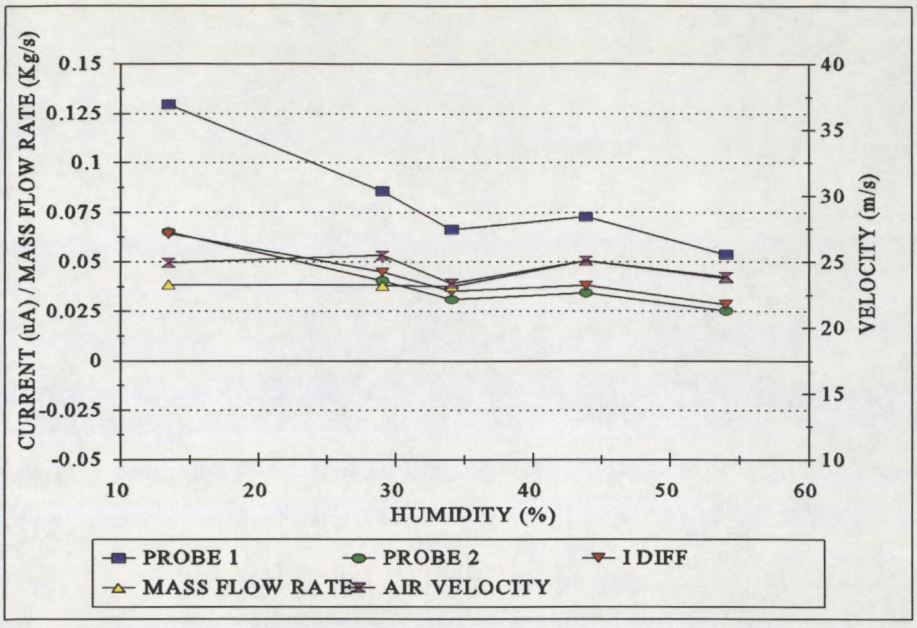

Figure 3.5.1-3 Effects of changing relative humidity at 70 degrees Celsius.

All three figures show that the probe current is related to the relative humidity by the form of Equation (20)

$$I \propto a^{rh} \qquad (20)$$

where I is the probe current

rh is the relative humidity

and $0>a<1$

The same relative humidity change from 20% to 50% in each of the three cases leads to a smaller decrease in probe current for each successive temperature. This means that the lower the ambient temperature the more significant are the effects of changing relative humidity on probe current.

It has been shown that the relative humidity and temperature both effect the probe current generated. Hence it would appear that Equation 13 is a simplification. However, as the temperature increases the relative humidity decreases and thus on a station where the temperature in the PF pipes is in the region of 90 degrees Celsius, and fairly constant around that temperature, it is possible that the minimal changes in the ambient relative humidity and temperature have negligible effect on probe current.

3.5.2 Particle velocity tests

Figure 3.5.2-1 shows the effect of changing air velocity on the probe current magnitude.

There is a steady increase in probe current as the air velocity increases. The slight variations from the curve can be attributed to the changes in mass flow rate and humidity.

Equation (13) shows that the mass flow rate is related to the velocity raised to a power of β. Since the curve shown here is almost linear, β must be unity. There is no reason why this is not possible since β is a characteristic of the material, in this case aluminium oxide. The value of β for PF will not necessarily be unity and in fact appears not to be.

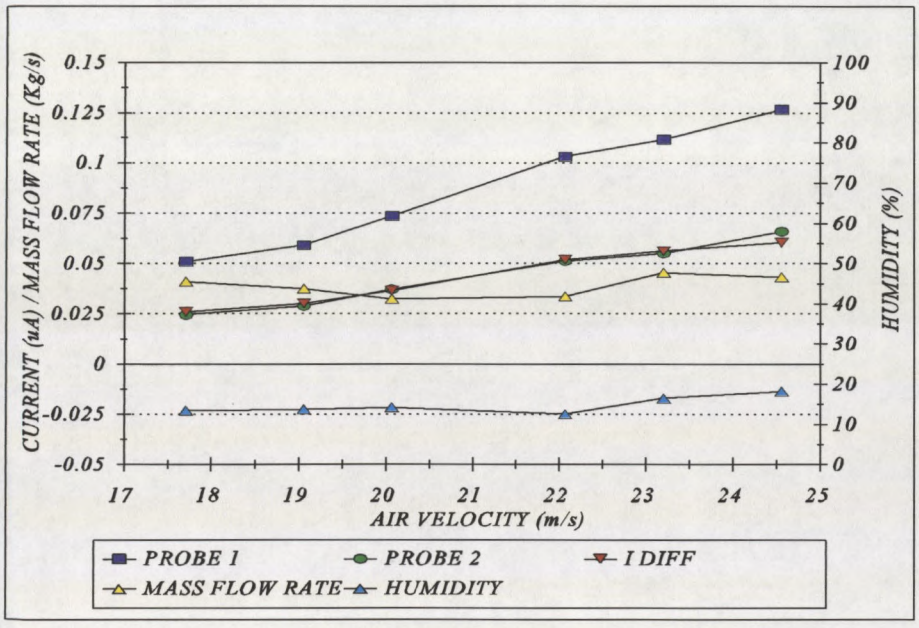

Figure 3.5.2-1 Effects of changing velocity on probe currents.

3.5.3 Mass flow rate test

Figure 3.5.3-1 shows the effects of a changing mass flow rate on probe current. The increase from 0.034 kg/s to 0.078 kg/s represents 26% of the total increase in mass flow rate over the entire test. For this change in mass flow rate the increase in probe current is however 90% of the total increase in probe current over the test.

The increase from 0.078 kg/s to 0.187 kg/s, while representing an increase in mass flow rate of 74% of the total range, only results in a 10% increase in probe current.

Thus the probe current is related to the mass flow rate by the form of Equation (21).

$$I \propto \ln M \qquad (21)$$

where I is the probe current
M is the mass flow rate

It is possible that the flattening of the curve is a result of a decrease in air/fuel ratio such that saturation of the air occurs. In this case the air/fuel ratio at the highest mass flow rate is less than 1. The mass flow rate of the air is 0.138 Kg/s. It is also possible that the probes themselves are saturated and are undergoing electron transfer at the maximum possible rate.

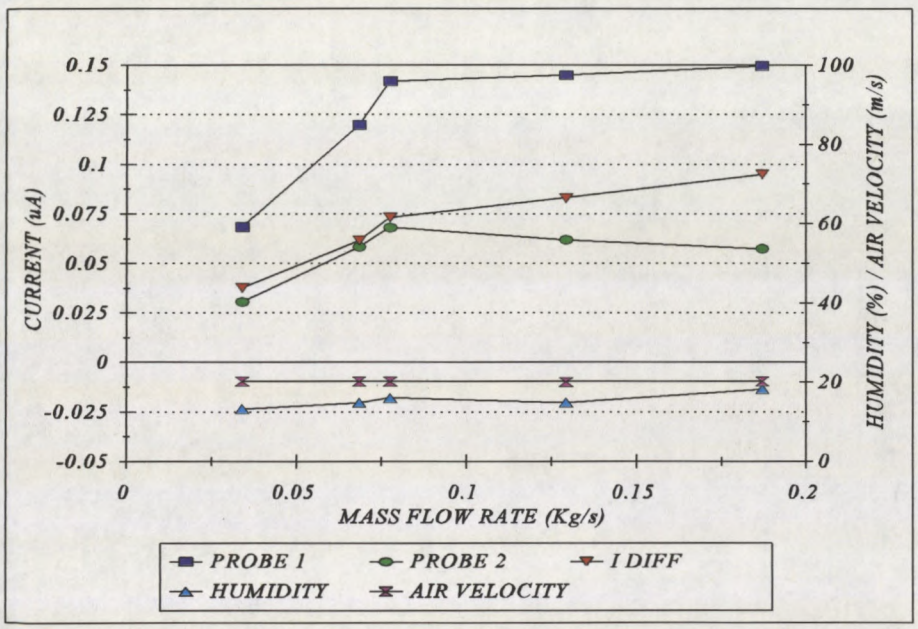

Figure 3.5.3-1 Effects of changing mass flow rate on probe current.

3.5.4 Particle size test

Figure 3.5.4-1 represents the change in probe current and probe current difference for three different particle sizes and three different mass flow rates. The lines of currents representing the mass flow rates, increase as expected with the increase in mass flow

rate. However, both the probe current and the probe current difference are related to particle size by the form of Equation 22.

$$I \alpha D_p^{\delta} \qquad (22)$$

where I is the probe current or probe current difference
D_p is the particle size
δ is the particle size index

One of the aims of these tests was to determine whether the voltage difference between the two probes was not effected by the change in particle size. This is clearly not the situation.

Equation (13) shows the average particle size to be raised to a power of unity. Since this response has been shown to be logarithmic it is clear that the power is not unity. Since the air fuel ratio at the station is higher than any of those which result from the mass flow rates used for these tests, a curve was fitted to the line representing the current on probe 1 at the highest flow rate. The result of this curve fitting is to find a value of 0.528 for δ. This value is discussed and used in Section 7 (pp 70).

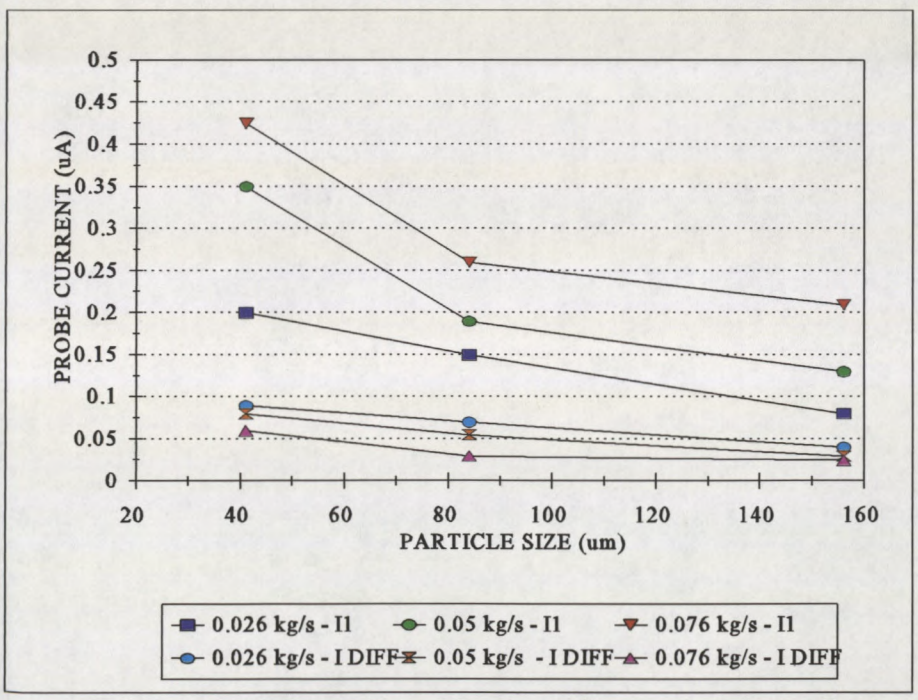

Figure 3.5.4-1 Effects of changing mass flow rate and particle size on probe current.

4 HENDRINA POWER STATION ISOKINETIC / ELECTROSTATIC TECHNIQUE COMPARISON TESTS - 1994

Hendrina Power Station approached T-R-I because the station required a means to measure the mass flow rate and the distribution of PF in the pipes. As a result tests were carried out at Hendrina on unit 5, mill F, to determine the feasibility of installing an on-line electrostatic device to measure the mass flow rate of PF in each pipe. This unit and mill were chosen because of easy accessibility and uniform pipe geometry (Figure 4.1-1).

4.1 Equipment setup

Figure 4.1-1 shows the equipment layout used at Hendrina Power Station. Coaxial cables from each Collapsible Grating Probe (two per pipe, resulting in a total of 12 channels) are connected to a high impedance buffer box which was located near the boiler. From the buffer box a single 16 core cable runs to the unit operating room where it was connected to the data acquisition computer.

This cable was routed clear of other high current cables since these could induce noise.

The pipe geometry of this mill was very suitable for the necessary tests. Due to the uniformity of the pipes (pipes 1 & 2 are a mirror image of pipes 3 & 4) between the mill and the boiler, the probe and sampling port positions for pipes 1, 2 and 5 are identical to those for pipes 3, 4 and 6 respectively (Figure 4.1-1). The sampling procedure is facilitated by the fact that all the sampling ports are easily accessible from floor levels and no scaffolding or platforms are necessary.

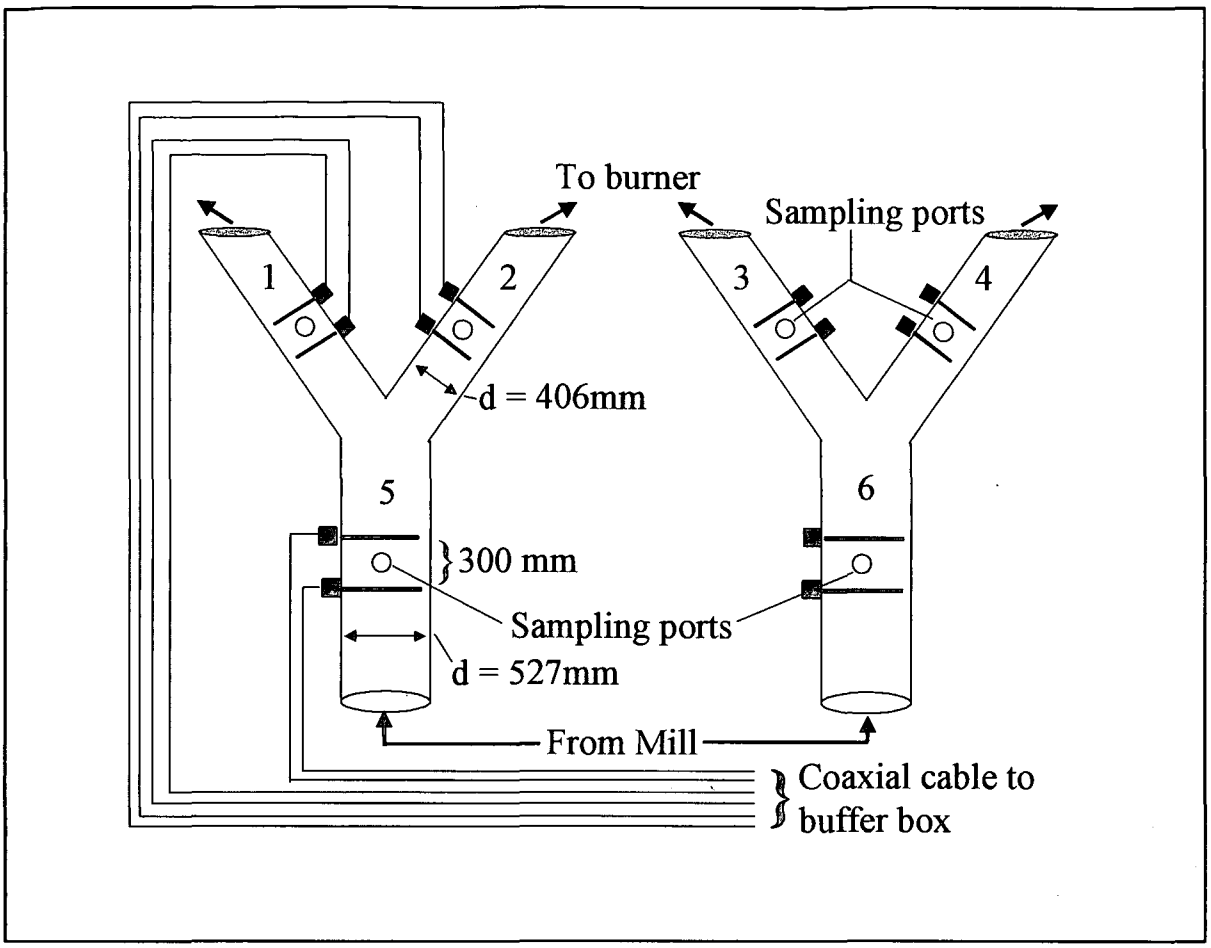

Figure 4.1-1 Hendrina Power Station, unit 5, mill F - pipe geometry and positioning points of electrostatic probes and measurement equipment.

4.2 Test procedure

The test procedure called for six tests to be done at two different loads with three different air/fuel ratios for each load. For each test the mass flow rate using the electrostatic technique was measured. Simultaneously iso-kinetic sampling was carried out. This was because each test condition would lead to different quantities of PF flowing at different velocities in the PF pipes. The conditions for these six tests are shown in Table 4.2-1

TEST No.	MILL LOAD (Tonnes/Hr)	AIR/FUEL RATIO
1	22.2	1.52
2	22.2	1.60
3	22.2	1.67
4	13.2	1.90
5	13.2	2.10
6	13.2	2.30

Table 4.2-1 Mill load conditions for the six tests analysed.

Once the mill had settled at the required test conditions as given in Table 4.2-1, the data logging computer was set to log data and the iso-kinetic sampling procedure was started. Each of the six pipes was sampled iso-kinetically by the Hendrina Power Station personnel using the sampling ports as seen in Figure 4.1-1. The start and finish times of the sampling procedure for each pipe were recorded manually. Attempts to minimise errors in the sampling procedure were made by using a 12 position target plate. Results of iso-kinetic sampling cannot however, be guaranteed to be accurate within 10% of the true mass flow rate and when roping is occurring in the PF pipes, errors of 20% of true mass flow rate are possible.

4.3 Test data processing procedure

The tests done at Hendrina in 1994 and Kendal in 1995 used similar data processing techniques.

The data was acquired using a National Instruments ATMIO-64-F analog to digital input card. The data was logged in byte format to a DAT (Data Acquisition Tape) drive. The DAT drive is used because of the size of the resultant files.

Data from the DAT drive was processed using a Labview application (Figure 4.3-1). Figure 4.3-1 shows the correlation module for a single pipe. The modules for the remaining pipes are in the background of the innermost loop. The following parameters were calculated by this application:

(i) The PF velocity was calculated using a cross correlation technique (Marantos

1992) over a range of 1000 points. Thus for each 1000 points recorded a single PF velocity was calculated.

(ii) The voltage reading for the same 1000 points used for each correlation (Marantos 1992) was averaged to give a single probe voltage. Since the data was recorded at a frequency of 6.7 kHz per channel this averaging process resulted in data arrays which contain over 6 points per second. The process being measured will only change over a period of approximately 30 seconds, and is thus slow changing when compared to this resultant sampling rate.

(iii) The mass flow rate is calculated directly from the iso-kinetic sampling results. This procedure is carried out by calculating the ratio of the sampling probe cross sectional area to the cross sectional area of the pipe. Since the time over which the sample was taken is known, the mass flow rate can be calculated. The iso-kinetic sampling results can be seen in Appendix F.

(iv) The values of K_m and β are calculated by using the mass flow rates calculated in (iii) above and then solving simultaneous equations. More than one value for each of the two constants is found and the average for each is used to calculate the mass flow rate for each pipe using Equation (13).

(v) For the two probes in each pipe the probe voltage difference, the probe voltage ratio and the product of these two parameters is calculated and the resultant values are compared to the mass flow rates as calculated in (iii) and (iv) above. This was just an experiment to see if any relationship between these parameters and mass flow rate was easily observable.

The resultant data is written to a text file which can be studied and analysed using a spreadsheet package. The results of this analysis and the comparisons made are detailed in the next section.

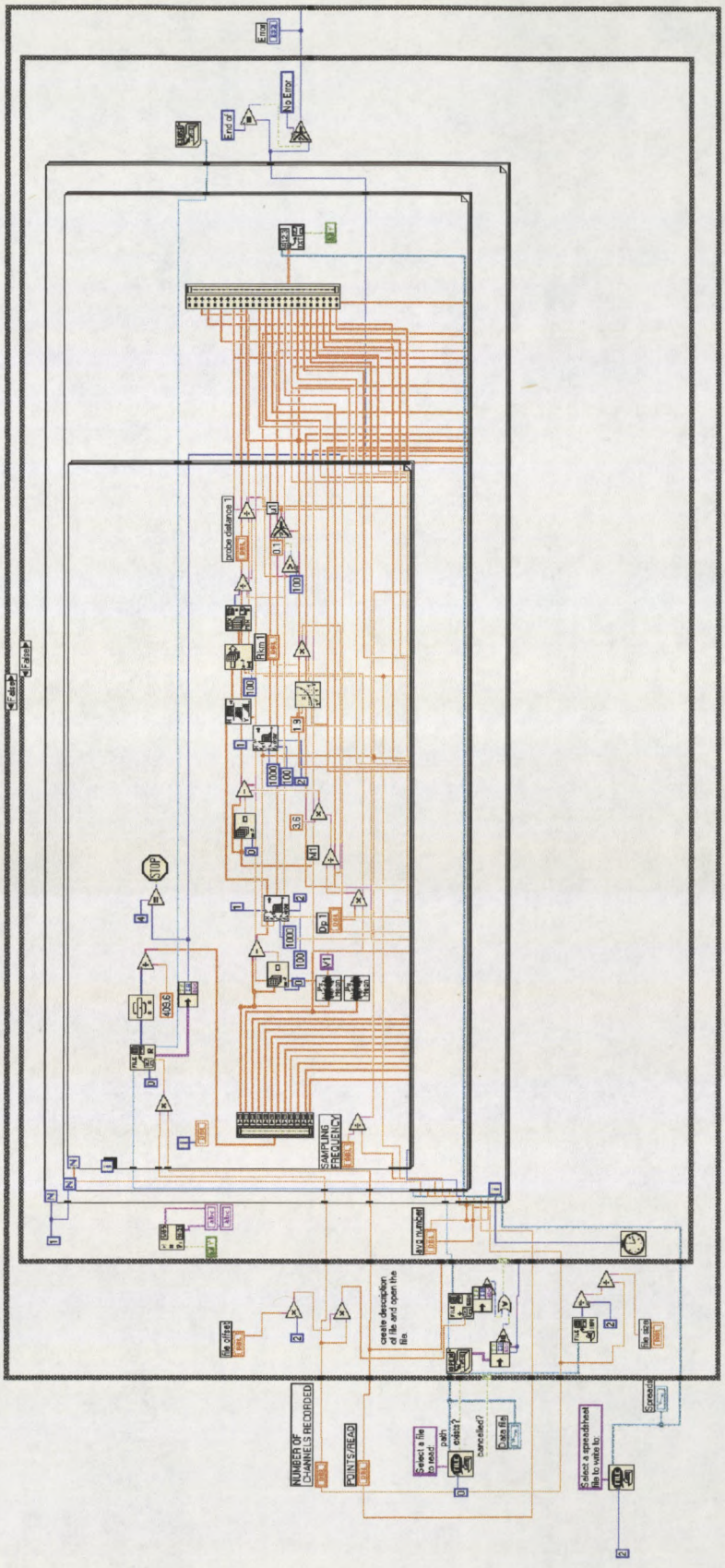

Figure 4.3-1: Labview application for processing of the power station test data

4.4 Test results

4.4.1 Comparison of electrostatic mass flow rate and probe voltage difference

Figures 4.4.1-1 and 4.4.1-2 represent graphically the mass flow rate as calculated using method (iii) of Section 4.3, the probe voltage difference, the probe voltage on probe 1, the product of the probe voltage difference and the probe voltage ratio, the particle size and the particle velocity for pipes 6 and 2 for the six tests described in Table 4.2-1.

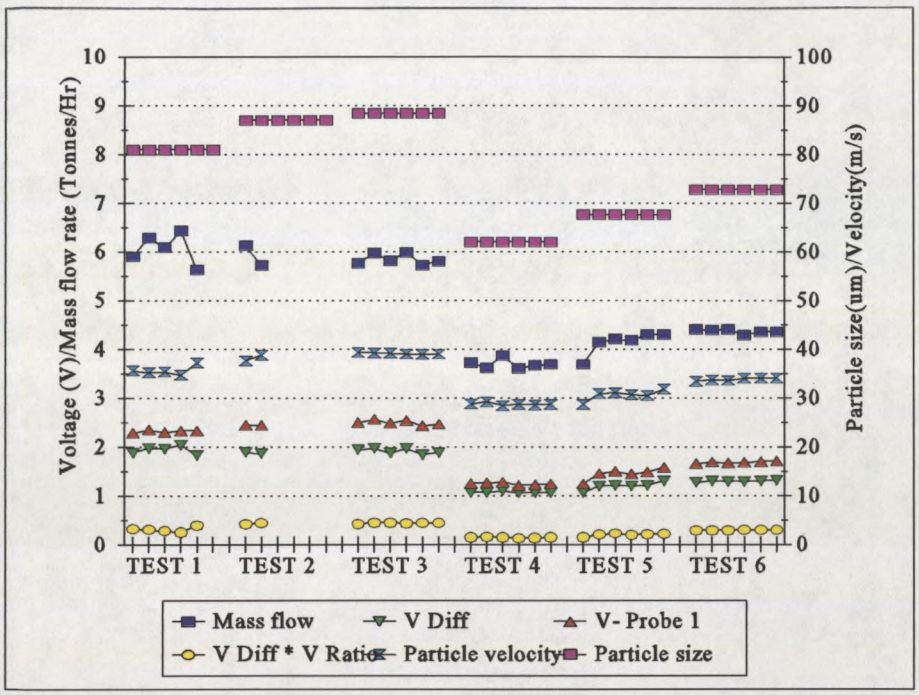

Figure 4.4.1-1 Pipe 6- Electrostatic mass flow rate, probe voltage parameters and particle size. 3 tests at 22 Tonnes/Hr (1, 2 & 3) and 3 tests at 13 Tonnes/Hr (4, 5 & 6)

Each of the six tests is represented by six markers. Each marker is the average value of the relevant parameter calculated for the period of time over which each pipe was sampled iso-kinetically. For example, in Figure 4.4.1-1 there are six markers representing test 1. The first marker is the recorded voltage in pipe 6 while pipe 1 was being iso-kinetically sampled. The second marker is the recorded voltage in pipe 6 while pipe 2 was being iso-kinetically sampled and so on. Where markers are missing the signal was lost due to problems with the cables from the sensors. Also the data logging process to the DAT tape drive was at times temperamental and the computer

sometimes reset for unknown reasons. This could have been the result of intermittent power failures or a glitch in the supply voltage. Also the computer is in the open on the station floor where the conditions are hot and dusty and not ideal for computer operation.

Table 4.2-1 shows the mill load for tests 1, 2 and 3 is 22.2 tonnes per hour and for tests 4, 5 and 6 it is 13.2 tonnes per hour. This represents a decrease in flow rate of 9 tonnes/hour, or 41%, between the first three tests and the next three. This is a significant drop in mill load. Figure 4.4.1-1 representing pipe 6, does show this marked decrease, both for the calculated values and the voltage parameters. Figure 4.4.1-2, representing pipe 2 does not, however, show the same marked decrease in the calculated values, while the voltage parameters do show the expected decrease.

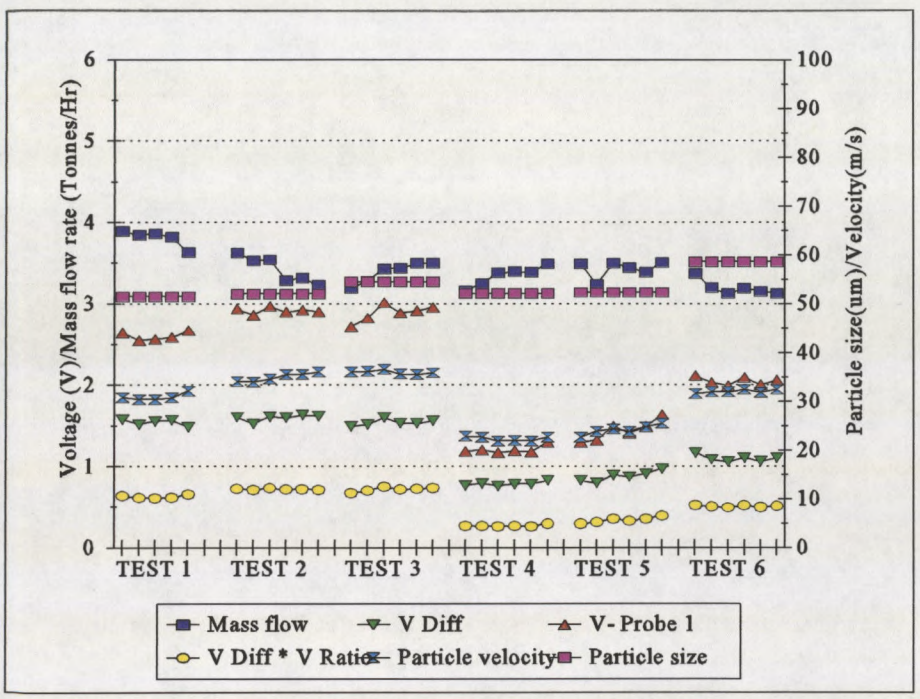

Figure 4.4.1-2 Pipe 2- Electrostatic mass flow rate, probe voltage parameters and particle size. 3 tests at 22 Tonnes/Hr (1, 2 &3) and 3 tests at 13 Tonnes/Hr (4, 5 & 6)

Graphs representing the remaining pipes can be seen in Appendix D. They also show that the calculated mass flow rate does not always show the marked decrease while the voltage parameters do.

Since the 41% drop in flow rate is a known fact the voltage parameters studied would appear to be more indicative of mass flow rate than the calculated value.

The method of calculation for the mass flow rate (method (iii) Section 4.3) uses values of k_m and β which are calculated from the iso-kinetic sampling results. The inaccuracy of iso-kinetic sampling has already been discussed. This inaccuracy may be the cause of the discrepancy in the calculated values.

The actual mass flow rates calculated directly from the iso-kinetic sampling results are given in Figure 4.4.1-3. The following can be observed.

(I) The sum of the mass flow rates in pipes 1 and 2 was greater than that for pipe 5 in three of the four tests. This is physically impossible since pipe 5 divides into pipes 1 and 2. However assuming an error band of 10% in a positive or negative direction, i.e. ± 10%, the first 5 tests all fall within the error band.

(ii) The sum of mass flow rates for pipes 3 and 4 is approximately 63% of the mass flow rate measured in pipe 6. Pipe 6 divides into pipes 3 and 4. Assuming a similar error band as in (I) above, none of the six tests fall within the error band.

(iii) The sum of pipes 5 and 6 when added together are within 9% of the expected values (22 Tonnes/Hr for tests 1 and 2, and 13 Tonnes/Hr for tests 3 and 4.) However the sum of pipes 1, 2, 3 and 4 are as much as 30% short of the expected values.

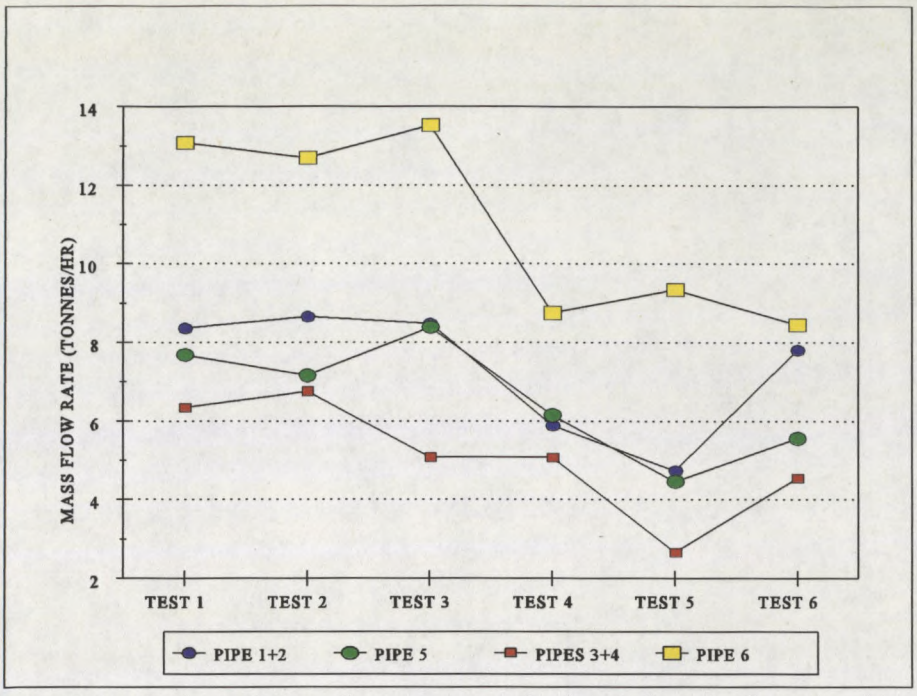

Figure 4.4.1-3 Mass flow rate as calculated directly from iso-kinetic sampling results.

These discrepancies prove the inaccuracy of the iso-kinetic sampling technique and more specifically the iso-kinetic sampling done during this test series.

4.4.2 Comparison of iso-kinetic sampling mass flow rate and probe voltages.

Figures 4.4.1-3 and 4.4.2-1 show the iso-kinetic sampling mass flow rate and the probe voltage representation of mass flow rate respectively. Note that the values in Figure 4.4.2-1 are not true mass flow rate but rather an indicative numerical value for mass flow rate which is the product of the probe voltage difference and the probe voltage ratio. (The absolute magnitude is the factor of interest in this case). This value is chosen for comparison because it always showed the decrease of 41% in mass flow rate between the first three tests and the second three (Figure 4.4.1-1).

The sampling results (Figure 4.4.1-3) for pipe 6 are difficult to explain since the sum of the mass flow rate in pipes 3 and 4 which split from pipe 6 (see Figure 4.1-1) is much lower than that of pipe 6. The electrostatic results (Figure 4.4.2-1) also show unexpected mass flow rate values for pipe 6. It is possible that the flow pattern in this pipe may be extreme i.e. a small, dense "rope". Further tests are necessary to determine the cause of these unusual results.

The electrostatic test results do follow the correct trend. i.e. from one test to the next test, if there is a change in the mass flow rate for the sum of pipes 1 and 2 then there is a similar change in the flow rate in pipe 5. The same statement holds true for pipes 3, 4 and 6. This trend is not always followed when observing the results for iso-kinetic sampling i.e. a measured change in mass flow rate in pipe 5 is not always followed by a similar measured change in pipes 1 and 2 (Figure 4.4.1-3).

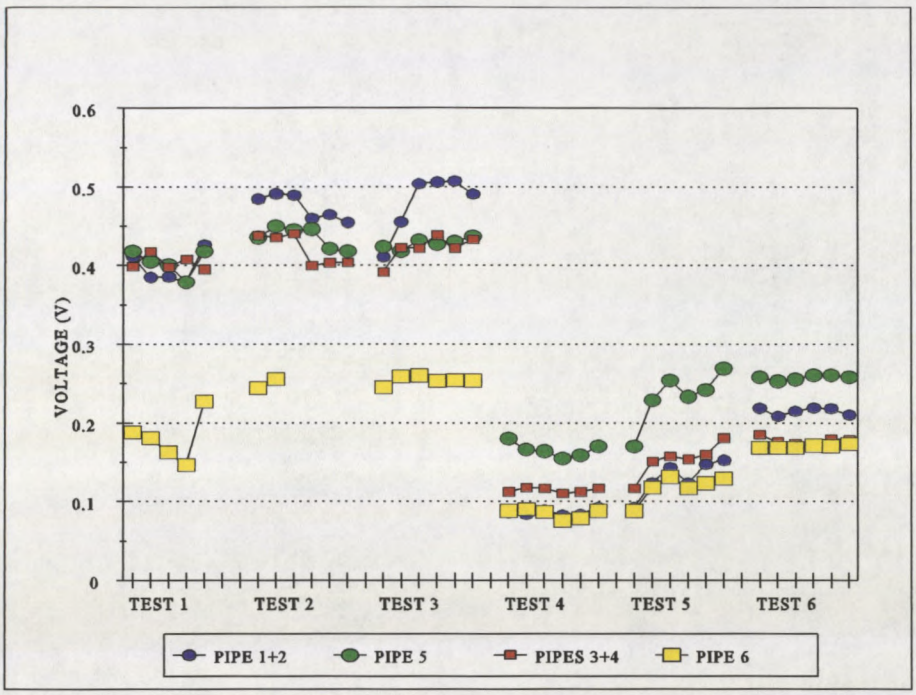

Figure 4.4.2-1 Numerical values representative of mass flow rate calculated from the product of probe voltage difference and probe voltage ratio.

4.4.3 Particle size analysis

Figure 4.4.3-1 shows a comparison between the particle size established at Hendrina Power Station using a sieving technique (represented by green squares) and that established at T-R-I using a laser analysis machine (represented by blue circles). The same samples were used for both measurements.

The discrepancy between the results the two methods produce can be explained as follows. The laser analysis machine assesses the average particle size by measuring the actual average diameter of particles and then calculating the overall average. The

sieving technique allows particles of smaller diameter through each successive sieve. The mass remaining in each sieve is then measured, and expressed as a percentage of the starting mass. Since the particles are not perfectly spherical, a single particle may remain on a sieve, if it lies with its long axis across the grating, even though the average particle size of that particle may be less than the grating size. Thus the Mastersizer will find a smaller average particle size.

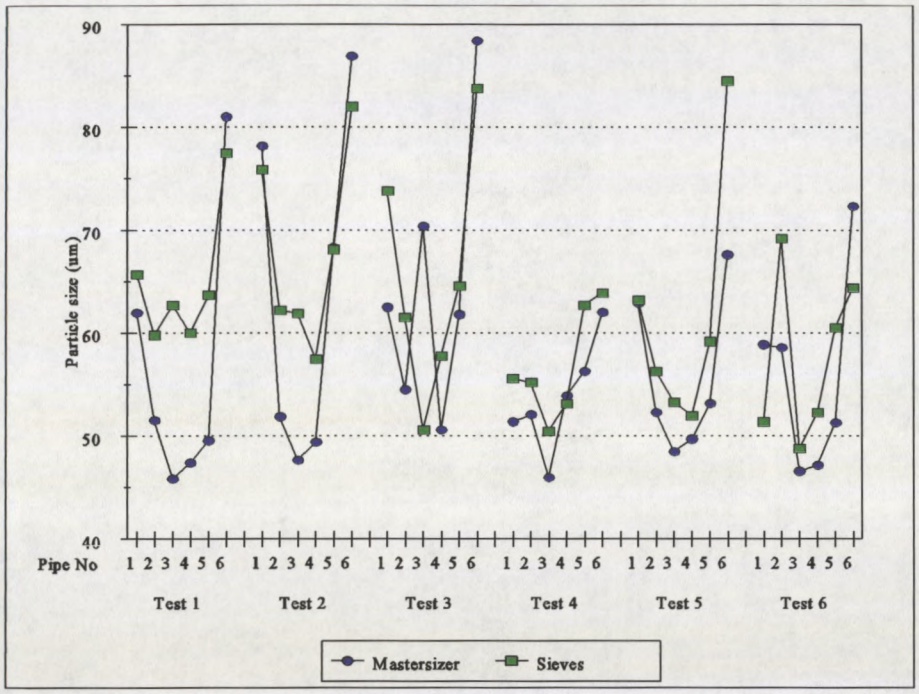

Figure 4.4.3-1 Comparison of average particle size measured using sieves and a Mastersizer particle size analyzer.

Figure 4.4.3-2 and 4.4.3-3 however again shows the weakness of the iso-kinetic sampling technique. Since pipes 1 and 2 split from pipe 5, and 3 and 4 split from pipe 6, the average weighted particle size in pipes 1 and 2 should be the same as that in pipe 5, and the average weighted particle size in pipes 3 and 4 the same as that in pipe 6. Figure 4.4.3-2 (pipes 1, 2 and 5) shows this to be true.

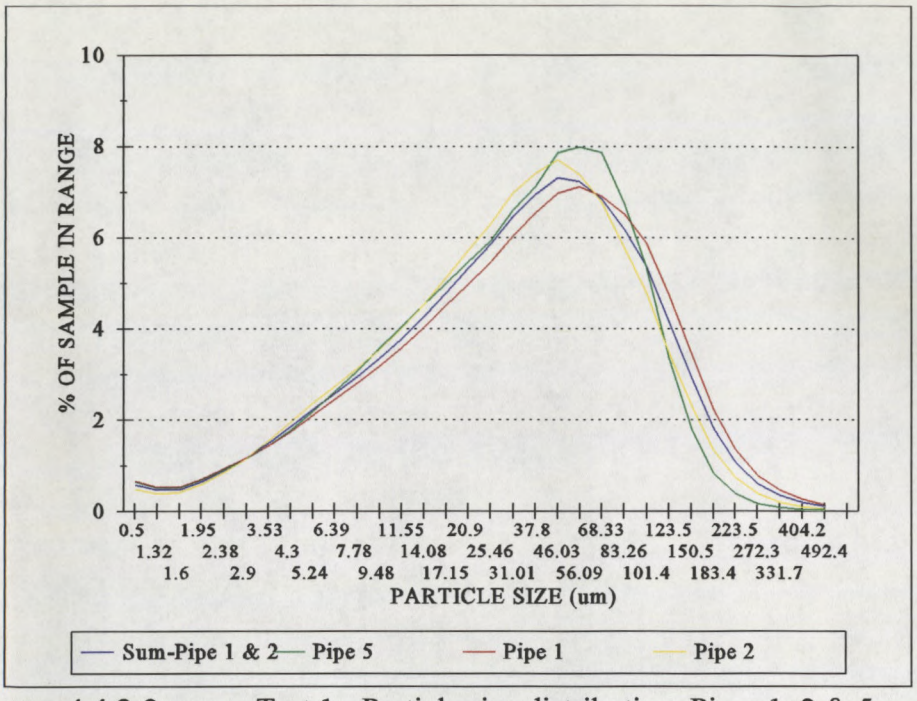

Figure 4.4.3-2 Test 1 - Particle size distribution. Pipes 1, 2 & 5

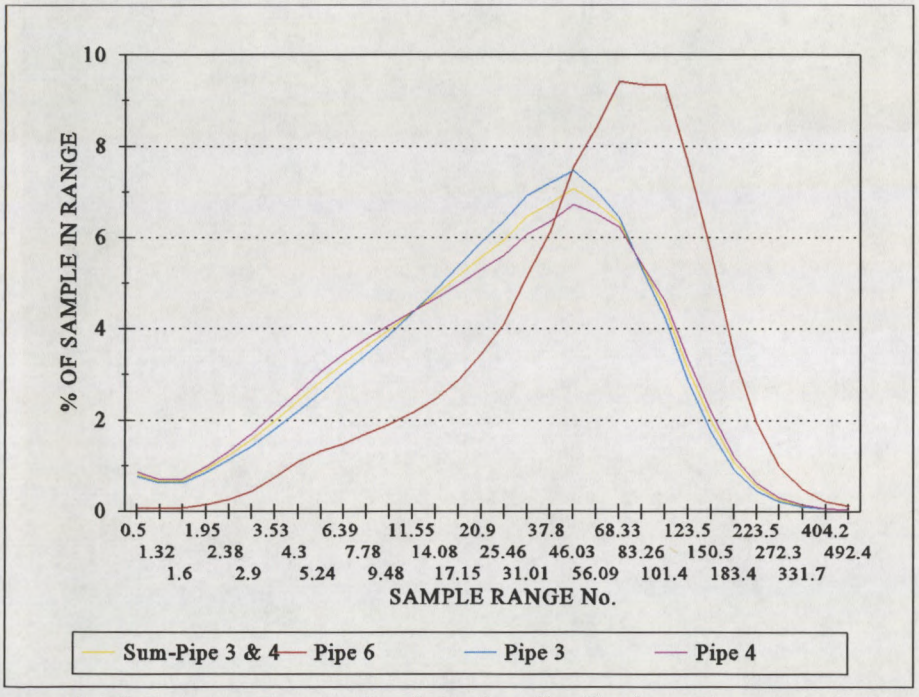

Figure 4.4.3-3 Test 1 - Particle size distribution. Pipes 3, 4 & 6

Figure 4.4.3-3 shows however a bigger average particle size in pipe 6 than that in pipes 3 and 4. This can be attributed to the fact that different size particles travel in different parts of the pipe (and at different velocities) in a consistent pattern. When the sampling is carried out not enough points are sampled to give an accurate result for particle size. This does not effect only the particle size analysis. The mass of the extracted sample will also be incorrect. Figures 4.4.3-2 and 4.4.3-3 give the results from test 1. The results for tests 2 to 6 give similar graphs and can be seen in Appendix E.

The particle size varies from pipe to pipe by as much as 70%. This is caused by the different air velocities in each pipe. The heavy, or larger particles are carried by the higher velocity while the smaller (lighter) particles are carried by the lower velocities.

4.4.4 Particle Velocity Measurement

Figure 4.4.4-1 shows the particle velocity measured in each pipe during each of the six tests. The air/fuel ratios increased from tests 1 to 3 while the load remained constant at 22 Tonnes/Hr and similarly for tests 4 to 6 where the load was 13 Tonnes/Hr. Since the amount of air flowing in each pipe must increase for the air/fuel ratio to increase, the resultant air velocity, and hence the particle velocity must increase. Figure 4.4.4-1 shows this successive increase from test to test.

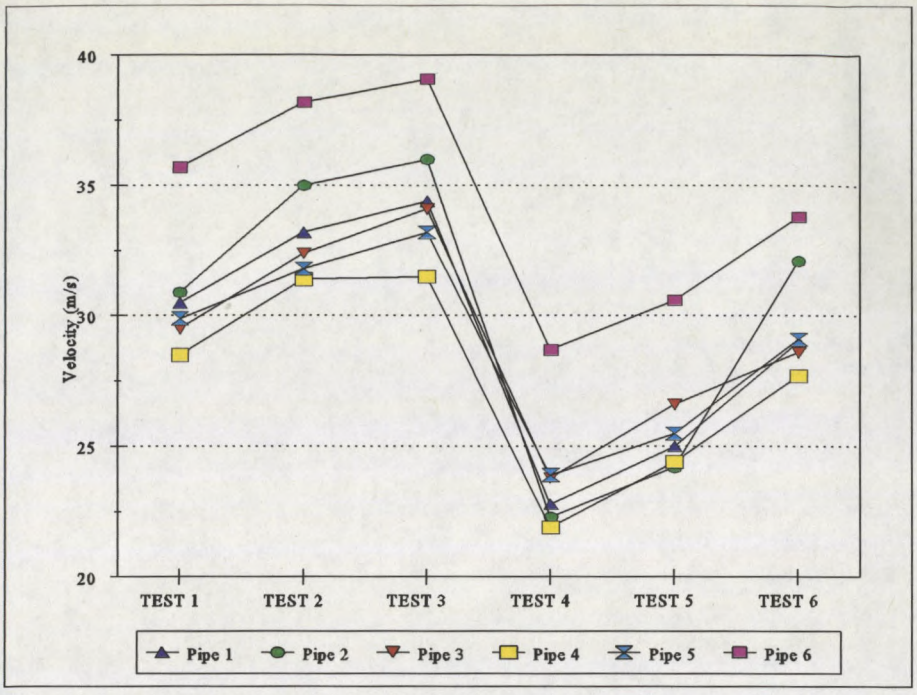

Figure 4.4.4-1 Particle velocity in each pipe for tests 1 to 6

4.5 Comparison of probe wear at Hendrina, Kendal and Lethabo Power Stations

The collapsible grating probes used at Hendrina wore away at a far higher rate than could reasonably have been expected. The photographs in Appendix A show the wear on various probes from different stations.

Photographs 1 and 2 show probes from Lethabo and Kendal power stations, respectively. The finger probes at Lethabo were installed for more than two years and the two probes shown are the cases of most and least wear. The Kendal probe was in for a period of approximately eighteen months and the wear can be seen on the grating which has sharp edges.

The probes shown in photographs 3, 4, 5 and 6 were collapsible grating probes which were installed at Hendrina for a period of 3 months. The 20 mm rod and the outer pipe (2.5 mm wall thickness) have been totally worn through.

The photographs clearly show that there is more wear on the Hendrina probes than there is on either the Lethabo or the Kendal probes despite the considerably shorter

period over which they were installed. The reason for this is that Hendrina has one of the most abrasive coals amongst the Eskom power stations and the particle velocity tends to be high.

These probes were made only of mild steel and a more permanent instrument could be made of harder material. Alternatively the probes can be coated with various materials. In order that the long term test could be carried out at Hendrina, new probes were made and were coated with a layer of Tungsten Carbide using a plasma transferred arc. The cost of this was R 625 per probe, an amount which would be less should the operation be carried out on a regular basis. Hence the problem of wear on the probes is not insurmountable.

4.6 Hendrina Power Station results - summary

(I) The comparison between the mass flow rate calculated using the electrostatic results with the particle size from the iso-kinetic sampling, and the probe voltage difference shows that the voltage difference always shows the correct trend while the calculated flow rate does not.

(ii) The mass flow rates calculated from the iso-kinetic sampling results show errors of up to 30%.

(iii) The particle size determined using a sieving technique on the iso-kinetic sample is sufficiently accurate when compared to that measured using a laser analysis machine.

(iv) The particle velocity measurements made using the electrostatic technique appear to be accurate.

5 KENDAL POWER STATION ISO-KINETIC / ELECTROSTATIC TECHNIQUE COMPARISON TESTS - 1995

As discussed in Section 4, PF sampling cannot be guaranteed better than 20% accurate for PF mass flow rate measurement. All the tests done in an attempt to verify the accuracy of the electrostatic mass flow rate measurement technique using iso-kinetic sampling results as a comparison have proven inconclusive because of the dubiety of the iso-kinetic results (Section 4, pp 38). The personnel working at Matimba Power Station have been working towards increasing the accuracy of the iso-kinetic technique. A second cyclone was added and the pipes between the sampler and the extraction probe were insulated.

With these refinements a recovery rate with an error of less than 2% has become possible. The recovery rate is calculated by comparing the mass of the extracted sample to the mill feeder speed. Since the test procedure requires that the mill be run under steady load conditions, the level of PF in the mill is assumed to remain constant. This means that coal going into the mill on the feeders must come out at the same rate in the form of PF. Hence feeder speed can be used to measure total coal flow through the mill and feeder speed is synonymous with mill load.

The primary objective of this set of tests was to compare the electrostatic measurements to the iso-kinetic sampling measurement and the mill feeder speed (mill load).

The secondary objective of this test series was to measure the temperature and relative humidity in the PF pipes and evaluate whether the amount by which these parameters change was of large enough magnitude to cause significant changes in probe current.

This series of tests was the first to be done at a power station after the findings of the rig tests (Section 3, pp 20). The rig tests highlighted the fact that temperature and relative humidity definitely have an effect on probe current.

5.1 Equipment setup

The tests were done at Kendal Power Station with the assistance of the Matimba personnel who carried out the iso-kinetic sampling procedure. Kendal was chosen because:

(I) The collapsible grating probes necessary were already made and the required sampling ports were available.

(ii) The mill selected had PF pipes with long straights where the probes were inserted and the sampling done. This meant that the effects of roping could be reduced to a minimum.

(iii) Kendal Power Station has tube mills and hence volumetric feeders from which coal flow can be calculated.

Figure 5.1-1 shows the equipment cofiguration with probe positions and sampling ports.

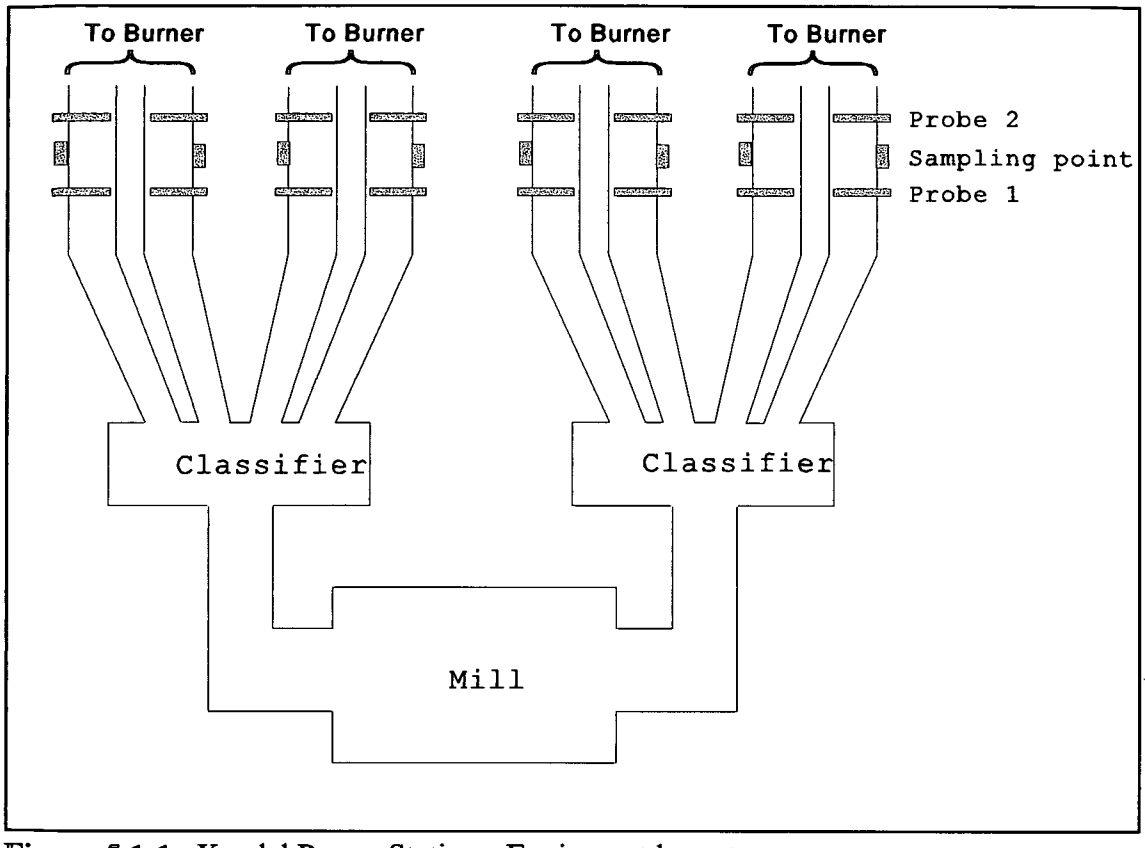

Figure 5.1-1: Kendal Power Station - Equipment layout

5.2 Test Procedure

Tests were done at three different mill loads of 40 %, 55 % and 70 %. Mill load is generally expressed as a percentage of total fuel flow through the mill. For example, if the mill runs at 100% load there may be a throughput of 30 Tonnes/Hr. Hence 40% load would correspond to a throughput of 12 Tonnes/Hr.

During each test PF sampling was carried out. After the sampling probe was removed

and the port was still open a temperature and relative humidity probe was inserted and the two measurements were observed.

5.3 Data processing procedure

5.3.1 Electrostatic data processing procedure

The electrostatic data processing procedure involved the use of a similar Labview application as that used for the Hendrina Power Station tests (Section 4.3 - Figure 4.3-1). The application read data recorded to the DAT tape during the test procedure, calculated the average current on each probe for every 1000 raw data points recorded and calculated the PF velocity over the same 1000 points for each pipe.

5.3.2 Iso-kinetic data processing procedure

The mass flow rate is also calculated from the iso-kinetic samples taken during the test procedure using Equation 23.

$$M = \frac{mR^2}{tnr^2} \qquad \text{Equation 23}$$

Where M = the mass flow rate in kg/s.
m = the mass of the sample extracted.
R = the radius of the PF pipe.
t = the sampling time.
n = the number of sampling points.
r = the radius of the sampling probe inlet.

The sum of the mass flow rates in the four pipes is compared to the feeder speed and the recovery rate determined.

5.3.3 Mill feeder speed

The mill feeder speed or mill load is steady for each test and recorded from the mill settings made by the operator.

All these results were then presented in graphic format using a spreadsheet package and the results studied and analysed.

5.4 Test results

5.4.1 Comparison between electrostatic results and mill load

The test results for the comparison between the mill load (feeder speed) and the electrostatic probe current are shown in Figure 5.4.1-1. The graph shows the average values of the 8 pipes at each mill load.

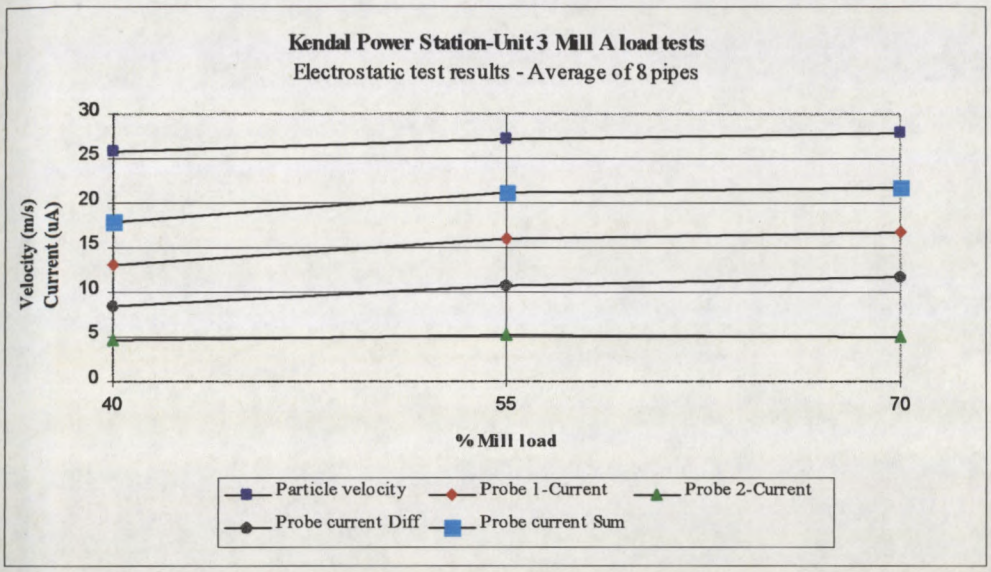

Figure 5.4.1-1 Comparison between electrostatic measurement and mill load.

The probe current, probe current sum and probe current difference all increase as the mill load increases. This is the expected result as shown in Section 3, Figure 3.5.3-1 where the flow rig tests show the probe currents increasing with an increase in mass flow rate. The probe current sum and difference are calculated in the same way as those in Section 4 (Hendrina Power Station tests).

5.4.2 Comparison between electrostatic results and iso-kinetic results

Figure 5.4.2-1 shows the comparison between the iso-kinetic sampling results and the corresponding electrostatic results for the test done at 70 % load . The pipe numbering arises from the fact that all those pipes designated with an L are from the motor drive end of the mill and those designated with a U from the non-drive end (Figure 5.1-1).

The graph shows that the iso-kinetic results and the electrostatic results do not match. Once again this poses the question of whether the iso-kinetic or the electrostatic results are at fault. However, the iso-kinetic sampling recovery rate is within 2% for the tests done at all three loads and this would suggest that the iso-kinetic sampling is accurate. Similar non-matching patterns occurred at 55 % and 40 % load. It is difficult to explain these inconsistencies. The chances of all three recovery rates being within 2% by coincidence are very slight. There is the possibility that the density and/or chemical makeup of the coarse coal passing through the feeder is changing. Changing chemical make-up may lead to changes in the quantity of charge transfer to the probes. Also the milled material may change shape and particle size with a change in chemical make-up. These types of changes will effect the probe current but not the iso-kinetic sampling recovery rate. Although these are possibilities it is unlikely that the chemical make-up of the coal will change over the short time period which covers this test series.

The PF sampling results can be seen in full in Appendix F.

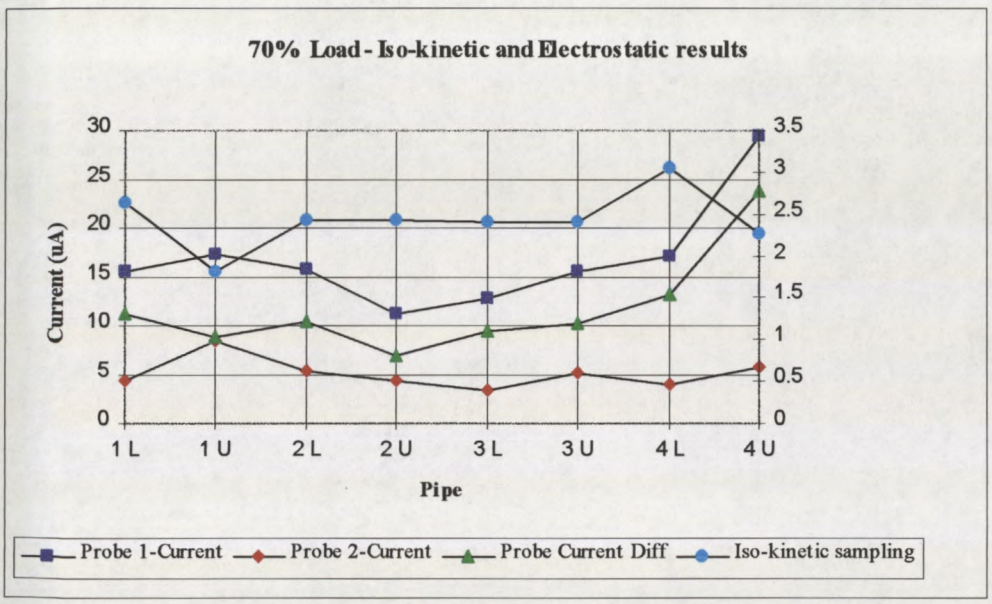

Figure 5.4.2-1 Comparison between iso-kinetic and electrostatic results for all 8 pipes at 70% mill load.

5.4.3 Comparison between mill feeder speed and electrostatic results at 40% load

Figure 5.4.3-1 show the electrostatic results for pipe 1 at a load of 40 % and Figure 5.4.3-2 the corresponding results recorded by the Kendal data logging system. Over the course of this test the mill load was oscillating. These oscillations can be clearly seen on both graphs. (Similar oscillations occurred for the other 7 pipes. Pipe 1 is merely used as an example.) This would tend to support the electrostatic technique since there is no question that the quantity of PF in the pipes was varying according to the oscillations. However the recovery rate calculated from the iso-kinetic results for this test is also within 2%. This would tend to support the accuracy of the iso-kinetic technique. This may be explained by the sampling time and the period of oscillation of the mill load. The time taken for a PF sample to be extracted is 6 minutes. The period of oscillation of the mill load is between 5 and 6 minutes. Hence the sampling time comes very close to covering the period of oscillation, and when the mass flow rate is calculated from the sample mass extracted a representative average will be obtained.

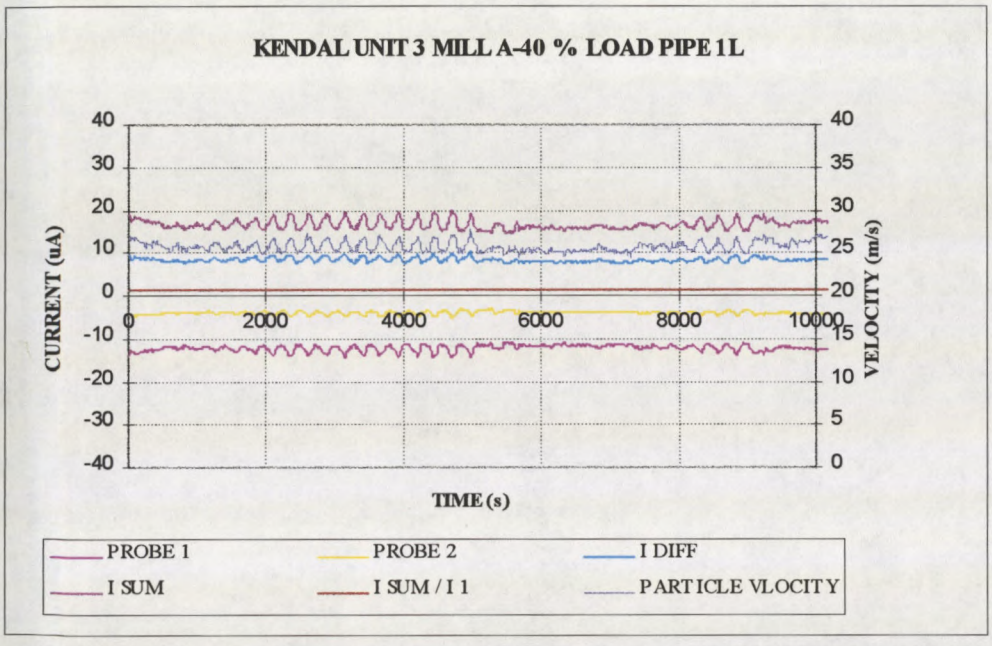

Figure 5.4.3-1 Pipe 1 electrostatic results showing the oscillations in the probe current and particle velocity at 40% mill load.

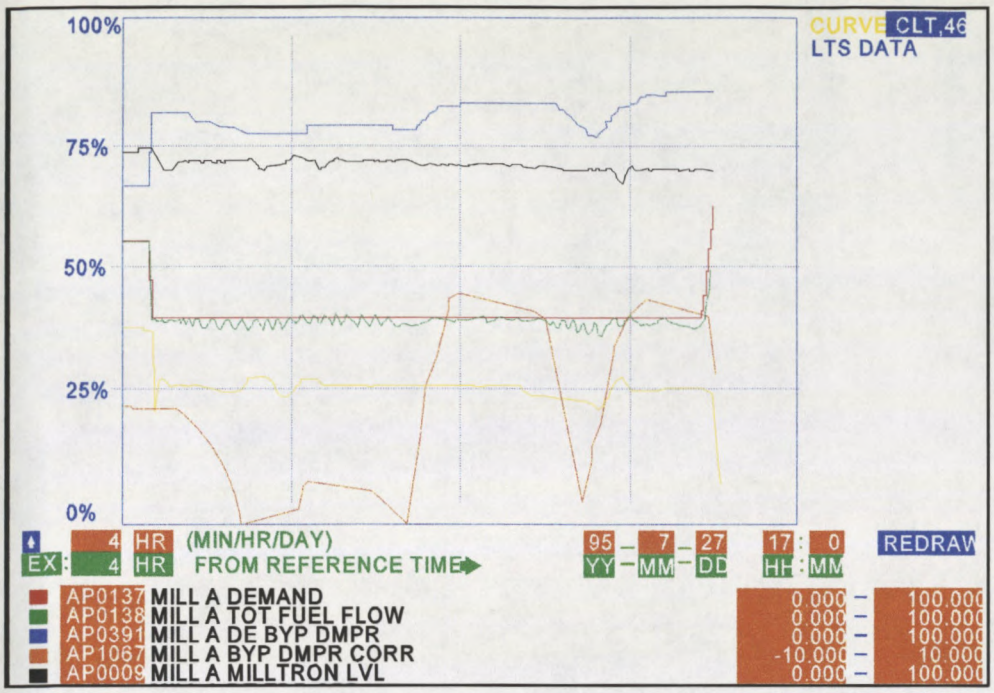

Figure 5.4.3-2 Kendal data showing the oscillations in total fuel flow

5.4.4 Effects of temperature and humidity on probe current

The relative humidity proved to be extremely low, in the order of 5 %. This value of relative humidity is lower than any value at which tests were done on the flow rig. Further it was constant from around that value, varying by less than 2 % relative humidity from one pipe to the next. The temperature was also relatively constant at values between 85°C and 90°C.

Using the results of the relationship found in Section 3 it was found that the variance in these parameters from one pipe to the next is minimal, and their effect on the measured probe current negligible.

5.5 Kendal power station tests - summary

The Kendal power station tests show the following:

(I) The iso-kinetic and electrostatic results are not conclusive.

(ii) The comparison between the electrostatic results and the Kendal computer results show the same oscillations. This is difficult to explain since the calculated recovery rate supports the accuracy of the iso-kinetic sampling and

the matching oscillations (mill load and electrostatic) support the accuracy of the electrostatic technique, and yet the comparison between the iso-kinetic and electrostatic results are inconclusive.

(iii) Even though tests were not done on the flow rig at the low relative humidities measured in the Kendal pipes the changes in temperature and relative humidity from one pipe to the next are small enough that their effect on probe current can be ignored.

6 HENDRINA POWER STATION STEP AND REPEATABILITY TESTS - 1995

A second short test series was done at Hendrina in 1995 (the results from a first test series done at Hendrina in 1995 are used in Section 7 for a statistical analysis) All the tests done so far in this study have been carried out in an attempt to determine with what accuracy the mass flow rate can be measured using an electrostatic technique. During all these tests, data was stored to disk immediately and no analysis was carried out, on line, and changes which occurred in the process were not detected until later data analysis. There was no real time representation of the data.

This is obviously not practical for an instrument which is measuring a process on-line and in real time. Hence the data acquisition and analysis technique were changed to provide a practical instrument which was tested at Hendrina Power Station. While testing the new presentation, tests were done to determine 2 things:

(I) The effect of step changes in the mill load on the electrostatic measurement.
(ii) The repeatability of the electrostatic measurement technique.

During these tests no iso-kinetic sampling was done so it is impossible to compare the electrostatic mass flow rate to any other mass flow rate. However the feeder speed is known and since the flow rate must increase with feeder speed there is some indication of what the mass flow rate should be.

6.1 Equipment setup

The equipment setup used is similar to that used in the first set of tests done at Hendrina in 1994. The collapsible grating probes used in 1994 are replaced by the permanent probes developed in 1995, shown in Figure 2.4-3 and only the four pipes after the split were monitored. i.e. data from 8 probes is recorded.

6.2 Data processing procedure

The data processing procedure for Hendrina in 1995 was substantially different from those which had been used previously. The previous method had the disadvantages that the data was being recorded at high frequency, thus requiring excessive disk space or the use of a DAT drive, and the recorded data could not be observed during the acquisition. This led to unknowingly losing data and some tests having to be repeated.

In the case of the 1995 Hendrina tests the data acquisition was done using the same National Instruments card but the data processing was done immediately and the resultant values represented graphically on the computer screen in the form of both bar graphs and trend graphs. This served two purposes:

(I) It highlighted problems with the data acquisition equipment and obvious flow problems, such as a blocked pipe, immediately.

(ii) The graphic format display of the data is more readily understood by the unit operator.

The displayed data is recorded simultaneously to computer disc for later analysis using a spreadsheet package. Since this data has already been processed it does not require the excessive disk space which was previously necessary.

Figure 6.2-1 shows the front panel and the application diagram of the Labview application used for this test series. The front panel is what the user sees on the computer monitor and consists of various graphic displays. The actual program (6.2-1c) is where the processing takes place. i.e. the data acquisition, the cross correlation (for velocity measurement), the calculations of mass flow rate and velocity are carried out by the program shown.

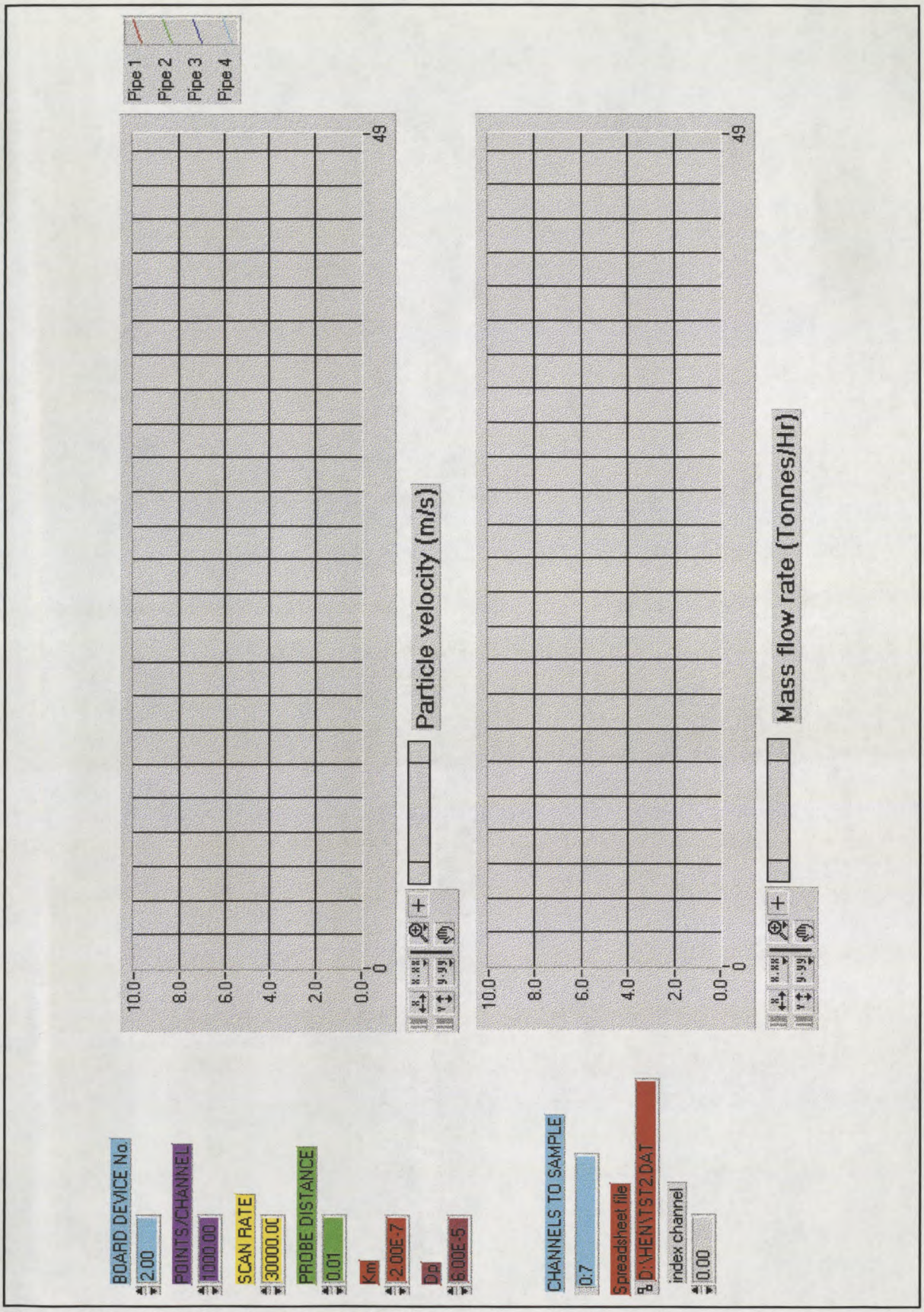

Figure 6.2-1a Labview front panel showing trend graphs of mass flow and velocity

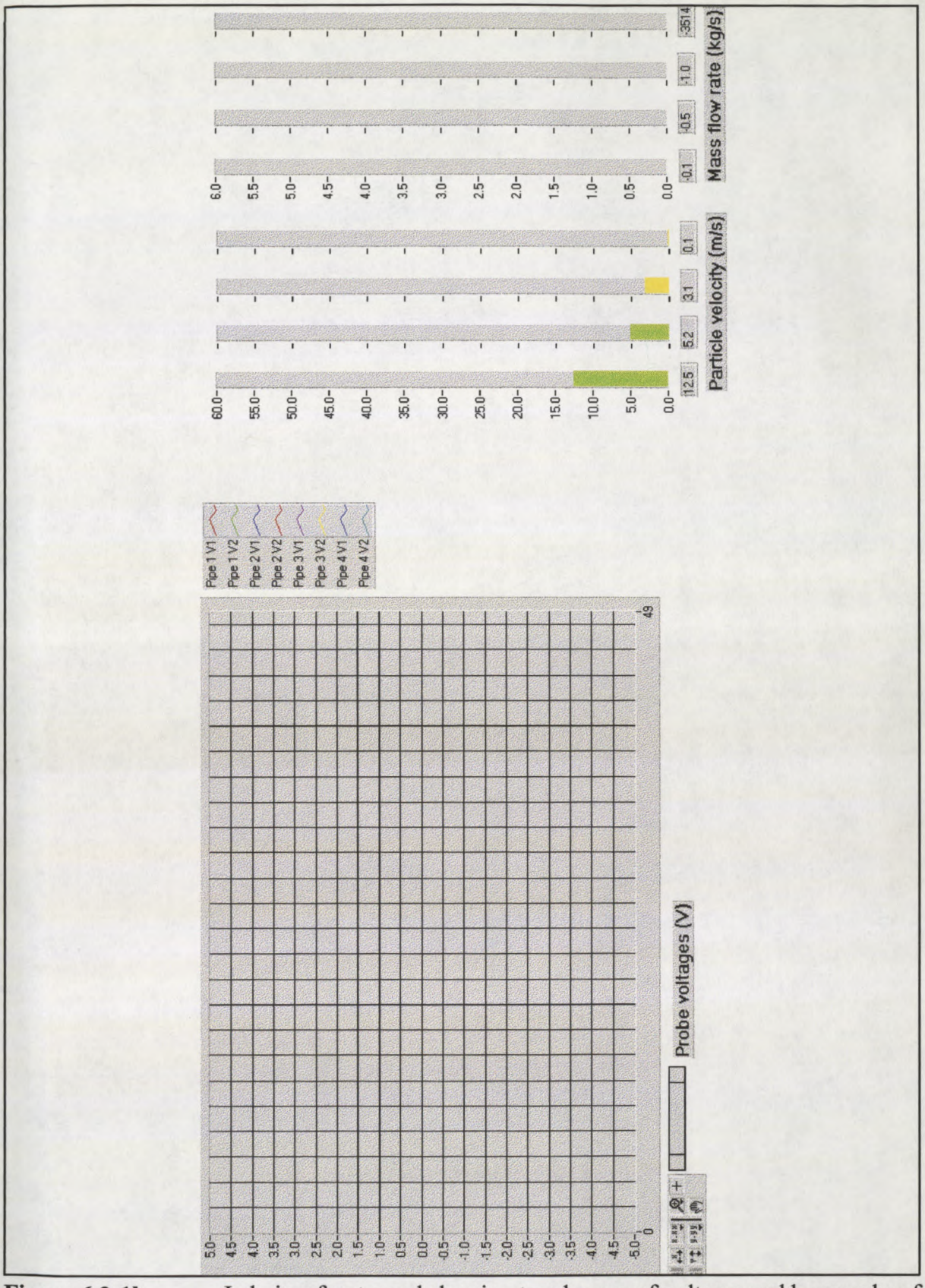

Figure 6.2-1b Labview front panel showing trend curve of voltages and bar graphs of mass flow and velocity

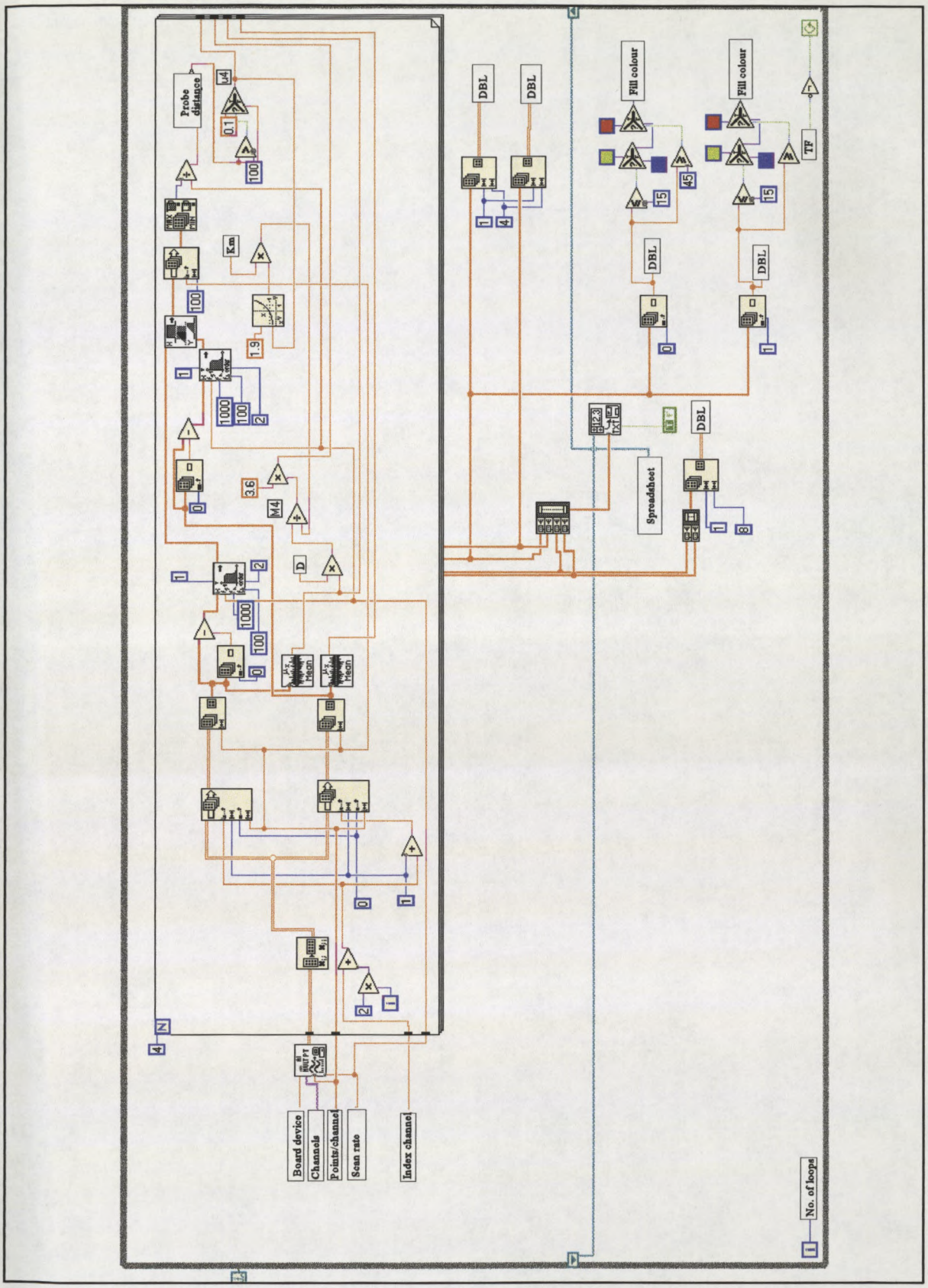

Figure 6.2-1c Labview graphical program for data processing and display for Hendrina Power Station

6.3 Test procedure

The test procedure for the two tests was straightforward.

6.3.1 Mill step test procedure

For the mill step test the mill was placed on manual control at each mill load and allowed to reach a steady state whereafter data acquisition was started and continued for 10 minutes. The mill load started at 50 % and went up in 10 % increments to 80 %. Ideally, in order to see the effect of these step changes across the entire mill load conditions, it would have been better to start lower and go higher but the mill trip conditions did not allow for this.

6.3.2 Mill repeatability test procedure

For the repeatability test the mill was run at steady load for three different mill loads on two consecutive days and the results recorded.

6.4 Test results

6.4.1 Step test

Figures 6.4.1-1 and 6.4.1-2 show the results of the calculated mass flow rate during this test. This flow rate is calculated on-line by the Labview application using Equation 13, a fixed particle size of 60μm and a value for β of 1.9. This fixed particle size will introduce an error the details of which are discussed in Section 7 (pp 70).

Figure 6.4.1-1 shows the results for each of the four pipes. The increase in each pipe is steady as the load increases. The distribution appears to be uneven with the maximum flow in pipe 1 and the minimum in pipe 3.

Figure 6.4.1-2 shows the total fuel flow and the relationship appears to be linear through the first three steps and then drops off. It is possible that the probe becomes saturated at some point and no further electron transfer can take place. This phenomenon can also be seen in Figures 5.4-1 and 5.4-2 where the Kendal results are illustrated and in Figure 3.5.3-1 where the flow rig results are illustrated. In the case of Kendal the probe current change (proportional to mass flow rate) from 40 % to 55

% mill load is greater than that from 55 % to 70 % mill load. It may be necessary to apply further research into the best possible probe configuration in order to overcome the problem.

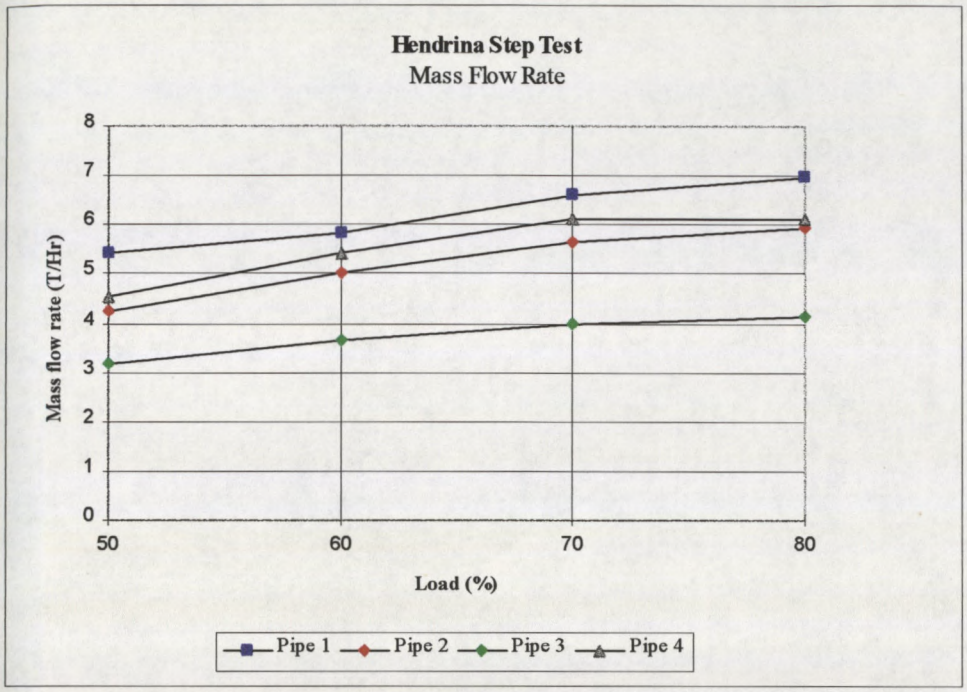

Figure 6.4.1-1 Hendrina step test-individual pipe results.

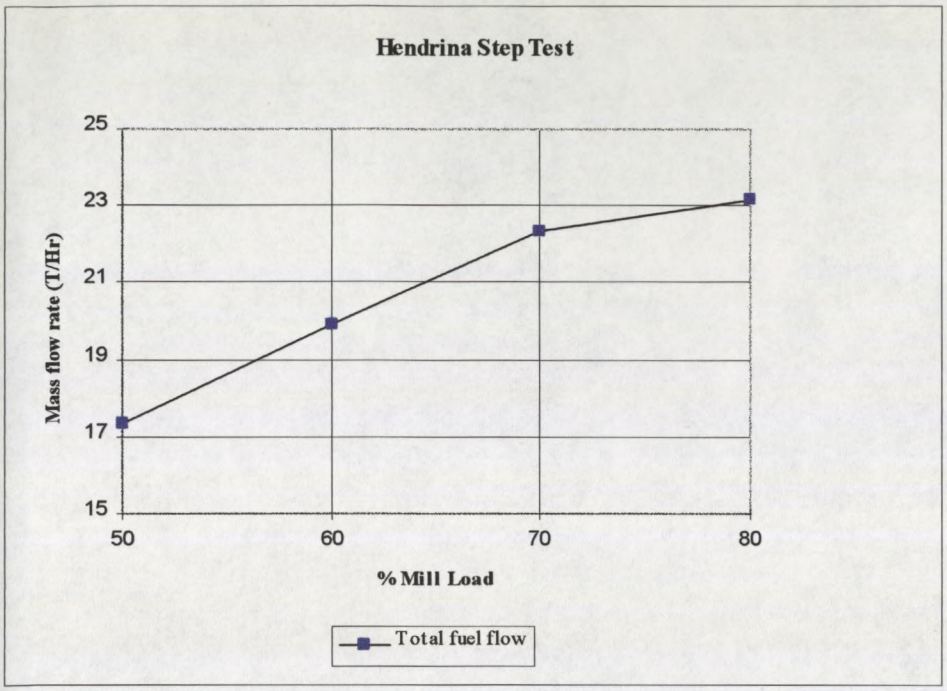

Figure 6.4.1-2 Hendrina step test - total fuel flow

6.4.2 System repeatability

The total mass flow at each load on the two days is shown in Figure 6.4.2-1.

The graph shows that the change in each case from day 1 to day 2 is less than 1 Tonne/Hour. This is less than 7 % in the case of the 50 % load and 5 % in the cases of the 70 % and 85 % loads.

The errors can be caused by changes in particle size which would effect the reading since a fixed particle size is used. This would probably be a very small change though because the mill conditions would not change dramatically overnight. The amount of wear on the mill components is negligible for that period of time.

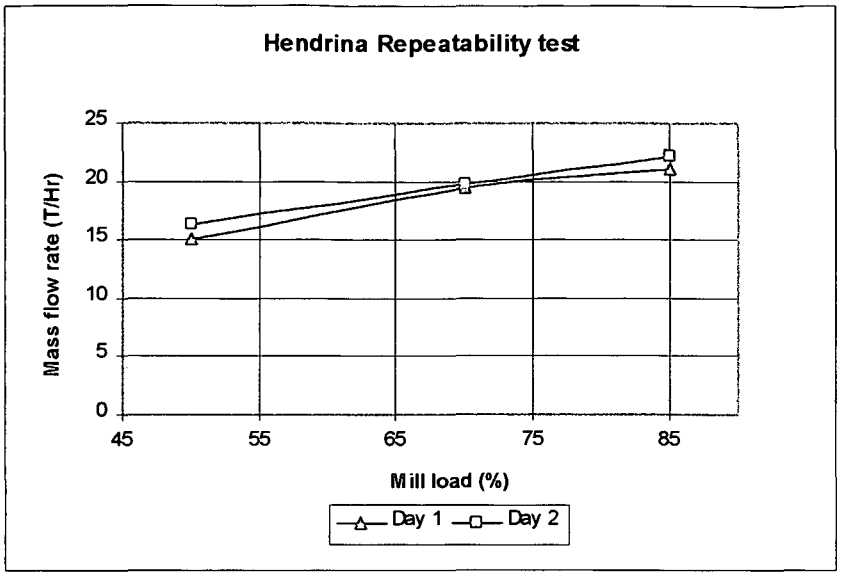

Figure 6.4.2-1 Hendrina repeatability test

It may be necessary that repeatability be tested over a much longer period of time in order to get a realistic idea of the changes in electrostatically measured flow rate for set mill conditions over the long time period.

6.5 Hendrina Power Station 1995 - summary

The tests showed that the relationship between mill load and mass flow rate calculated using the electrostatic technique is linear up to a point. The apparent non-linearity, at high mill load conditions, may be caused by probe saturation.

The system repeatability is within 7% and improves at high load conditions.

7 STATISTICAL ANALYSIS ON THE MEASUREMENT ACCURACY OF AN ELECTROSTATIC FLOW RATE DEVICE

The tests done at Kendal Power Station in 1995 showed that the effects of changing temperature and relative humidity can be ignored. Hence the remaining factor which cannot be measured on-line in real time, and which has the biggest effect on probe current, is particle size. The particle size will change with load, mill characteristic and coal quality and the value used in Equation 13 to calculate mass flow rate cannot be changed. An average value for particle size must be used to calculate the mass flow rate. This average value is generally found by extracting a PF sample using iso-kinetic sampling, a process which has already been proven to have doubtful accuracy.

Tests were done at Hendrina in 1995 on a single mill at loads of 50 %, 70 % and 85 %. This was done by determining the mass flow rate, both electrostatically, and by using iso-kinetic sampling. The iso-kinetic sampling results are summarised in the tables shown in Appendix F. These tables show the average particle size of the extracted sample and the mass flow rate for each of the four pipes calculated using Equation 23. The results from these tests, and those done at Hendrina in 1994, are used for a statistical analysis to determine the error incurred in electrostatic mass flow rate measurement, caused by the inability to measure particle size on-line. This analysis was done with the help of the statistics section at T-R-I.

It is important to note that although the changing particle size is probably the major contributing factor which can cause electrostatic measurement error, it is not the only factor which will lead to measurement errors. As mentioned above temperature and relative humidity may have an effect though it is probably negligible. Changing particle shape and coal quality may also be factors, although the chances of these parameters changing over a short term period are low. Changing mill characteristics, which may lead to changes in particle shape, will only occur over a long period of time and the coal quality will only change through different coal being mined.

Table 7-1 gives a summary of the statistical analysis results.

HENDRINA 1994				HENDRINA 1995			
LOAD		D^1	$D^{0.528}$	LOAD		D^1	$D^{0.528}$
13 T/Hr	M_{AVG}	2.55	2.55	50 %	M_{AVG}	2.56	2.61
	Std dev	0.26	0.14		Std dev	0.57	0.33
	Possible % error	10.20	5.49		Possible % error	22.27	12.64
16 T/Hr	M_{AVG}	3.54	3.53	70 %	M_{AVG}	3.52	3.60
	Std dev	0.64	0.33		Std dev	1.03	0.54
	Possible % error	18.08	9.35		Possible % error	29.26	15.00
Total	M_{AVG}	3.03	2.99	85 %	M_{AVG}	3.82	4.12
	Std dev	0.46	0.23		Std dev	1.35	0.72
	Possible % error	15.18	7.69		Possible % error	35.34	17.48
				Total	M_{AVG}	3.29	3.44
					Std dev	0.94	0.50
					Possible % error	28.57	14.54

Table 7-1: Statistical analysis summary for particle size error

Following is an explanation of Table 7-1.

7.1 Statistical analysis procedure

The example shown below details the method of calculation of mass flow rate and standard deviation given in Table 7-1 for the test done at Hendrina in 1994 at an expected mass flow rate of 13 T/Hr and using a value for δ of 1. The values for this test as given in Table 7-1 should be:

$M_{avg} = 2.55$
Std dev = 0.26

The figures are derived as follows:

There are three tests done and four PF pipes are sampled during each test. Hence there are a total of 12 samples. The average particle size of each sample is found using a Mastersizer. The assumption is then made that these 12 particle sizes represent the full range of particle sizes that are possible for the mill under test. Each of these values is used to calculate a mass flow rate for each pipe using Equation 24. Hence 12 flow rates are calculated for each pipe.

$$M_{avg} = I \frac{\overline{D_p}^{\delta}}{K_m \overline{u}^{\beta}} \qquad (24)$$

where

M_{avg}	is the mass flow rate.
I	is the probe current.
$\overline{D}_p$	is the average particle size.
δ	is the particle size index.
$\overline{u}$	is the average air velocity.
β	is the material constant.
K_m	is the probe constant.

Equation (24) is similar to Equation (13) given in Section 2. There is a difference however. Equation (13) has the average particle size raised to a power of one. The flow rig tests done in 1994 showed that this exponent (δ) was not 1 and when a curve was fitted to the particle size/probe current curve shown in Figure 3.5.4-1 it was found that the exponent should be 0.528. All values shown in Table 7-1 are calculated for exponents of 1 and 0.528. Hence the two columns labelled "D^1" and "$D^{0.528}$".

Values for K_m and β are found by using the chi squared test. The chi squared test is used to compare observed and expected values. In this case different values of K_m and β are used to calculate the mass flow rate and the resultant mass flow rate is compared to the iso-kinetic mass flow rate. The values of K_m and β used in the final analysis are those which gave the smallest error when applying the chi squared test. Table 7-2 shows the values of K_m and β used for each test.

	1994		1995	
	K_m	β	K_m	β
D^1	2.77E-6	1.159	5.60E-8	2.177
$D^{0.528}$	4.42E-4	1.028	5.10E-7	2.850

Table 7-2: K_m and β values found using the chi-squared test.

The average and first standard deviation (67%) of these 12 values are calculated for each pipe. The standard deviation is calculated assuming a normal distribution curve, an example of which is shown in Figure 7-1. Each of the flow rates falls into a "bin". The bins are 0.3 T/Hr apart.

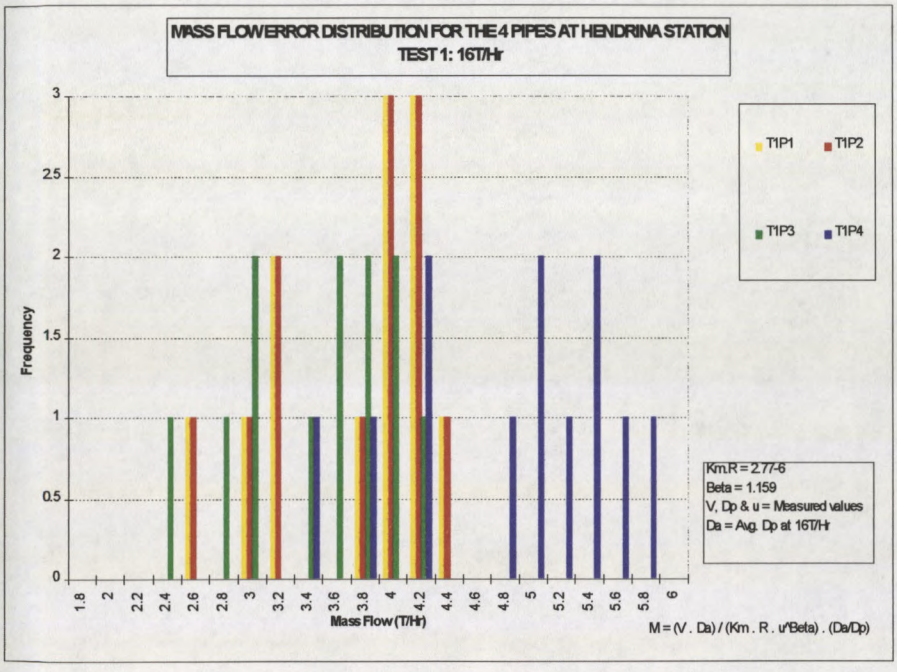

Figure 7-1: Distribution curve example

Table 7-3 shows the values for the first of the three tests done at 13 T/Hr flow rate. The other two tests are similar. The mass flow rate and standard deviation are shown in red. The corresponding mass flow rates and standard deviation are also shown in red in Table 7-4. Table 7-4 summarises the results for all three tests and shows the average mass flow rate and standard deviation for the test done at 13 T/Hr. These two values should and do correspond to the values given above.

PIPE	VOLT (V)	VELOC (u)	Dp_mean	MFR T/Hr	MFR avg	Std Dev
1	1.3	22.5	51.39	2.353666	2.397024	0.246181
	1.3	22.5	52.13	2.387559		
	1.3	22.5	45.95	2.104514		
	1.3	22.5	53.93	2.469999		
	1.3	22.5	62.86	2.878993		
	1.3	22.5	52.26	2.393513		
	1.3	22.5	48.54	2.223136		
	1.3	22.5	49.67	2.27489		
	1.3	22.5	58.9	2.697625		
	1.3	22.5	58.59	2.683427		
	1.3	22.5	46.6	2.134284		
	1.3	22.5	47.22	2.16268		
2	1.2	22	51.39	2.229947	2.271025	0.233240
	1.2	22	52.13	2.262057		
	1.2	22	45.95	1.993891		
	1.2	22	53.93	2.340164		
	1.2	22	62.86	2.72766		
	1.2	22	52.26	2.267698		
	1.2	22	48.54	2.106278		
	1.2	22	49.67	2.155311		
	1.2	22	58.9	2.555825		
	1.2	22	58.59	2.542373		
	1.2	22	46.6	2.022096		
	1.2	22	47.22	2.048999		
3	1.2	23	51.39	2.11797	2.156986	0.221528
	1.2	23	52.13	2.148468		
	1.2	23	45.95	1.893768		
	1.2	23	53.93	2.222653		
	1.2	23	62.86	2.590691		
	1.2	23	52.26	2.153826		
	1.2	23	48.54	2.000511		
	1.2	23	49.67	2.047082		
	1.2	23	58.9	2.427484		
	1.2	23	58.59	2.414708		
	1.2	23	46.6	1.920556		
	1.2	23	47.22	1.946109		
4	1.7	21.5	51.39	3.244396	3.304162	0.339346
	1.7	21.5	52.13	3.291114		
	1.7	21.5	45.95	2.900953		
	1.7	21.5	53.93	3.404753		
	1.7	21.5	62.86	3.968529		
	1.7	21.5	52.26	3.299321		
	1.7	21.5	48.54	3.064467		
	1.7	21.5	49.67	3.135807		
	1.7	21.5	58.9	3.718523		

	1.7	21.5	58.59	3.698952
	1.7	21.5	46.6	2.941990
	1.7	21.5	47.22	2.981132

Table 7-3: Mass flow rates calculated for test 1 at 13 T/Hr for each particle size and each pipe.

Pipe	Test	MFR	Std Dev	Average MFR (T/Hr)	Average Std Dev
1	1	2.397024	0.246181	**2.550414**	**0.261934**
1	2	2.505857	0.257358		
1	3	2.361219	0.242504		
2	1	2.271025	0.233240		
2	2	2.454533	0.252087		
2	3	2.451713	0.251797		
3	1	2.156986	0.221528		
3	2	2.08971	0.214619		
3	3	2.173077	0.223181		
4	1	3.304162	0.339346		
4	2	3.155829	0.324112		
4	3	3.28383	0.337258		
		2.550414	0.261934		

Table 7-4: Summary of mass flow rates and standard deviations calculated for all three tests done at a flow rate of 13 T/Hr.

The results given in Table 7-1 show the following:

(I) There is a 67 % chance that the maximum error will be 35.34 % (85 % load - Hendrina 1995)

(ii) The error is reduced by half when a value for δ of 0.528 is used. This would support the findings of the flow rig tests (1994) that the exponent of the average particle is in fact not one.

These results are promising. Although the ultimate solution to the particle size measurement problem is to find an on-line measurement device (work is being done at T-R-I to do so) it seems unlikely that such a device will exist in the near future. The figures shown in Table 7-1 also give possible % error and it is likely that the actual errors will not be as high as those reflected.

There are also methods which can be used to minimise the particle size error further. If each pipe was sampled on a regular basis a particle size trend could be obtained for

each pipe and a different particle size could be used to calculate the mass flow rate in each pipe instead of one common one. This is not unreasonable because a mill normally runs at fairly consistent loads. At this normal load the particle size may differ from pipe to pipe, but it is unlikely to change on an ongoing basis in the same pipe. i.e. if the particle size in pipe 4 is 60 microns it is not going to jump quickly to 80 microns and then down to 40 microns. It should remain fairly constant.

8 CONCLUSION

In conclusion the following facts have been established.

Tests on the flow rig showed that such things as humidity have a major effect on the probe current developed when solid particles strike an insulated object. More specifically the following facts emerged from this investigation:

(I) Probe current and humidity share an exponential relationship. At lower temperatures the effect of changing humidity is enhanced.

(ii) The particle velocity has a linear relationship to probe current although this result may be specific to the material used in these rig tests. In this case the material is Aluminium Oxide and the linear relationship suggests that the value of β is 1 in Equation (13).

(iii) Probe current and mass flow rate share a logarithmic relationship. The probe current increases as the mass flow rate increases. However there may also be a certain amount of probe current saturation which would definitely effect this result should that be the case.

(iv) Probe current and particle size share an exponential relationship showing that the exponent of the average particle size as used in Equation (13) is not one and in fact when a curve is fitted the value of the exponent is found to be 0.528.

Tests done at the two power stations showed that iso-kinetic sampling is not an accurate means of two-phase flow rate measurement. It has consistently proved inaccurate. However at this stage it remains the only method of flow rate measurement to which comparisons can be made with electrostatic flow rate measurements.

The Kendal tests show there is a comparison between the electrostatic probe results and the Kendal computer data. The two results clearly show the oscillations. The problem is that the comparison is between total fuel flow and that of an individual pipe. The total fuel flow signal cannot be used to determine the PF distribution in each pipe. Hence the continued reliance on PF sampling.

The step test done at Hendrina in 1995 shows the relationship between mill load and mass flow rate measured electrostatically to be a linear one up to a certain point. Thereafter the relationship changes and this may be due to probe saturation.

The statistical analysis carried out on the Hendrina results to determine the possible errors induced through the inability to continually monitor the particle size showed that there is a 67% chance that the error will be less than 29% using an exponent for particle size of one in Equation (13) and less than 15% when using a value of 0.58 for the exponent. This result supports the findings of the rig tests that the exponent of the particle size is not unity.

The humidity does have a major effect as shown by the test rig results. The effect of humidity and temperature on the station can possibly be ignored because. Measurement of both temperature and humidity done during the Kendal test showed that the parameters change by very small amounts over a period of time. When the rig results are used to evaluate the changes on the station their effect is negligible.

The use of an electrostatic technique for the measurement of flow rate of two phase flow is feasible provided an accuracy of better than ±15% is not required. These limits are set by the continued inability to measure particle size on-line. This may become possible in the future. It is also conceivable that more complex analysis techniques for such data as probe current difference and probe current ratio could reduce the need for particle size measurement.

8.1 Recommendations

These test results show that there are various things that need further study. These are as follows.

(I) It must be established whether the decreasing probe current after it reaches a certain level shows the true relationship between the mass flow rate and the probe current or whether the probes are becoming saturated.

(ii) The changes in temperature and humidity in the PF pipes should be monitored more closely in order to determine if they cause changes in probe current which cannot be ignored. Temperature is not so critical since the PF pipes are actually set to operate at a specific temperature and the primary air

is pre-heated to this temperature.

(iii) It would appear that continued attempts to compare iso-kinetic sampling and electrostatic results would prove fruitless, since the PF sampling has consistently been inaccurate. The best approach may be to install the system, which exists presently, on an entire unit giving the boiler operator trend curves representing the mass flow rate in each of the pipes. It is certain that the velocity can be accurately determined and even this parameter is of use. For example if a pipe became blocked or partially blocked then the velocity would decrease and this could be immediately detected and the mill replaced by the standby mill rather than trip. This would avoid a load loss. A clear idea of distribution can also be gained by observing the calculated mass flow rate in each pipe. Again if the distribution is poor the mill could be taken out of commission and the problem found. This would avoid a situation where the boiler efficiency is decreased through poor distribution.

(iv) Analysis techniques for probe current parameters such as difference and ratio should be investigated and tested. This could be some sort of neural network or fuzzy logic technique.

9 REFERENCES

Beck, M.S., Green, R.G., Plaskowski, A.B, and Stott, A.L. (1990). Capacitance measurement applied to a pneumatic conveyor with very low solids loading. Measurement Science and Technology. Vol. 1. No. 7. pp 561-564. July.

Cheng, L., Tung, S. K. and Soo. S. L. (1970). Electrical measurement of flow rate of pulverised coal suspension. Journal of Engineering for Power. pp 135-149. April.

Cole, B. N., Baum, M. R. and Mobbs, F. R. (1969-1970). An investigation of electrostatic charging effects in high speed gas-solids pipe flows. Proc. Instn. Mech. Eng, Vol 184 Pt 3C. pp 77-83.

Coulthard, J., Byrne, B., and YoungYan. (1991). Measurement of solids mass flow rate in pneumatic conveying systems. Computech. pp 15-18. October.

de Villiers, A. (1994). Personal communication. Mechanical Technology, Eskom
T-R-I. July.

Dicken, F.J., Hoyle, B.S., Hunt, A., Huang, S.M., Ilyas, O., Lenn, C., Waterfall, R.C., Williams, R.A., Xie, C.G. and Beck, M.S. (1992). Tomographic imaging of industrial process equipment. Techniques and applications. IEEE Proceedings, Part G: Circuits, Devices and Systems. Vol. 139. No. 1. pp 72-82. February.

du Randt, C. (1994). Personal communication. Lethabo Power Station. Eskom.

Halliday, D. and Resnick, R. (1970). Fundamentals of Physics. Second edition. John Wiley and Sons, New York. pp 281-285.

Huang, S.M., Beck M.S., Xie, C.G., and Plaskowski A.B. (1989). Tomographic imaging of 2-component flow using capacitance sensors. Journal of Physics E-Scientific Instruments. Voll 22. Iss 3. pp 173-177.

Ighodaro, D.A. and Oneill, B.C. (1991). Powder flow rate measurements by means of a pulse charge injection technique. Institute of Physics Conference Series. Iss 118. pp 135-140.

Izakov, F.Y., Zubtsov, P.A., Malyshev, G.N. and Ivin, L.A. (1979). Flowmeter for loose materials. Izmeritel 'naya Tekhnika (Translation). No10. pp 50-51. October

Marantos, S. (1991). Coal flame control and monitoring technology. Eskom, report No. TRR/E/91/C014. October.

Marantos, S. (1992). Instrumentation for on-line PF flow measurement. Eskom report No. TRR/E/92/PS009.December.

Marantos, S. (1993). Reliability of an electrostatic technique for on-line PF flow measurement. Eskom report No. TRR/E/93/EL008. June.

Marantos, S. (1993). Mass flow rate measurements and the effects of particle size. Eskom report No. TRR/E/93/EL071. December.

Masuda, H., Komatsu, T., Mitsui, N. and Iinoya, K. (1976-1977). Electrification of gas-solid suspensions flowing in steel and insulating coated pipes. Journal of electrostatics. Vol. 2.pp 341-350.

Parkinson M.J. (1969). On-line measurement of mass flow and velocity of particle laden gases. Chemistry and Industry. No. 39. pp. 1362-1363.

Potgieter, I. (1994). Personal communication. Combustion Group, Eskom T-R-I. July.

Sartori, A.J. Experiments on a new method of PF flow measurement. Eskom report No. ESC 4-3-5/92C

Scott, T.A. (1995) Personal communication. NCS Resins. January.

Steyn, A.G.W., Smit, C.F., du Toit S.H.C. and Strasheim, C (1994). Modern Statistics in Practice. First Edition. J.L. van Schaik, pp 196-199.

Vetter, A.A. and Culick, F.E.C, (1987). Acoustical reonance measurement of particle loading in gas-solids flow. Journal of Engineering for Gas Turbines and Power. Vol 109. pp 331-335. July.

von Bormann, F. (1994). Personal communication. Mechanical Technology, Eskom T-R-I. July.

Xie, C.G., Stott, A.L., Huang, S.M., Plaskowski, A., and Beck, M.S. (1989). Mass flow measurement of solids using electrodynamic and capacitance transducers. J. Phys. E: Sci. Instrum. April

10 APPENDICES

Appendix A Photographic comparison of probe erosion

This appendix shows the photographs taken of the probes which were installed at Lethabo, Kendal and Hendrina power station. The appendix is referred to in the Background (Section 2, pp 6) and the Hendrina 1994 tests covered in Section 4 (pp 38).

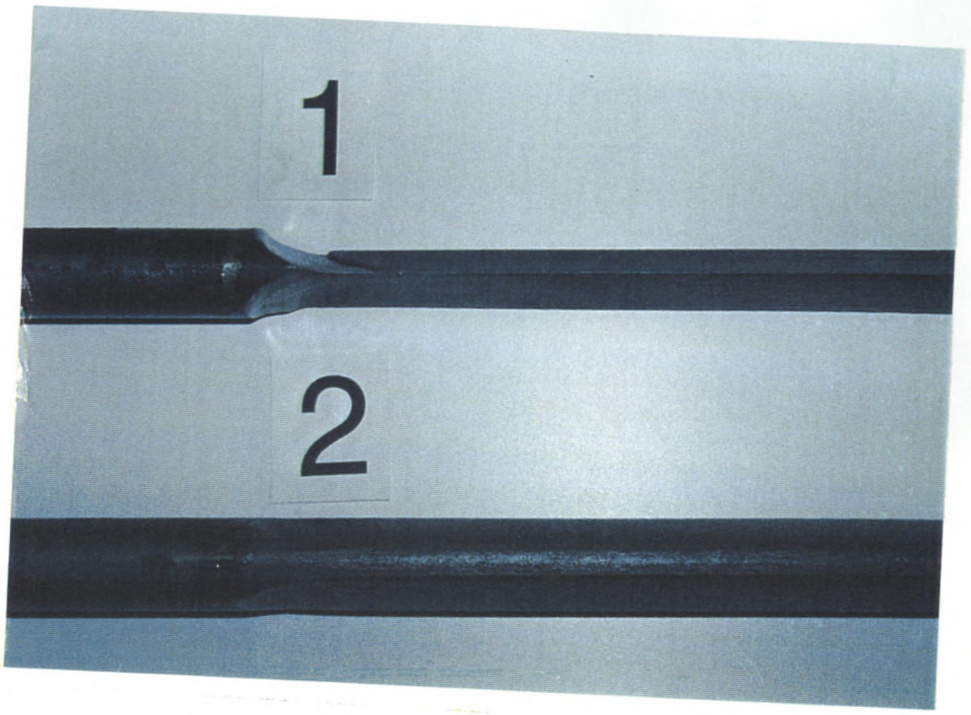

PHOTO 1

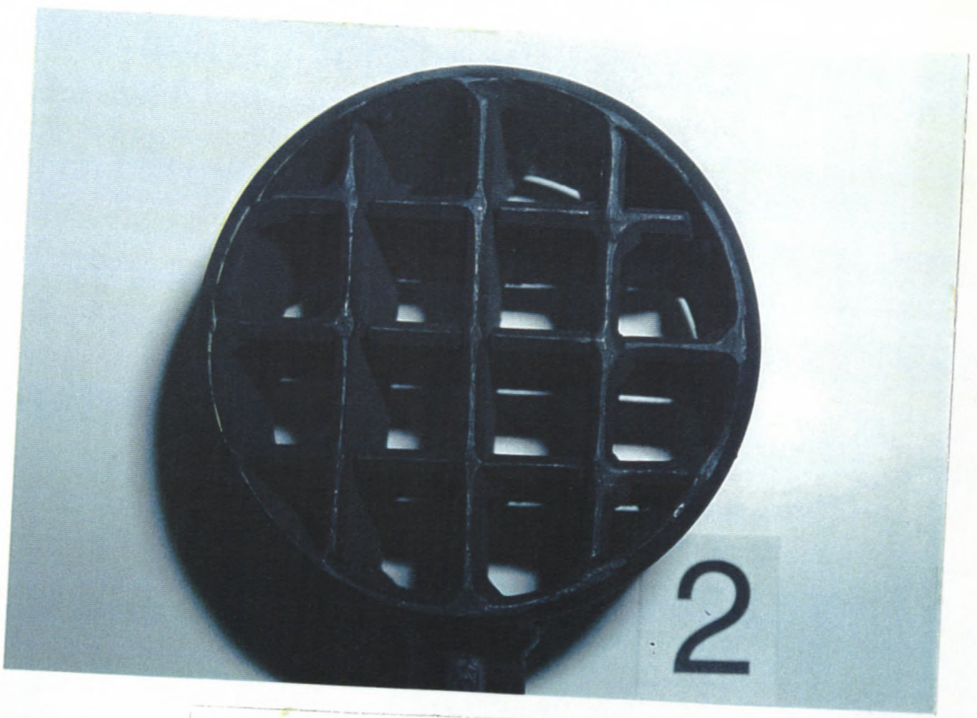

PHOTO 2

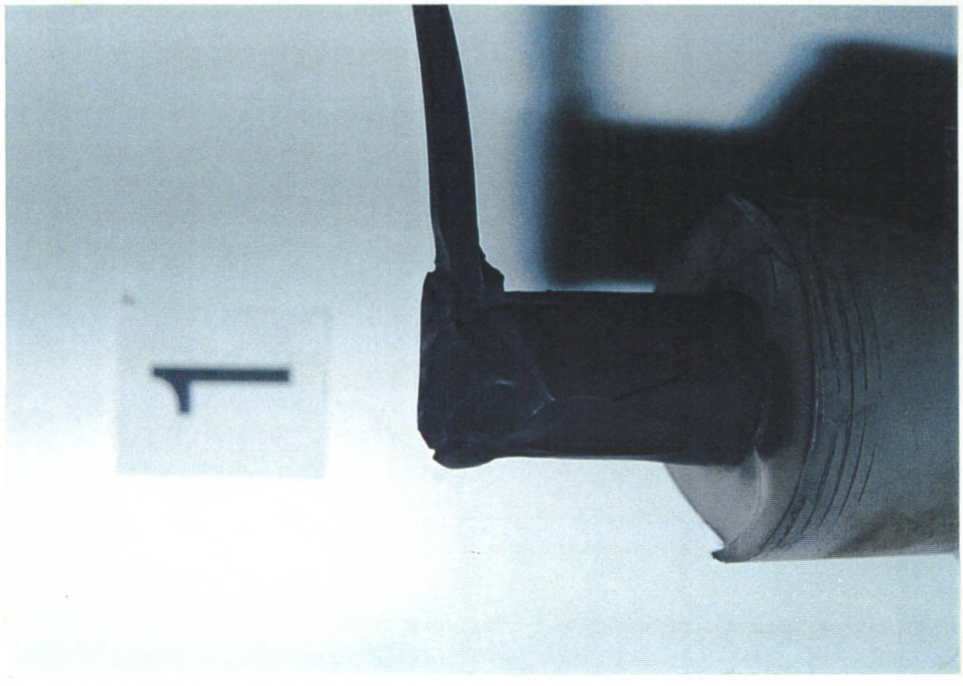

PHOTO 3

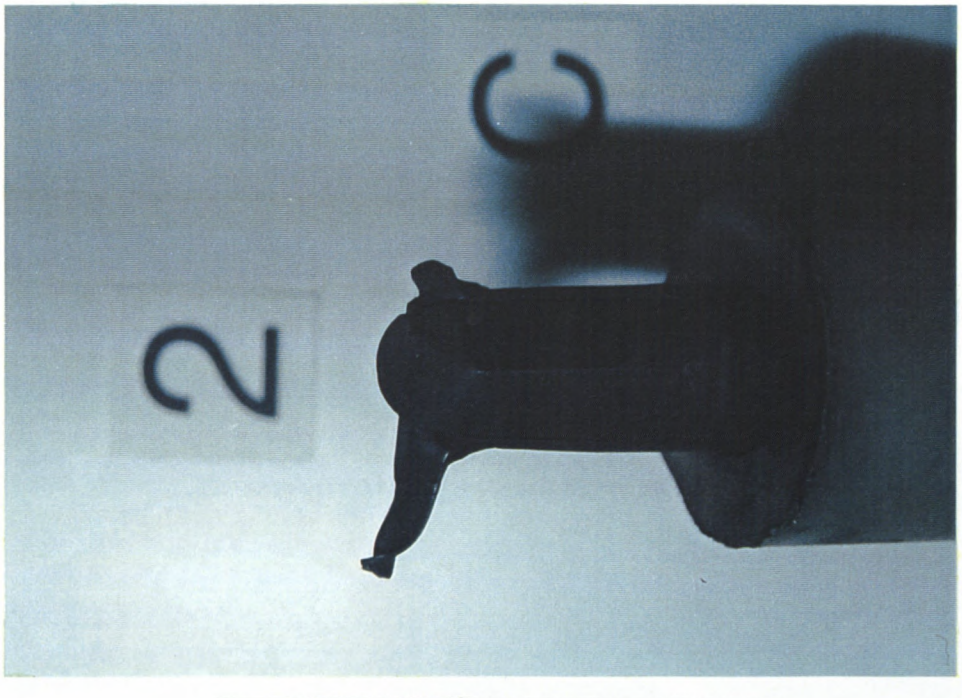

PHOTO 4

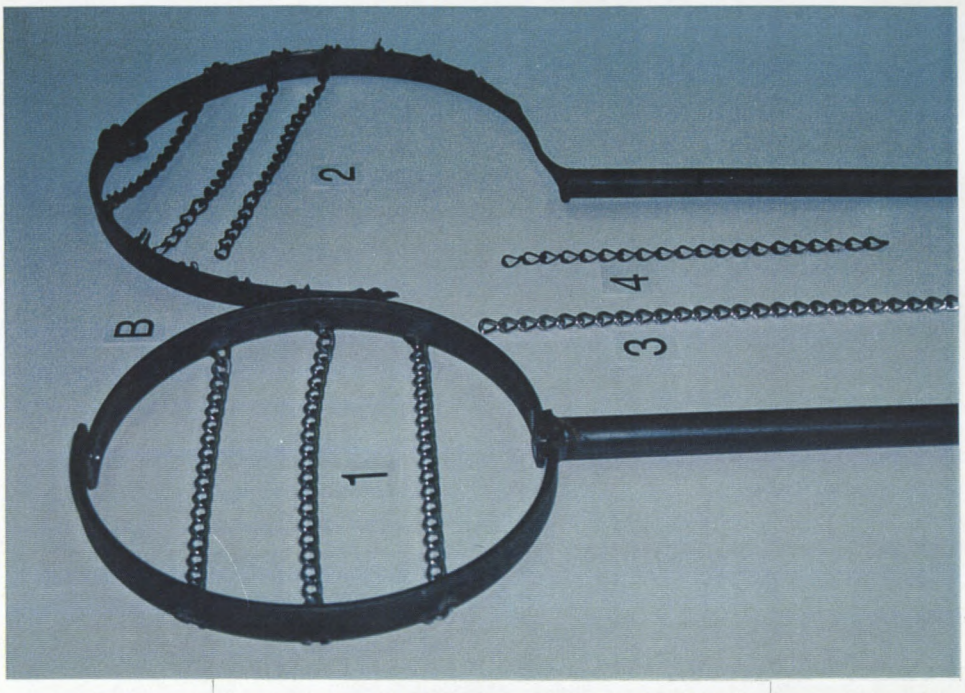

PHOTO 5

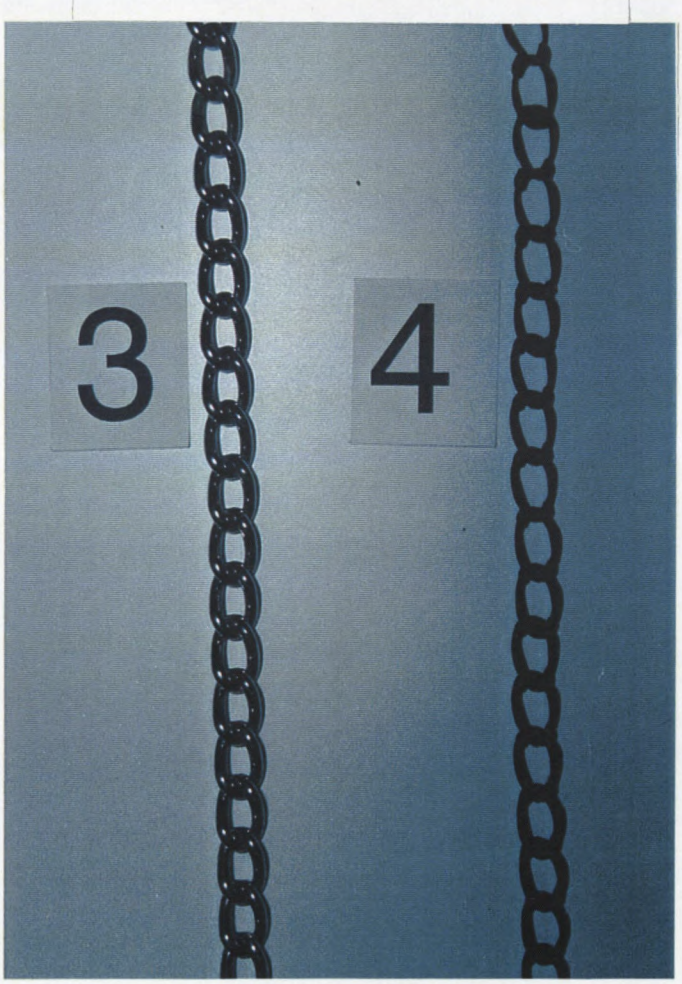

PHOTO 6

Appendix B Computer Fluid Dynamics study

This study was done by Martin van Staden and Gunter Hasse who work for the computer fluid dynamics simulation group. At the time of the study they were employed by Eskom T-R-I.

MEMORANDUM

Technology Research & Investigations

Lower Germiston Road
Cleveland Transvaal
SOUTH AFRICA

Private Bag 40175
Cleveland 2022
Telex 4-28860
Telephone (011) 629-5169
Facsimile (011) 629-5229

Tegnologie Navorsing & Ondersoeke

Laer Germistonweg
Cleveland Transvaal
SUID-AFRIKA

Privaatsak 40175
Cleveland 2022
Teleks 4-28860
Telefoon (011) 629-5169
Faksimilee (011) 629-5229

Email: MARTIN@TRI.ESKOM.CO.ZA

Company: **Eskom TRI**

Fax number: **Internal post**

Attention: **Evan Hole**

From: **Martin van Staden**

Date / Datum	**Your Ref. / U Verw.**	**Ons Verw. / Our Ref.**	**Enquiries / Navrae**
24 August 1995		OT120 M9543	Martin van Staden

Dear Evan

RESULTS OF CFD SIMULATIONS FOR THE PROPOSED ELECTROSTATIC MEASUREMENT DEVICE

The results of the CFD simulations for the proposed electrostatic measurement device (project number: 7753F284I) is included in this memorandum. Should there be any further enquiries please don't hesitate to contact us.

Regards

Martin van Staden
Computational Fluid Dynamics

Copies to circ file

CFD SIMULATION RESULTS FOR THE PROPOSED ELECTROSTATIC MEASURING DEVICE

1. Introduction

Methods to determine the massflow of pulverised coal fuel (PF) flow or ash flow in operational conditions of a Power station, is at this stage still inaccurate to be used to enhance and optimise plant performance. An electrostatic method to determine PF massflow has been investigated by Eskom TRI. In this method two sets of electrodes are placed behind each other in a PF pipe and the coal particles electrically discharge when colliding with these electrodes to induce and electrical potential difference between these electrodes. The potential difference recorded in this way can be related to the actual PF massflow. The optimal distance between the two sets of electrodes in a typical PF pipe is still to be determined for various particle sizes and fluid flow velocities. It has been proposed to investigate this problem using CFD.

2. Aim of the investigation

The behaviour of the dispersed coal/ash particles in the region of the electrostatic electrodes of the proposed PF massflow measuring device was investigated. The aim of the simulations was to be in a position to determine the optimal distance between the electrostatic electrodes for PF measurement purposes.

3. Project disclosures

It was not the scope of this investigation to determine the interparticle behaviour due to collisions of the particles in the flow field. Electrostatic charges which might existed on the particles were assumed to be neglible to have an influence on the ultimate behaviour of the particles.

4. Problem set-up

4.1 Description of the modelling domain

A two dimensional numerical mesh domain was developed for the cross sectional area on the centerline of PF pipe as indicated in Figure A. The mesh domain consisted out of 18000 fluid cells in order to be able to capture the flow behaviour in the vicinity of the electrodes. Refer to Figure 1 for the mesh domain.

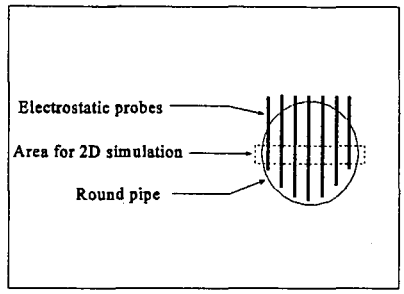

Figure A: Schematic layout of the modeling domain for the measuring device

4.2 Air flow boundary conditions

An uniform fluid velocity profile for the inlet boundary and a normal outlet boundary were applied to the numerical domain. The inlet velocities varied from 20 to 40 m/s with increments of 5 m/s. Isothermal flow field conditions were assumed to be 25 °C for the whole flow field. Steady, incompressible, turbulent and viscous flow field conditions were assumed.

4.3 Particle boundary and initial conditions

The two phase flow (particle) boundary conditions consisted of a distribution of 500 particles with sizes ranging form 5 - 400 micron which is normally found in the exhaust gasses of Eskoms Power stations. It was assumed that no heat or mass transfer took place between the particles and the air. The density of particles was set to 1710 Kg/m^3. An even distribution of particles was assumed to fill the pipe diameter for these simulations. It was also assumed that the mass of the particles relative to that of the air was small in order to have an significant effect on the air flow field behaviour and the so called: "uncoupled" modelling approach was followed.

5. Results

5.1 Velocity flow field behaviour for various pipe inlet velocities

The velocity plots for the modelling domain (Figures 2 - 6) show very high local velocities between the electrostatic electrodes for the different pipe inlet velocities. These local higher velocities (>30 ms/) are due to a decrease in cros sectional area where the mass equation must hold. Very low local velocities appeared behind the electrodes and formed a so called 'wake' of turbulent and recirculating air. This low velocity regions behind the electrodes are due to the boundary layers on the electrode which braked away as a result of a sudden increase in the local pressure. It can also be seen that the second row of electrodes are exposed to a low velocity wake from the first row of electrodes and that high velocity 'streets' formed between the electrodes in the flow direction.

5.2 Pressure flow field behaviour for various pipe inlet velocities

The pressure plots for the modelling domain (Figures 7 - 11) show an increase in the overall pressure drop from 0.57 kPa to 2 kPa for inlet velocities ranging from 20 - 40 m/s. Empirical calculations indicated that the maximum pressure drop for an inlet air velocity of 40 m/s with an electrode arrangement might be as high as 1.7 kPa ± 20% and correlates with the pressure order of magnitude of the simulations. It can also be seen that a pressure recovery took place behind the first row of electrodes and again behind the second row of electrodes. These pressure recoveries were due to the decrease in the local velocity.

5.3 Particle behaviour for various pipe inlet velocities

The behaviour of particles of various sizes for different pipe inlet velocities are shown in Figures 12 - 17.

Particles normally loose kinetic energy when colliding with a solid obstacle due to plastic and elastic deformation of the particle which is never fully recovered. The exact amount of energy lost for a specific type and mass of particle during a collision is still unknown and therefore an engineering guess had to be taken for these values. It was assumed that the particles lose 70% of their velocity energy normal and 10% of their kinetic energy tangentially with respect to the colliding surface. Figure 12 show that particles without any energy loss behave more erratic in the region of the electrodes compared to particles with an assumed energy loss (Figure 13).

Figures 13 - 17 show that smaller particles (5 - 20 micron) tended to follow the velocity stream lines while larger particles (80 - 400 micron) tended to behave in a more erratic manner. This behaviour may be explained by the small body forces and inertial forces and large drag forces on the smaller particles. The bigger particles experiences larger body and inertial forces compared to smaller particles and therefore the more erratic behaviour of the larger particles after collision with the electrodes.

Particles of all sizes which did not collide with the first row of electrodes normally did not collide with the second set of electrodes and would not have discharged. Different pipe inlet velocities did not have a significant effect on the behaviour of the various particle sizes when compared in Figures 13 and 17. It can also be seen that larger particles (160 - 400 micron) had multiple collisions against electrodes of the same electrode set.

6. Conclusions

The behaviour of particles of various sizes which were normally found in a power plant was investigated for different pipe inlet velocities. A two dimensional computational mesh domain was created with two sets of electrodes. The following tendencies in fluid flow and particles behaviour were found:

6.1 High overall pressure drop

The overall pressure drop increased from 0.57 kPa to 2 kPa for the two set electrode arrangement for an increase in inlet pipe velocities from 20 to 40 m/s. This pressure drop is very high and may affect the classifier performance when this device is installed in one of the PF pipes going to the boiler.

6.2 Influence of inlet velocity on particle behaviour

The simulation results indicated that an increase of the pipe inlet velocity did not significantly effect the overall behaviour of particles of various sizes.

6.3 Particle collisions with electrodes

Very small particles (5 micron) tended to follow the streamlines around the electrodes instead of colliding with the electrodes. Lager particles collided with the electrodes (10 - 40 micron) and multiple collisions with the same electrode set occurred for particle sizes of 80 - 400 micron. Most of the particles which did not collide with the first set of electrodes, did also not collide with the second set of electrodes.

6.4 Optimal distance between the two electrode sets

The simulation results indicated that the current distance between the two electrode sets did not influence the behaviour of particles of different sizes significantly with respect to the multiple collisions of the heavier particles with the same electrode set. Moving the electrode sets closer to each other might lower the overall pressure drop but inhibit collision of particles with the second electrode set. Moving the electrode sets farther apart would create the same pressure drop as in the current simulations because pressure recovery already took place behind the first set of electrodes. It is therefore difficult to conclude on the optimal distance between the electrode sets without further simulations.

7. Recommendations

The simulations which have been done provided information about dynamic behaviour of particles of different sizes for the two row electrode set-up. The extraction of the particle data from the electronic signals is as important as the dynamic behaviour of the particles. It is recommended that the capabilities and limitations of the signal conditioning process be known and that further CFD simulations planned in conjunction with this information.

The following recommendations on the dynamic behaviour of the particles could be made:

7.1 Staggered electrode arrangement

In order to ensure that all the particles in the domain collide with the electrodes, a staggered electrode arrangement could be considered. However the overall pressure drop will increase for such an arrangement and may have an influence on classifier behaviour if the device is installed in the PF piping system.

7.2 Effect of uneven particle distribution

The behaviour of the particles with an uneven particle distribution could be investigated to simulate the 'roping' behaviour of PF coal particles normally found in Eskoms power station plant.

7.3 Coupled modelling approach

Large mass and volume fractions of particles relative to the air in the piping could disturb the air flow patterns and the ultimate behaviour of the particles. A coupled modelling approach is recommended if such a situation is expected.

7.4 Calibration of electrodes

It might be possible to calibrate the electronic signals to compensate for the particles which did not collide with the electrodes. If such a calibration is possible it might be worthwhile to investigate the possibility to reduce the number of electrodes and also reduce the total pressure drop across the device. These investigations could be carried out for an uneven distribution of particles to ensure favrouble dynamic behaviour of the particles and adequate signal conditioning.

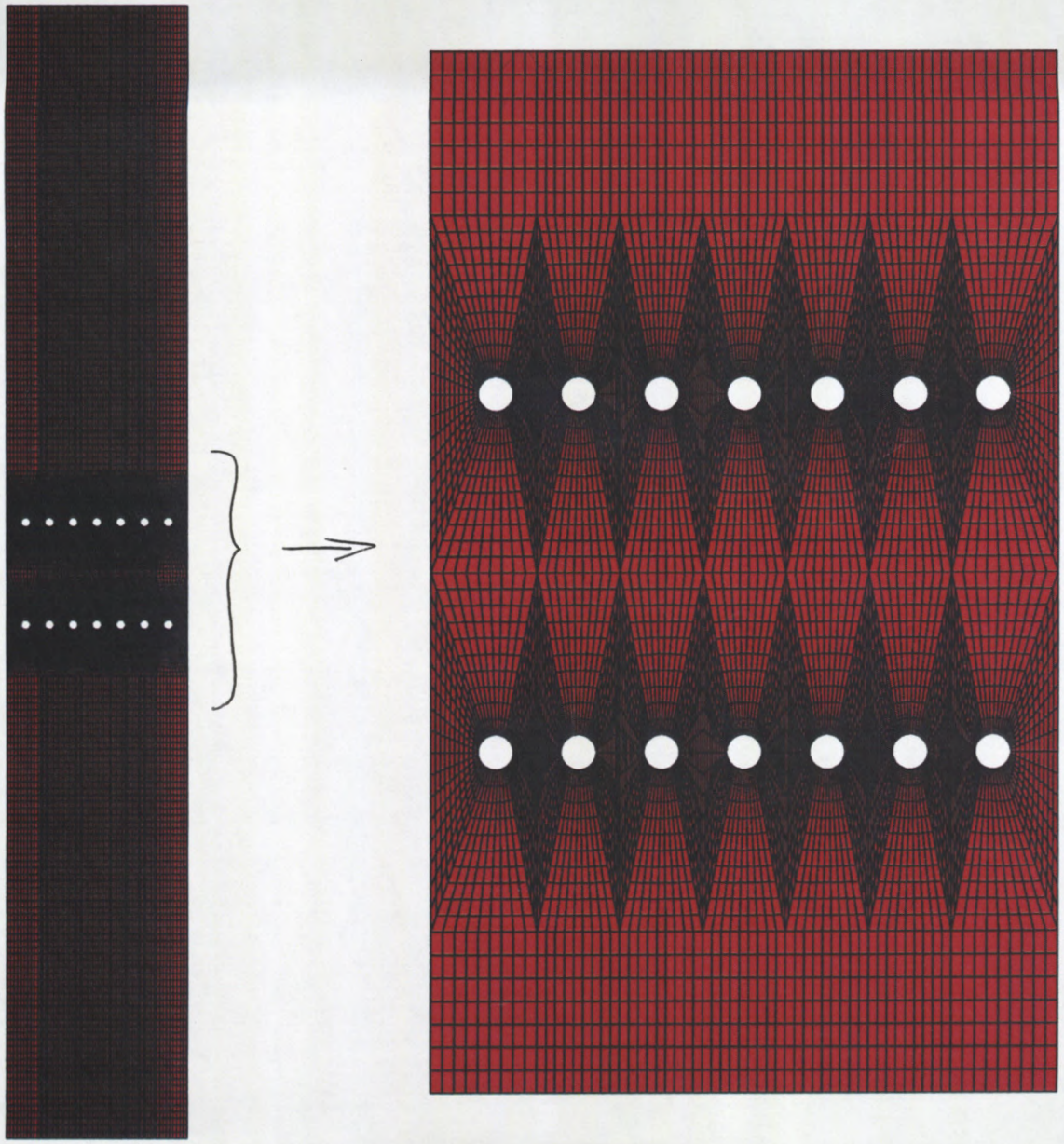

GEOMETRY PLOT FOR ELECTROSTATIC MEASURING DEVICE
two sets of seven electrodes with diameter = 20mm spaced 200mm apart

Figure: 1

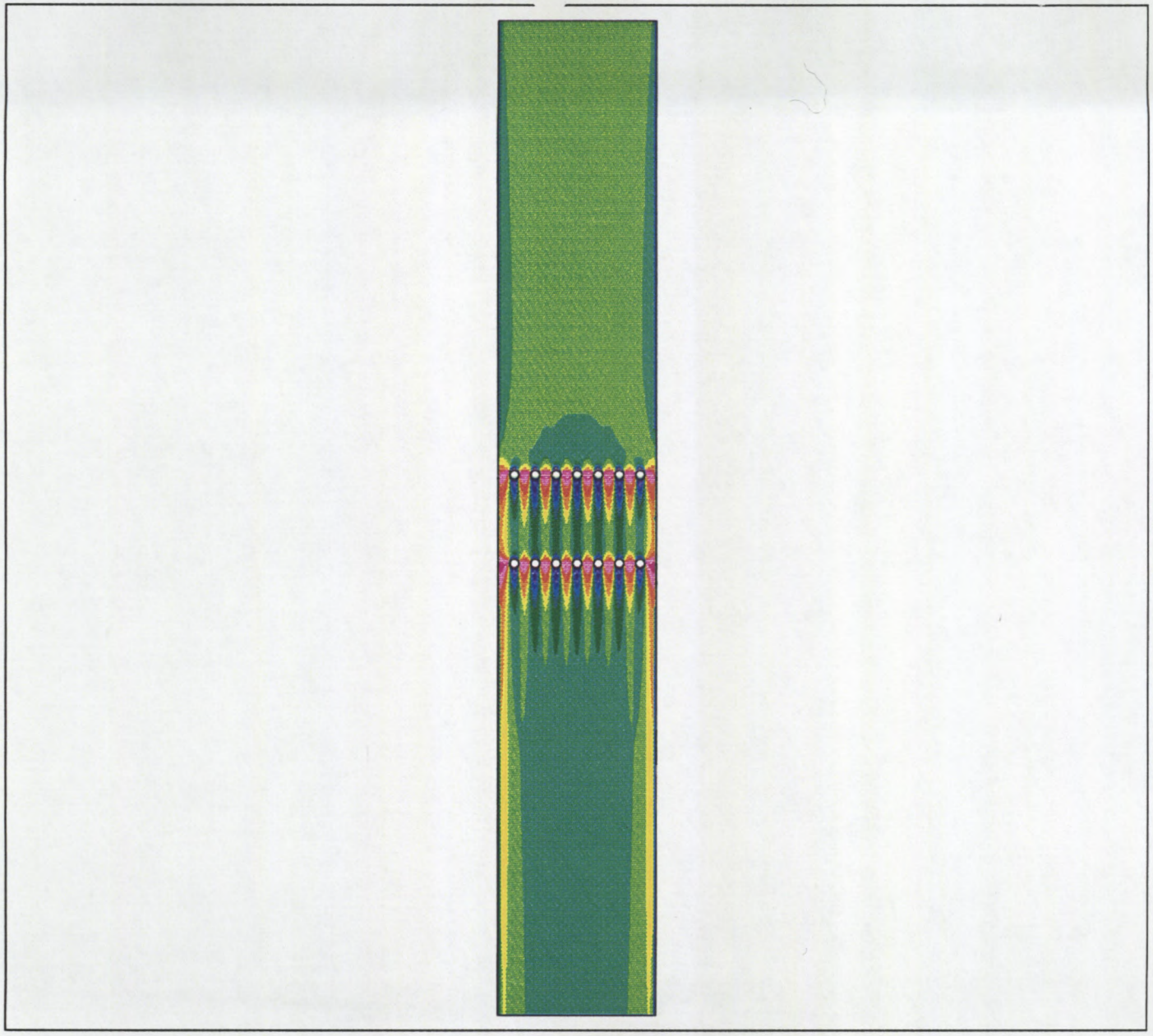

FLOW FIELD BEHAVIOUR FOR FLUID VELOCITY = 20 m/s

Figure: 2

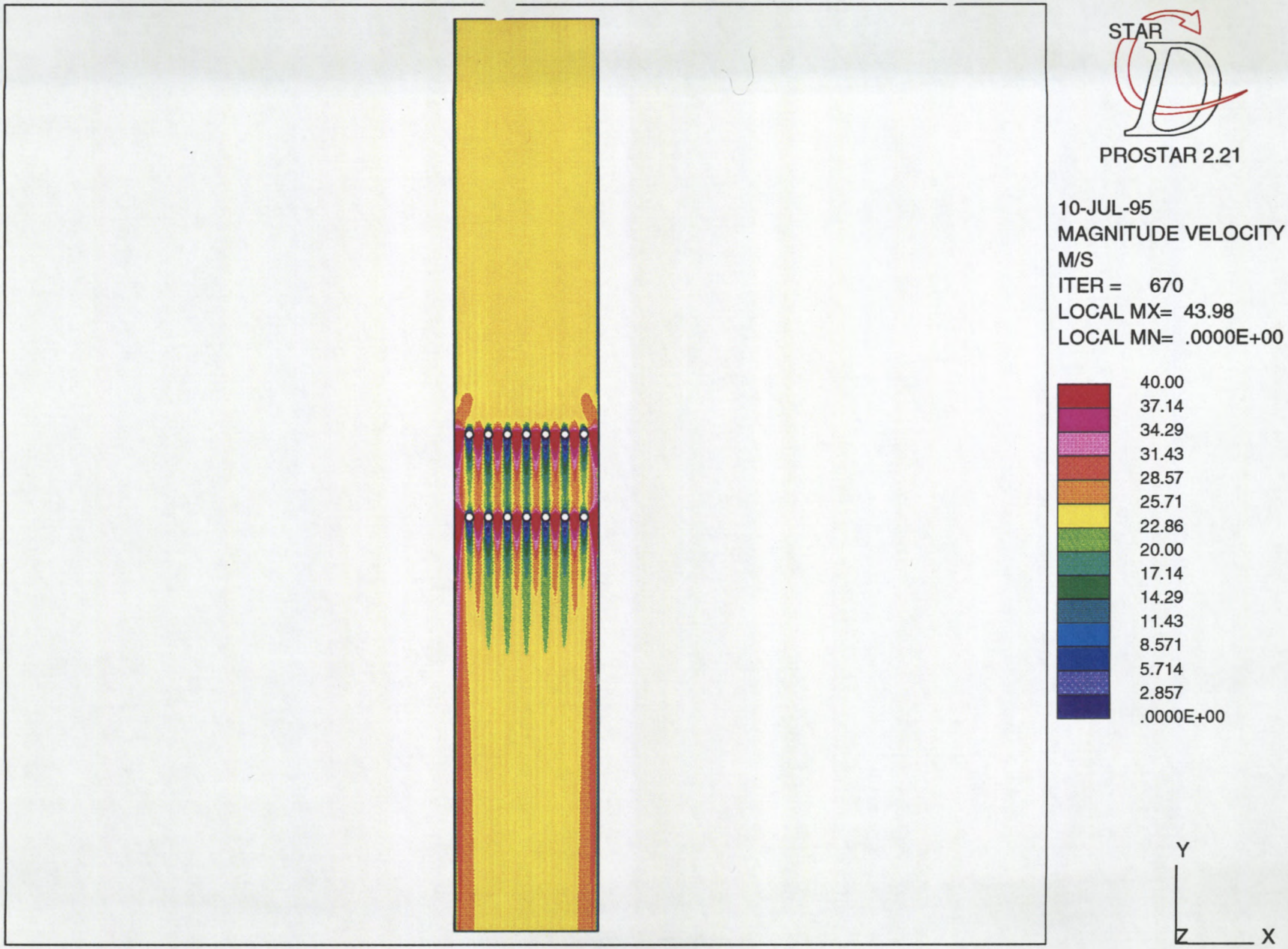

FLOW FIELD BEHAVIOUR FOR FLUID VELOCITY = 25 m/s

Figure: 3

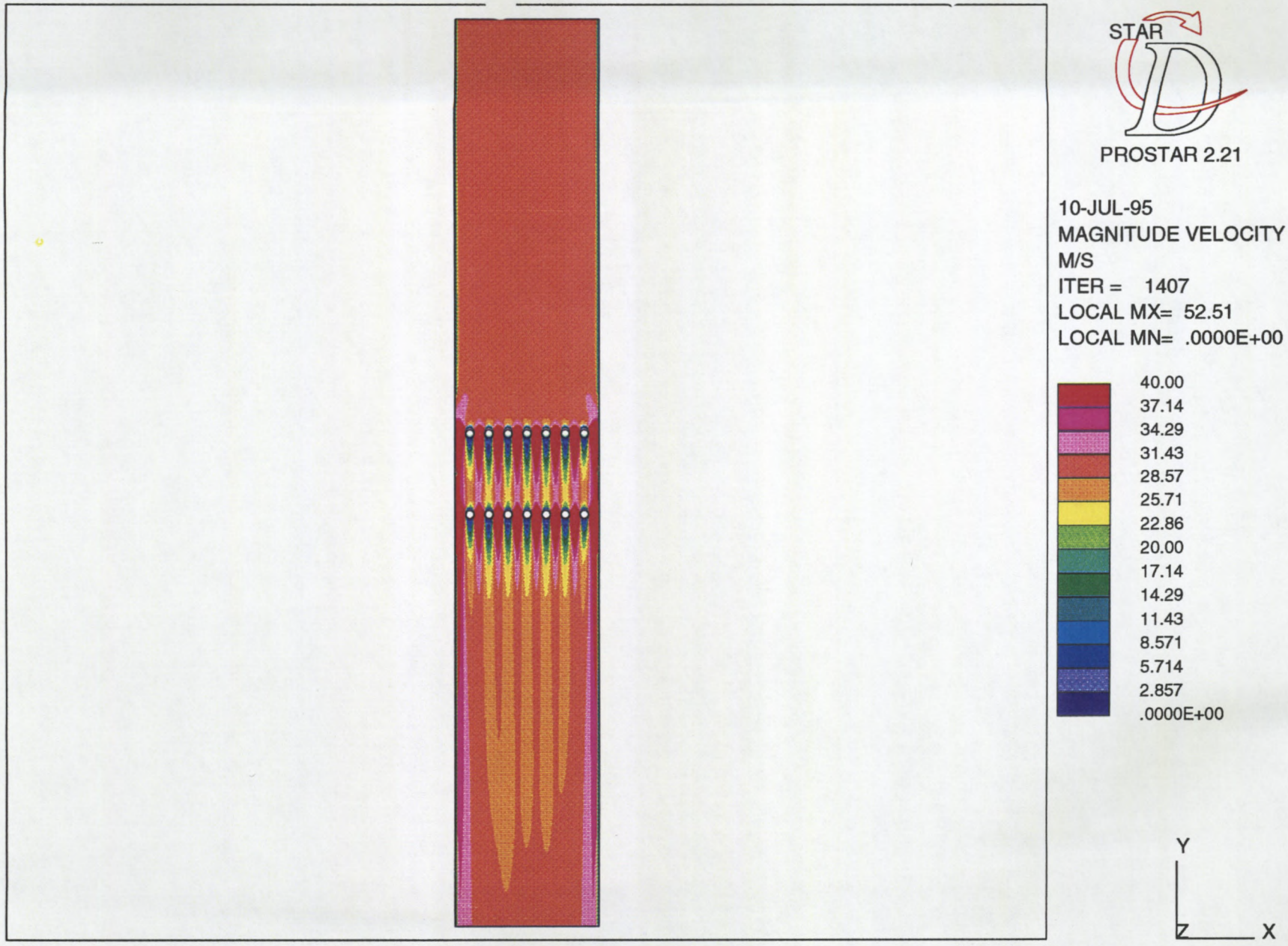

FLOW FIELD BEHAVIOUR FOR FLUID VELOCITY = 30 m/s

Figure : 4

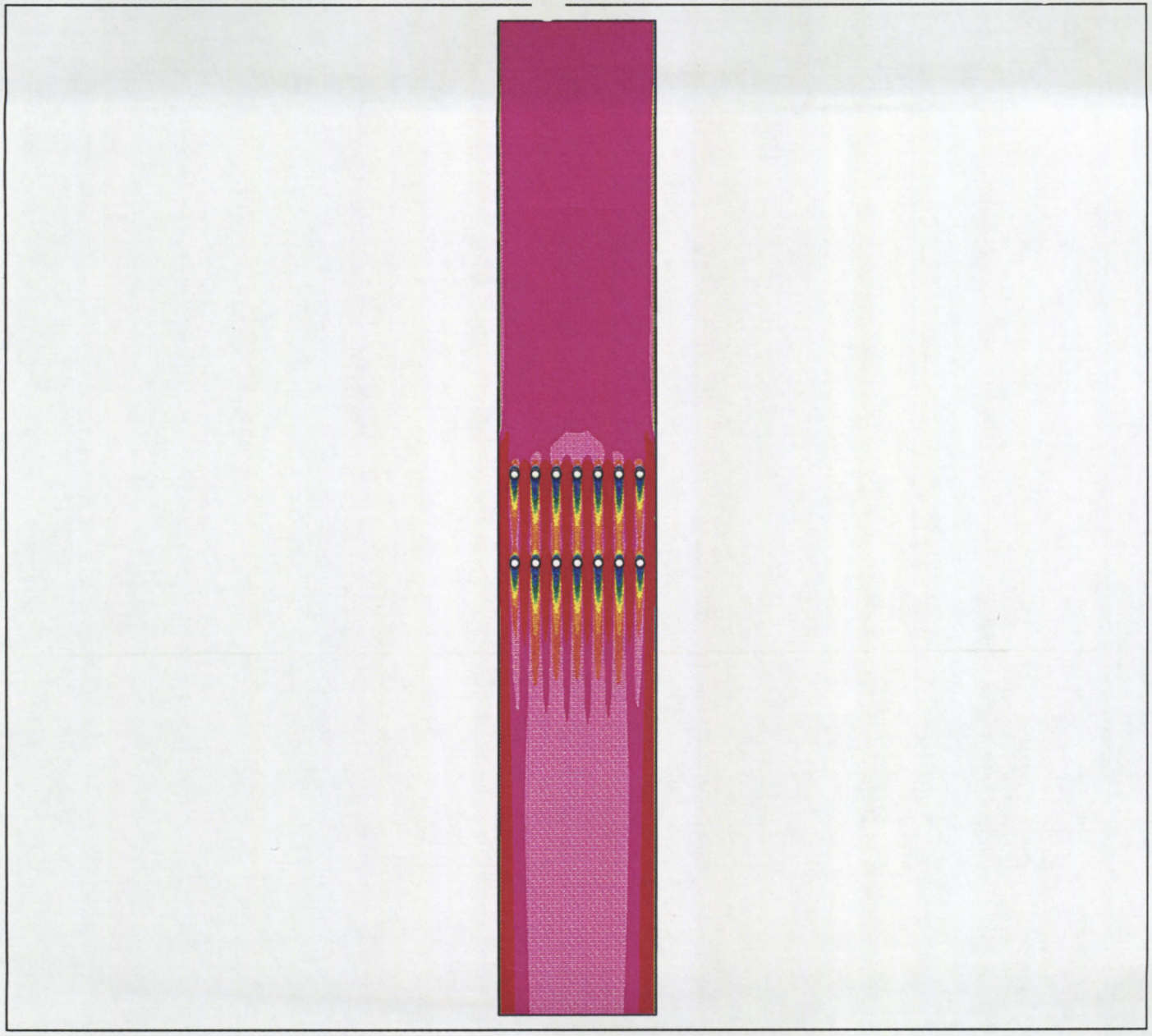

FLOW FIELD BEHAVIOUR FOR FLUID VELOCITY = 35 m/s

Figure : 5

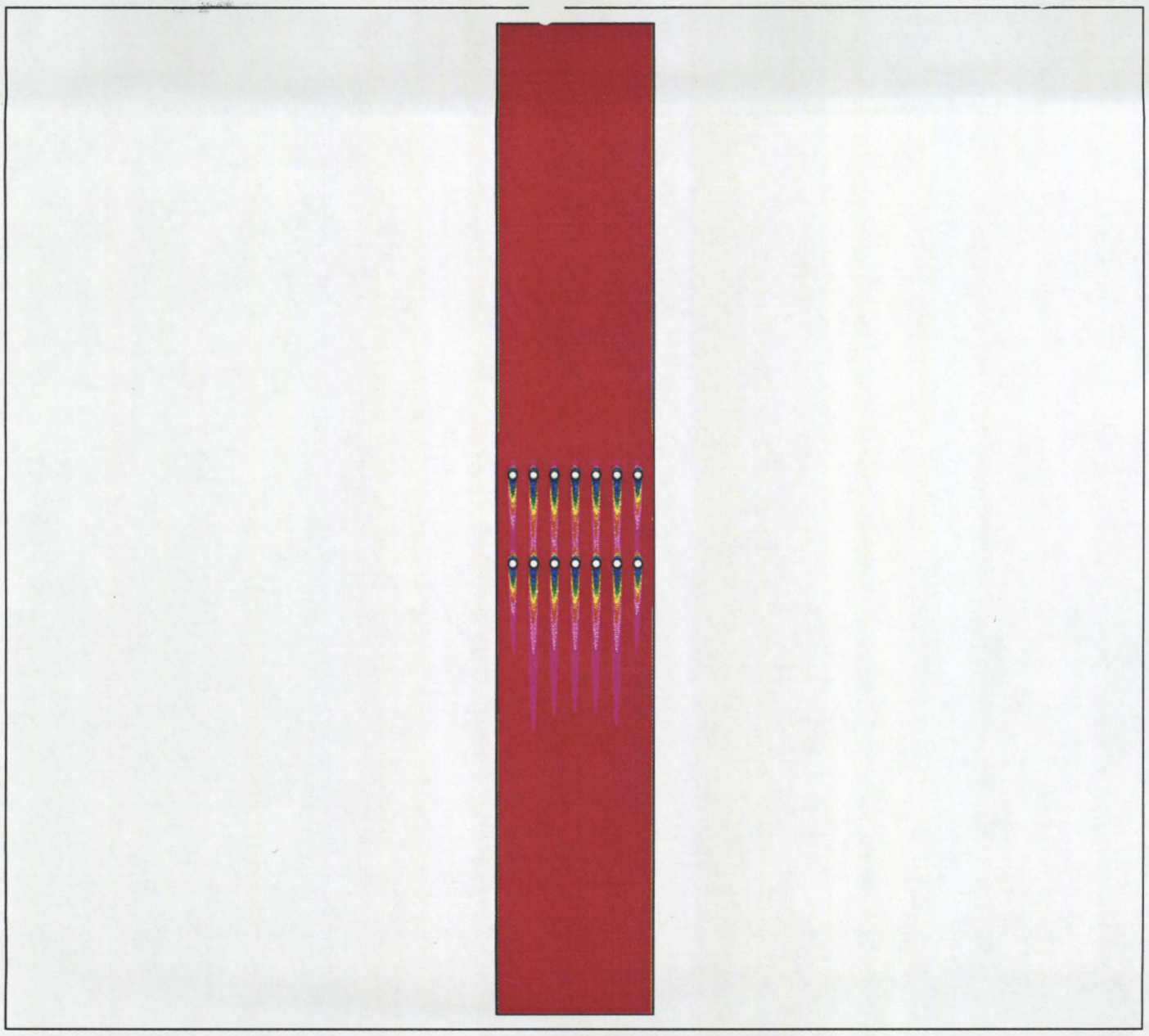

FLOW FIELD BEHAVIOUR FOR FLUID VELOCITY = 40 m/s

Figure: 6

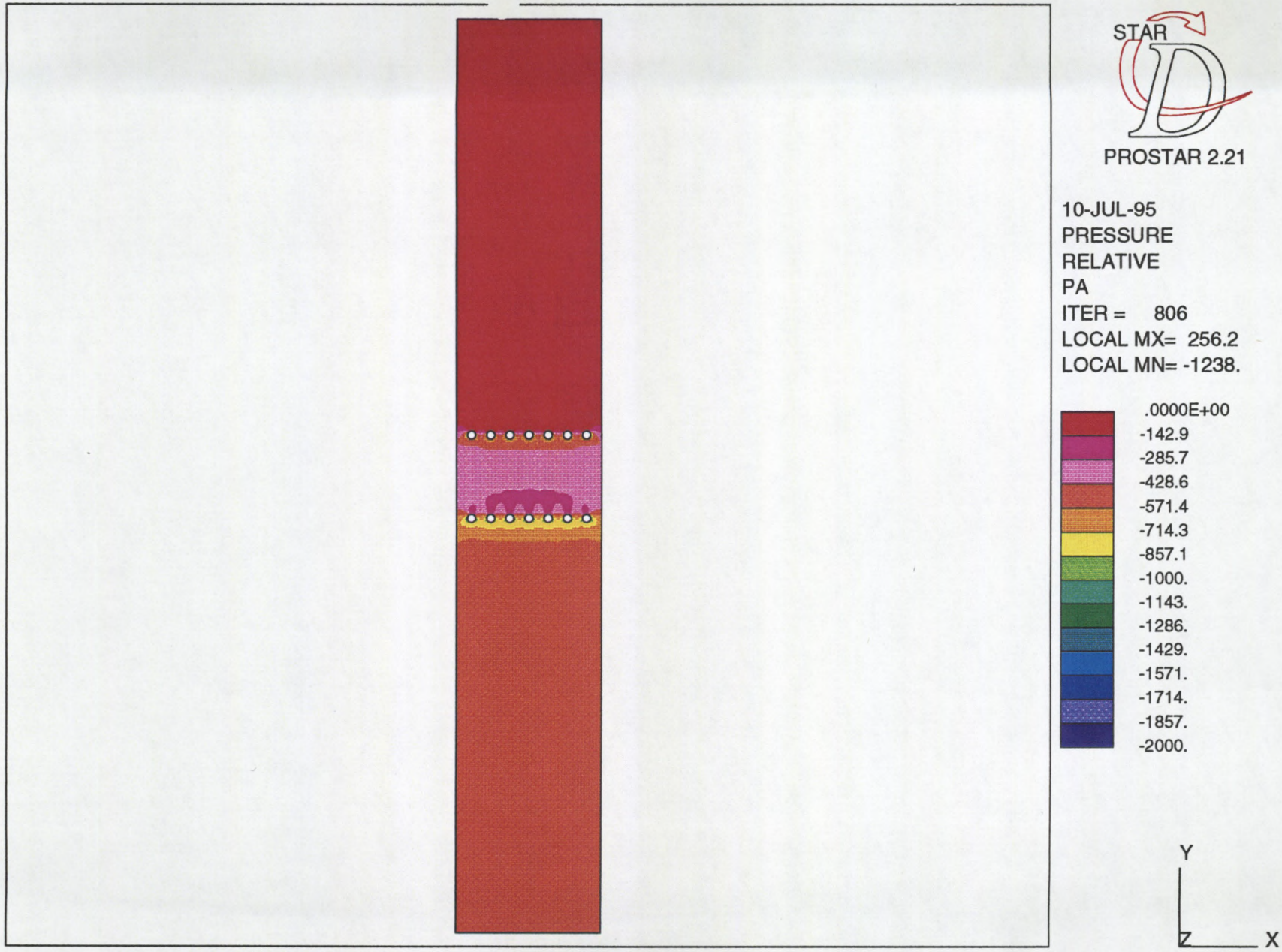

FLOW FIELD BEHAVIOUR FOR FLUID VELOCITY = 20 m/s

Figure: 7

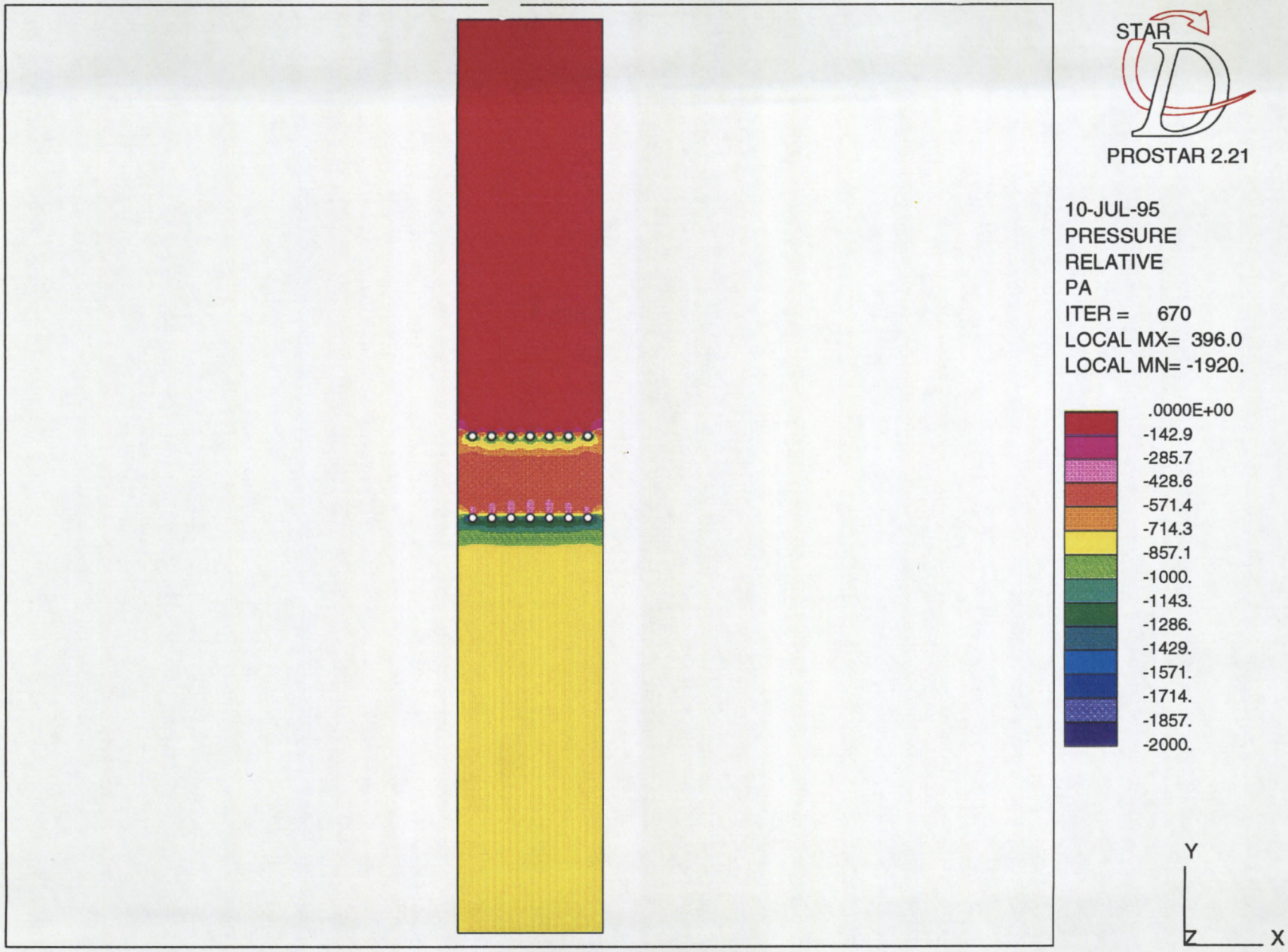

FLOW FIELD BEHAVIOUR FOR FLUID VELOCITY = 25 m/s

Figure: 8

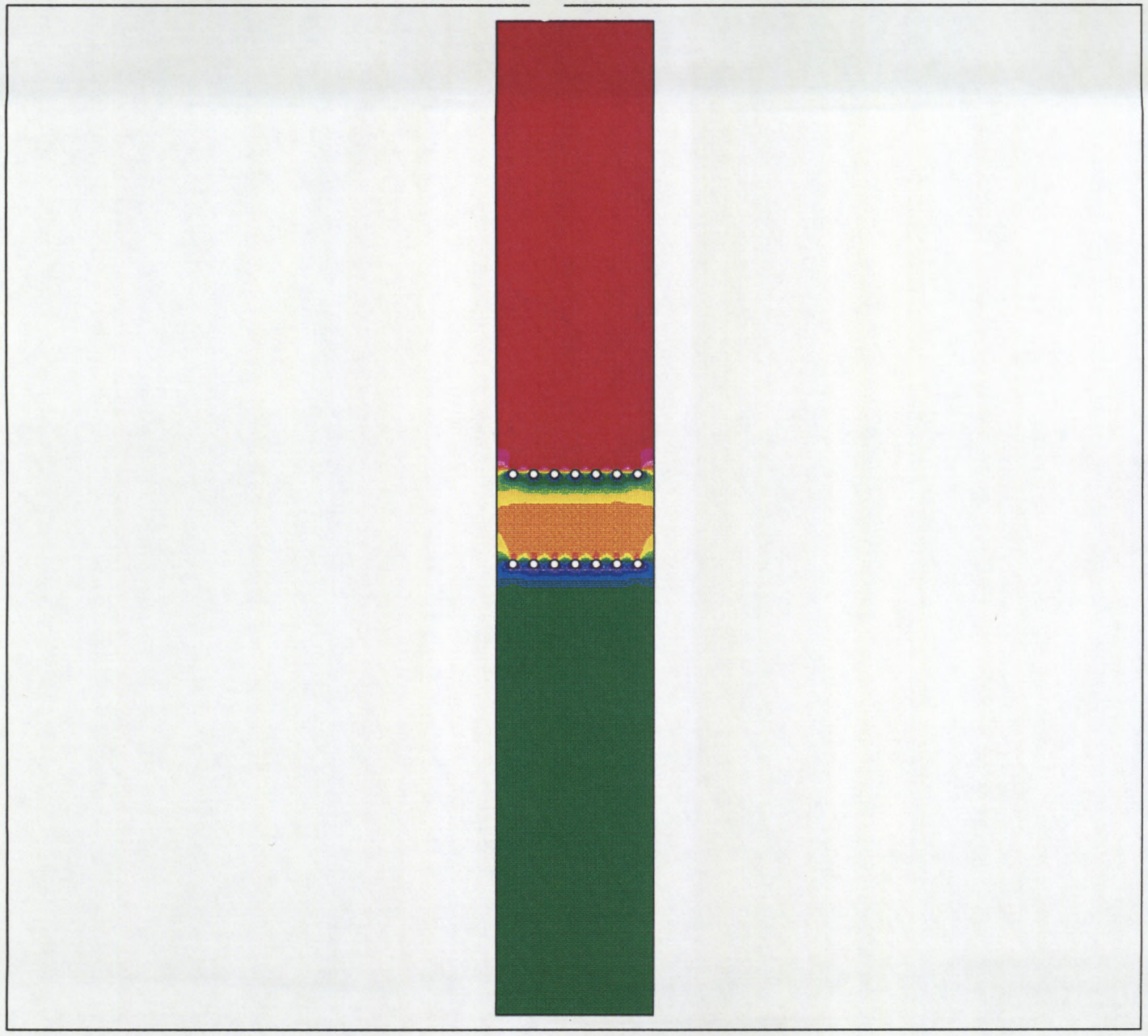

FLOW FIELD BEHAVIOUR FOR FLUID VELOCITY = 30 m/s

Figure : 9

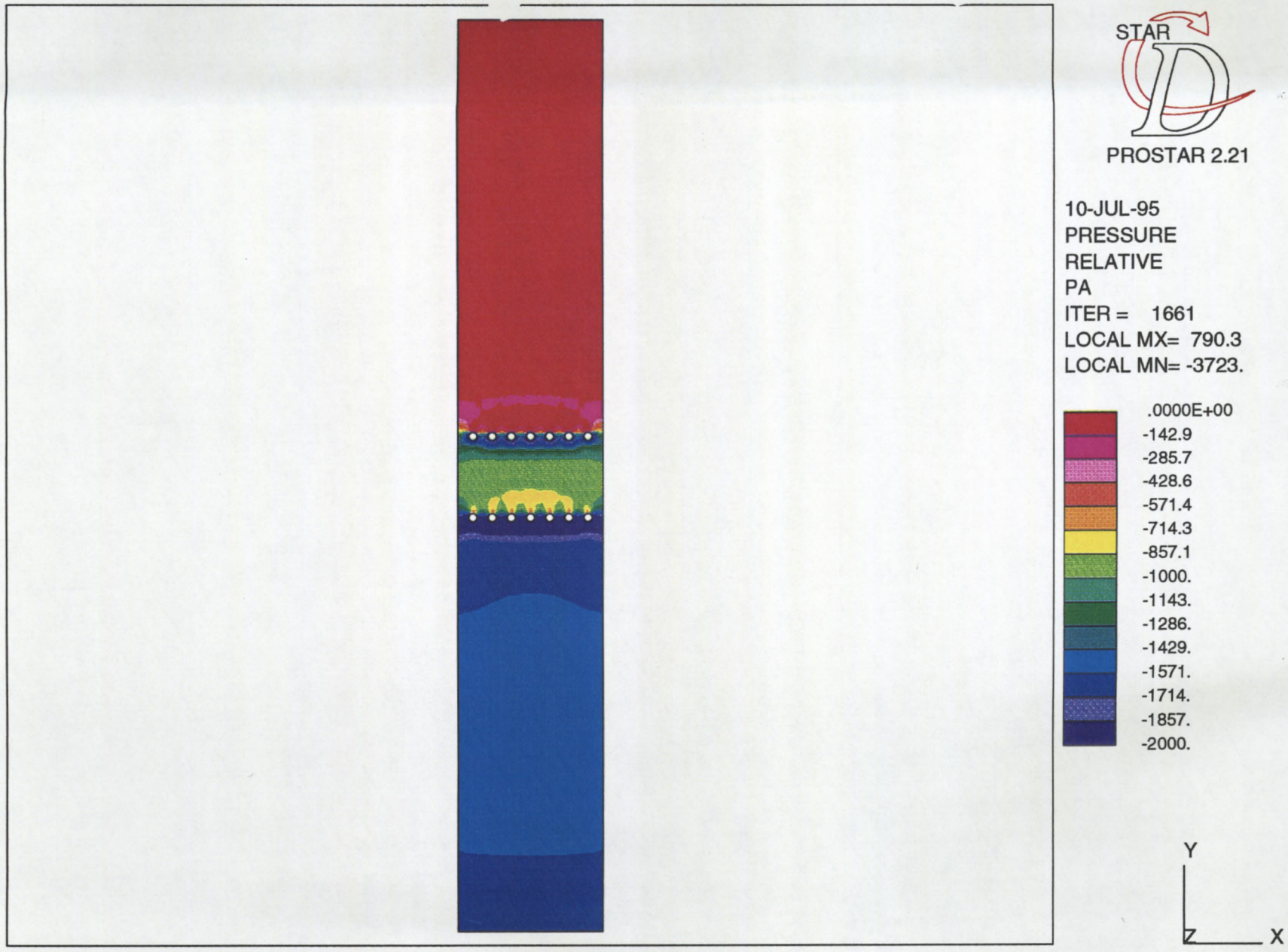

FLOW FIELD BEHAVIOUR FOR FLUID VELOCITY = 35 m/s

Figure: 10

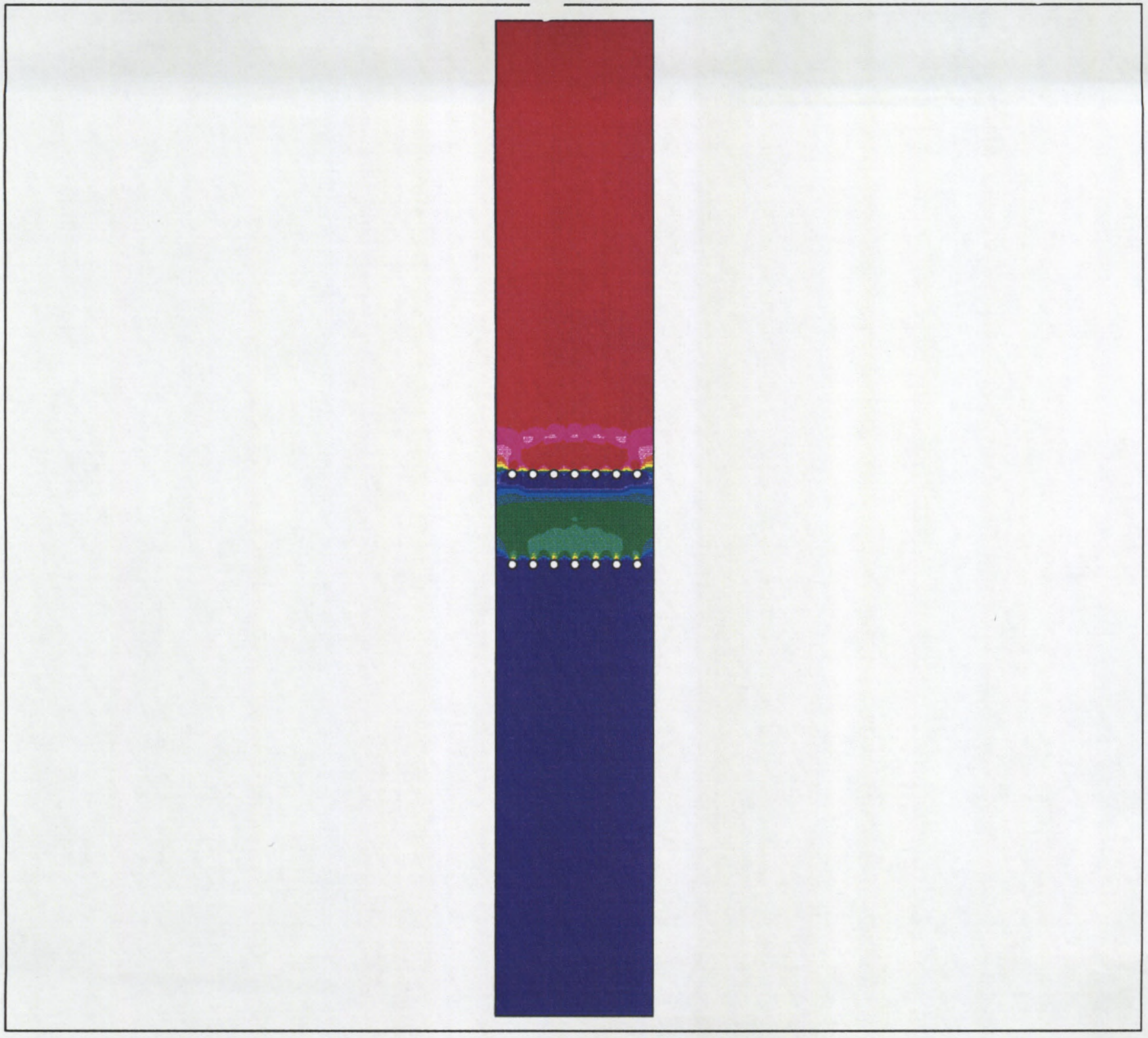

FLOW FIELD BEHAVIOUR FOR FLUID VELOCITY = 40 m/s

Figure: 11

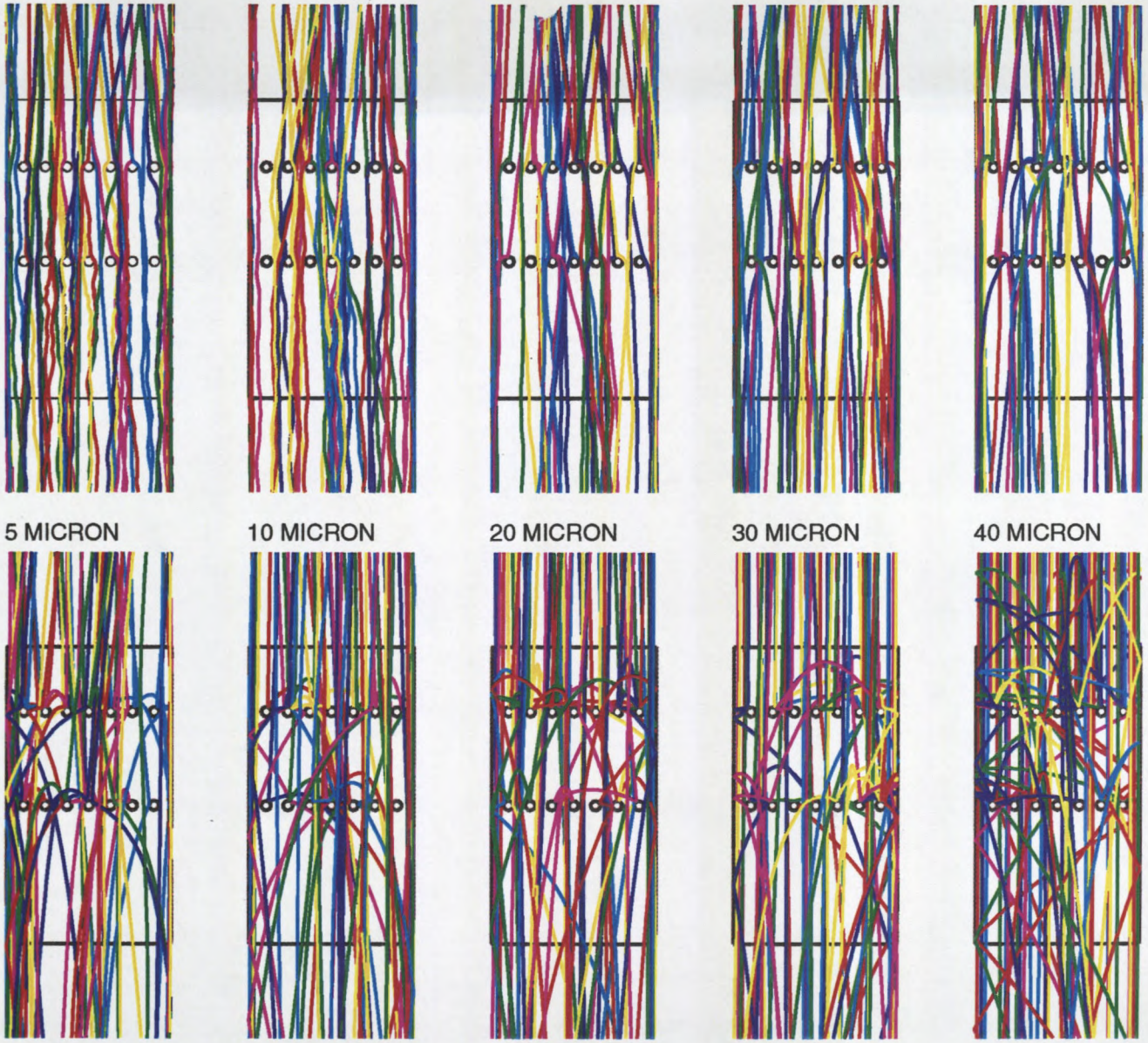

PARTICLE BEHAVIOUR FOR FLUID VELOCITY = 20 m/s
50 particles per size, uncoupled, no gravity
particle energy loss at wall: rebounce (no loss)

Figure: 12

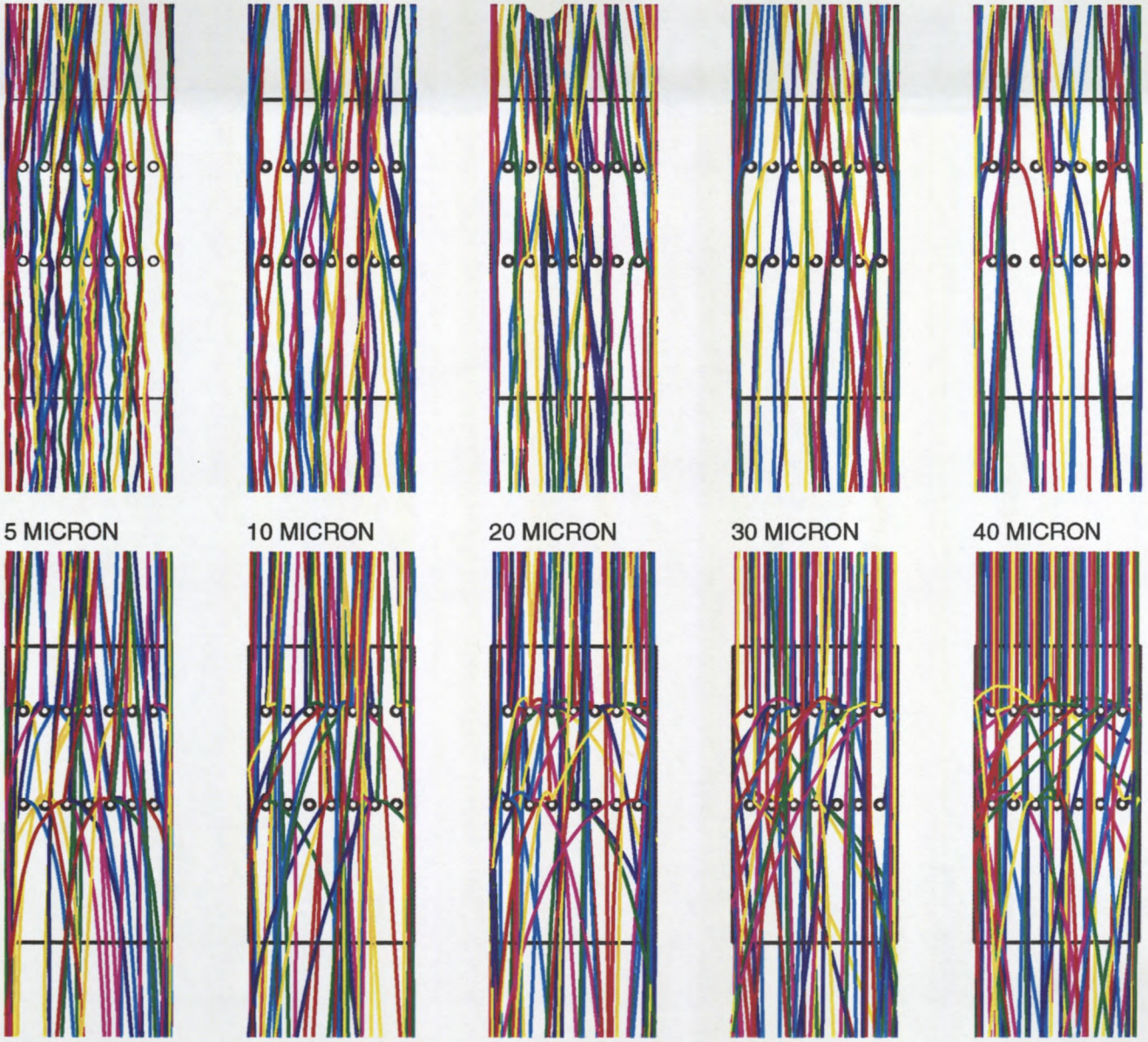

PARTICLE BEHAVIOUR FOR FLUID VELOCITY = 20 m/s
50 particles per size, uncoupled, no gravity
particle energy loss at wall: 70% normal 10% tangential

Figure : 13

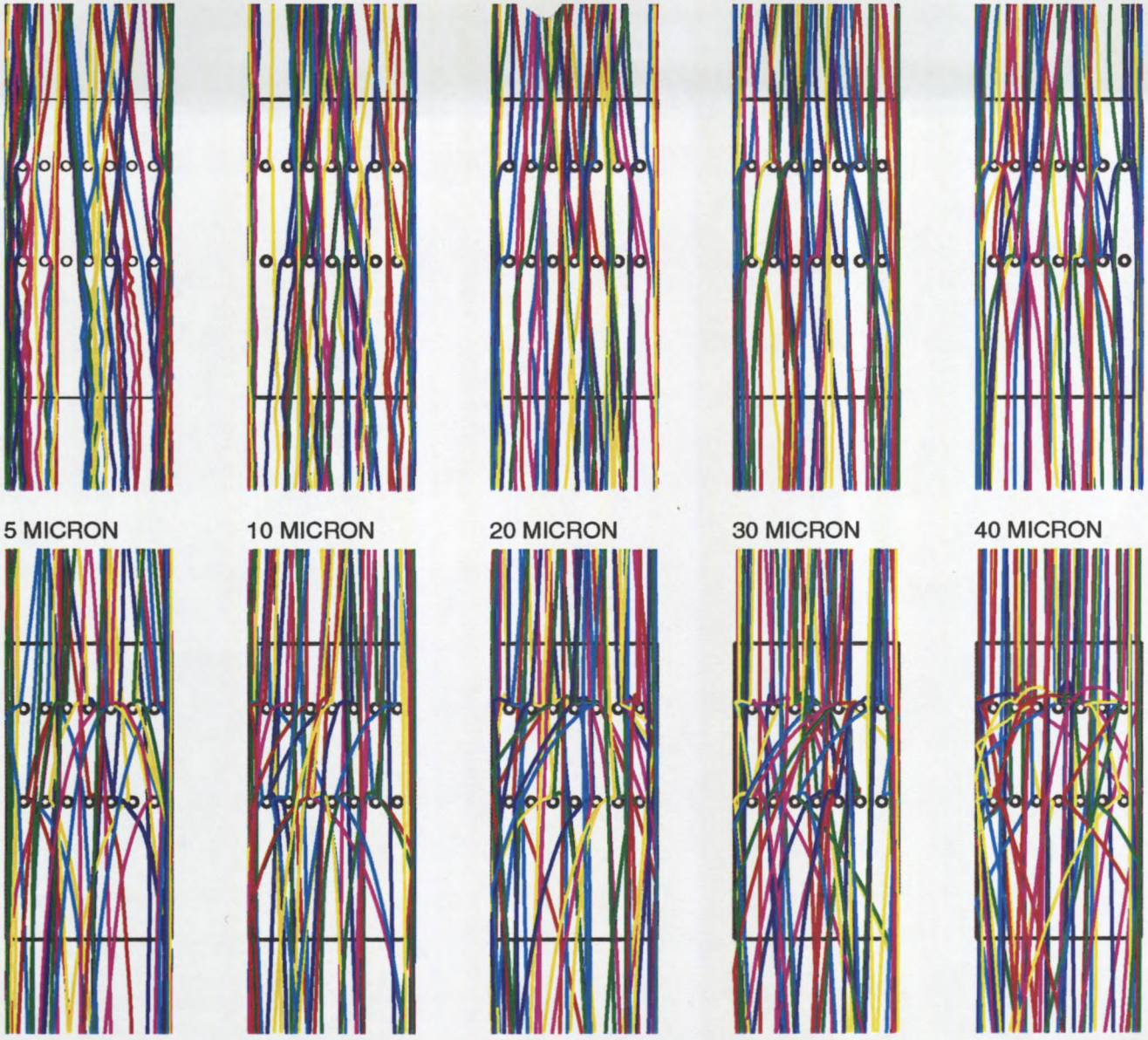

PARTICLE BEHAVIOUR FOR FLUID VELOCITY = 25 m/s
50 particles per size, uncoupled, no gravity
particle energy loss at wall: 70% normal 10% tangential

Figure: 14

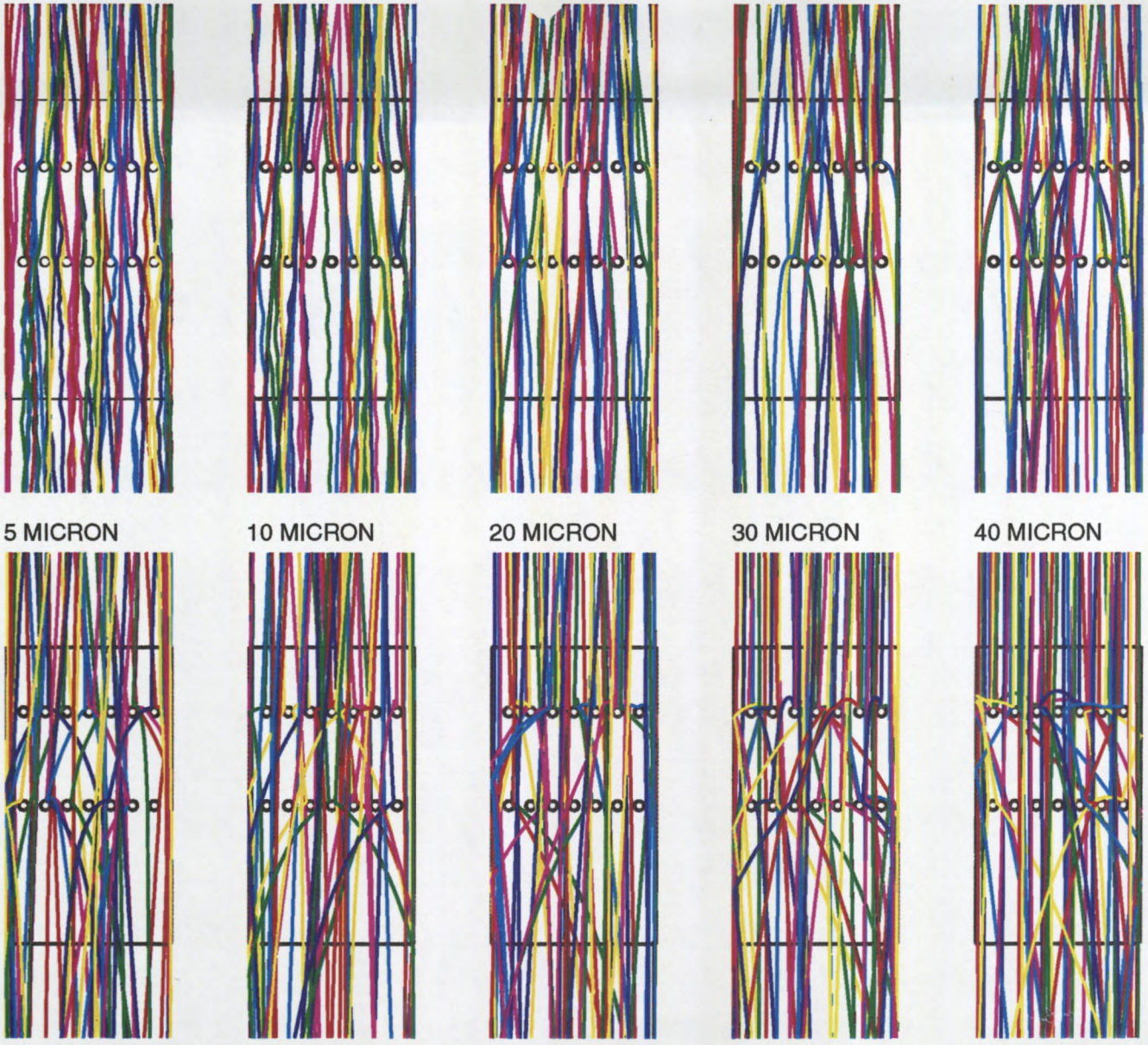

PARTICLE BEHAVIOUR FOR FLUID VELOCITY = 30 m/s
50 particles per size, uncoupled, no gravity
particle energy loss at wall: 70% normal 10% tangential

Figure 15

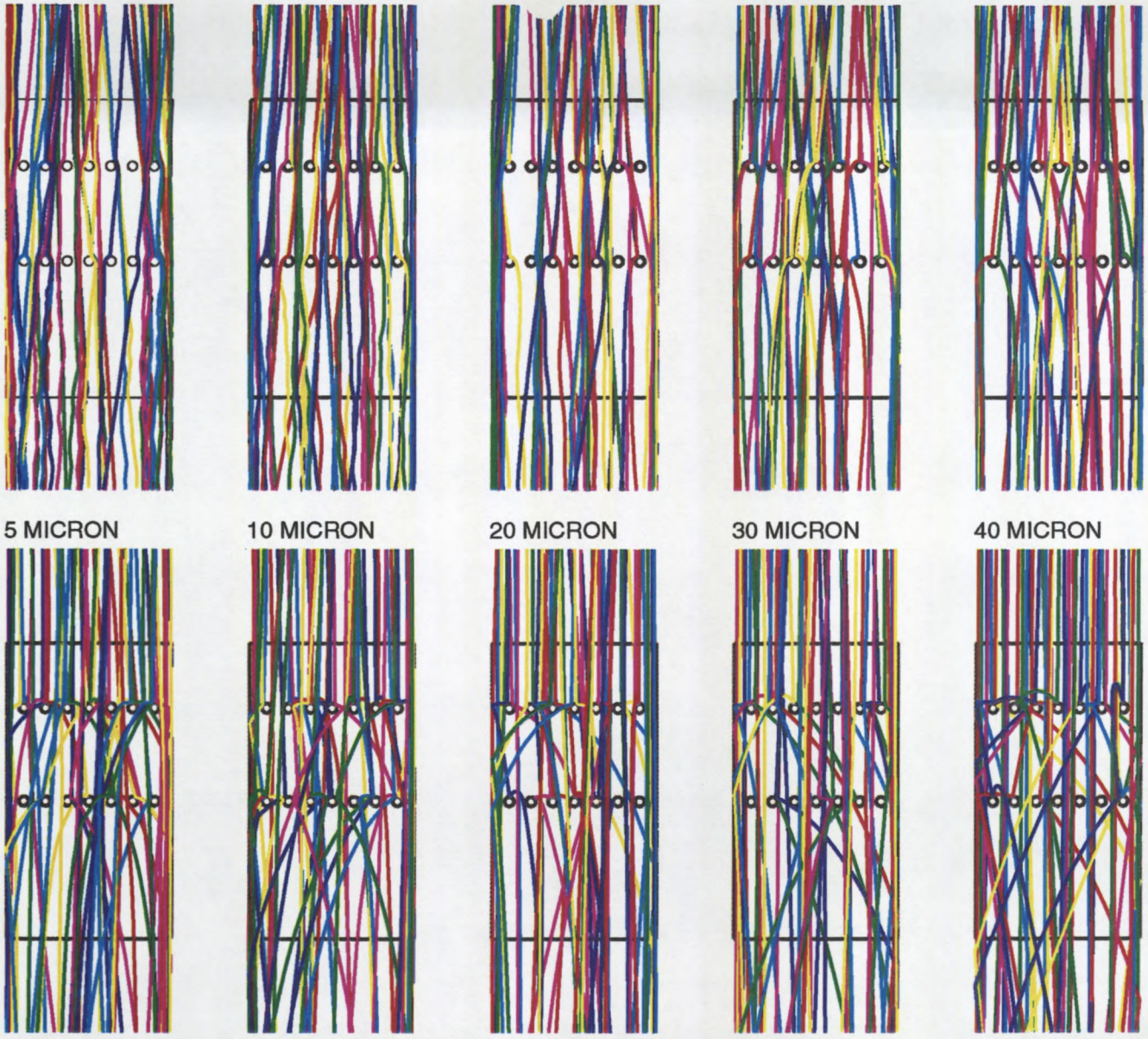

PARTICLE BEHAVIOUR FOR FLUID VELOCITY = 35 m/s
50 particles per size, uncoupled, no gravity
particle energy loss at wall: 70% normal 10% tangential

Figure : 16

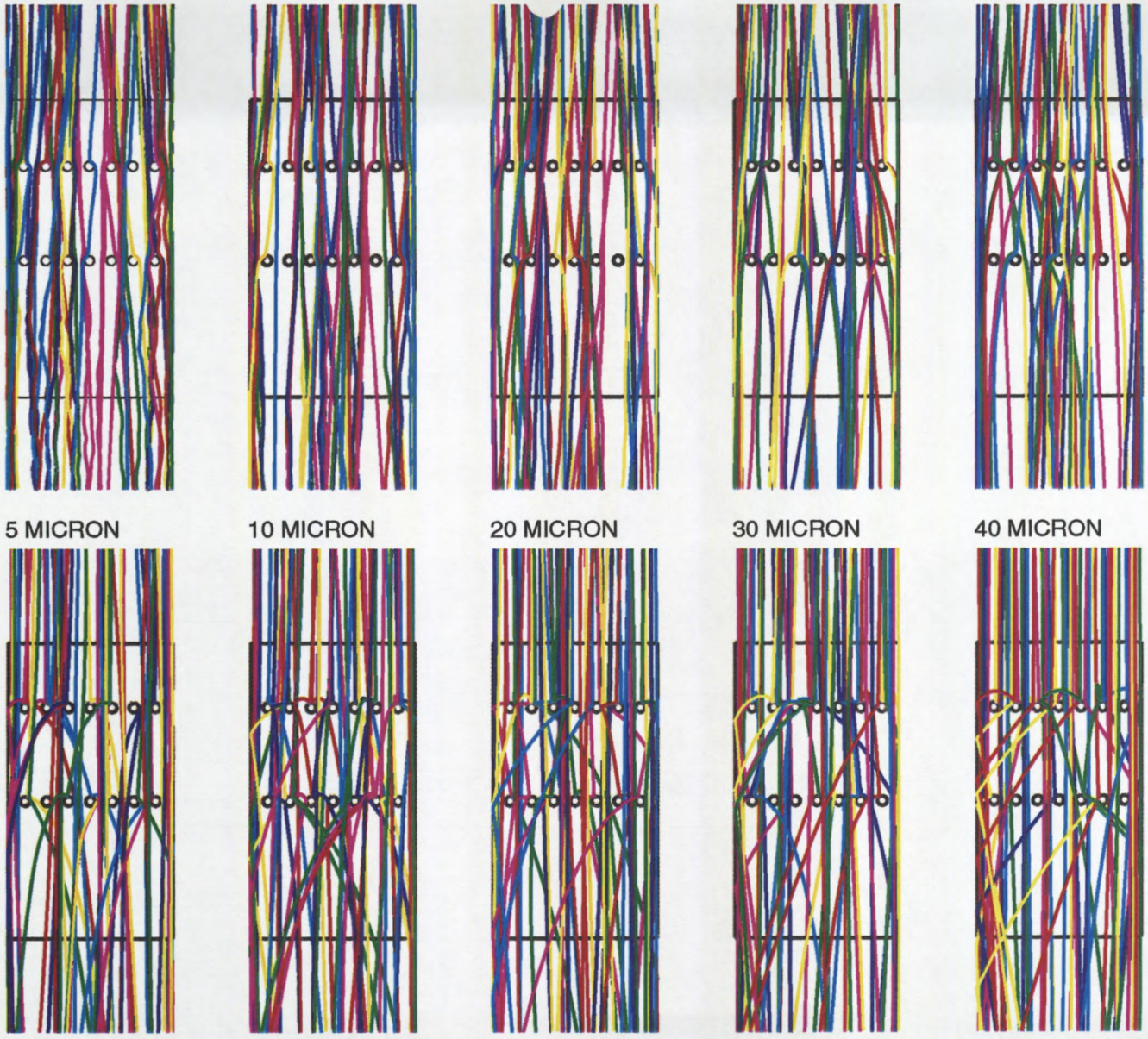

PARTICLE BEHAVIOUR FOR FLUID VELOCITY = 40 m/s
50 particles per size, uncoupled, no gravity
particle energy loss at wall: 70% normal 10% tangential

Figure: 17

Appendix C Flow rig development

The flow rig went through various stages of development. To start with it was a closed loop system from where it moved to a once through system. Since then things such as the material feeder and the methods of data acquisition have been improved.

C.1 Flow rig 1992

The earliest version of the flow rig is shown in Figure C.1-1. This system was a closed loop one used for the tests to determine which flow technique should be explored in more detail.

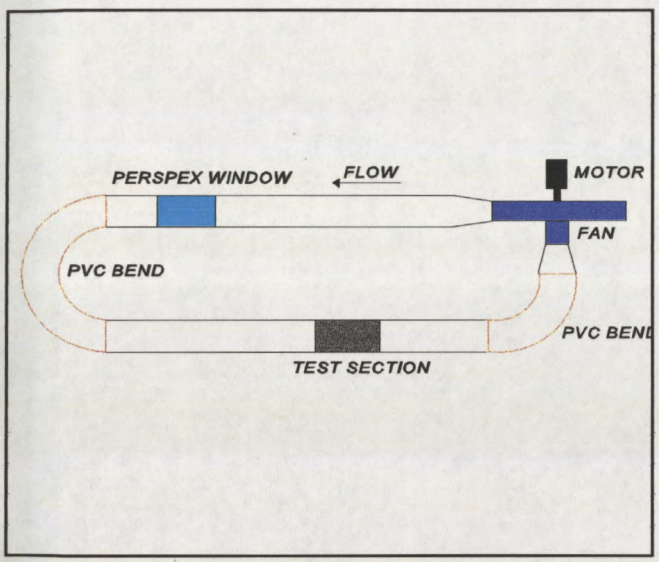

Figure C.1-1 1992 test rig

Various different capacitive and light methods were explored by inserting different sections in the test section (Marantos 1992).

C.2 Flow rig 1993-Closed loop

Once it was established that tests would be done using the electrostatic method the focus of the research immediately moved to power stations. Tests were done at Kendal and Lethabo power stations. Although the results looked promising (there was a definite relationship between mass flow rate and charge magnitude), there still existed too many inexplicable results. Thus in 1993 electrostatic tests were carried out on the flow rig shown in Figure C.2-1.

These tests were primarily to measure the effect of changing particle size on the charge magnitude. Two small collapsible grating probes were used in order that the particle velocity could be calculated using the cross correlation technique described in the Background. The air velocity was measured using a Pitot tube before the PF was introduced. Attempts to measure air velocity using the Pitot tube during the test run proved futile since the Pitot continually got blocked. The air velocity was varied by adjusting the fan speed. Once the test was complete the extraction port was opened and the PF caught in the cyclone.

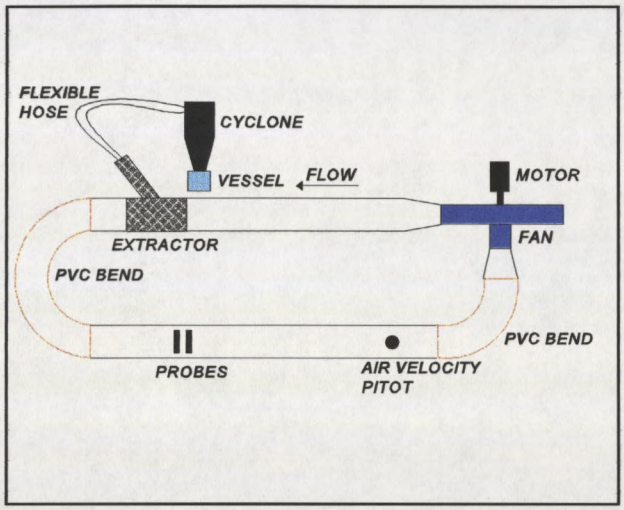

Figure C.2-1. 1993 test rig-closed loop

C.2.1 Method of data acquisition

Figure C.2.1-1 shows a schematic of the data acquisition mechanism used for this flow rig.

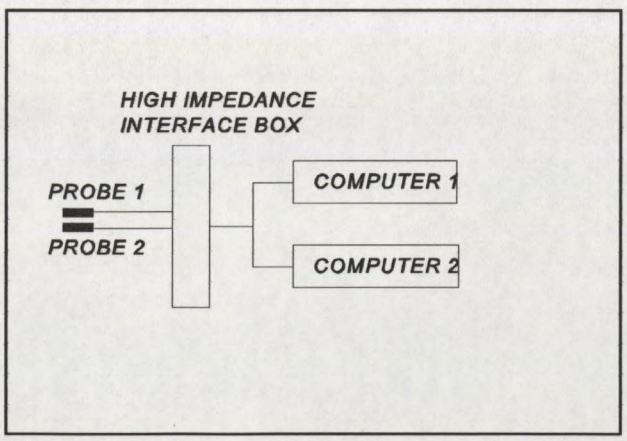

Figure C.2.1-1. Data acquisition mechanism

Computer 1 had an Eagle Electronics PC-60 A/D input card installed. Using software written in Pascal the probe voltages were recorded at 1 second intervals.

Computer 2 also had an A/D input card but this time it was a PC-30 card. This card can log data at much higher frequencies. Using this data the particle velocity can be calculated. The higher frequency is necessary in order that the two waveforms can be matched to each other.

Unfortunately it was impossible to log data to both computers at the same time. Thus when the test was run for a 5 minute period data was only logged to the second computer for a period of a few seconds in each minute.

The test results from this closed loop system were not particularly convincing since odd things happened which were not easily explained. The polarity of the probe voltage changed over a period of time and if "clean" air were allowed into the system the polarity immediately reverted back to its original state. None of the literature studied had covered this phenomenon and as such it was unexpected. It is possible that it has something to do with the ionisation of the air in the system. However this is just speculation. No attempt was made to explain the oddity. Rather a change to an open loop system was made which was more real to the power station environment anyway.

C.3 Flow rig 1993-Open loop

The open loop rig is shown in Figure C.3-1. The data acquisition mechanism was exactly the same except that both computers logged at the same time.

The feeder was made from a PVC tube with a piston sliding inside it. The piston was driven by a windscreen wiper motor attached to a helical drive rod. The feedrate was varied by adjusting the voltage on the motor.

Tests were done at various air velocities. The air velocity was measured by a Pitot tube placed in the pipe in the opposite direction to that in which it should have been placed. The air flowing past the Pitot creates a vacuum in the Pitot (Halliday and Resnick, 1970) and this vacuum when measured (the measured pressure is still positive since it is the difference between the vacuum and static pressure) using a manometer is proportional to the air velocity. It was discovered later that the air velocity measurement was inaccurate however because of varying back pressure in the system. This varying back pressure is created because the bag fillers become

less and less porous as they fill with particles. The less porous they became the higher the back pressure.

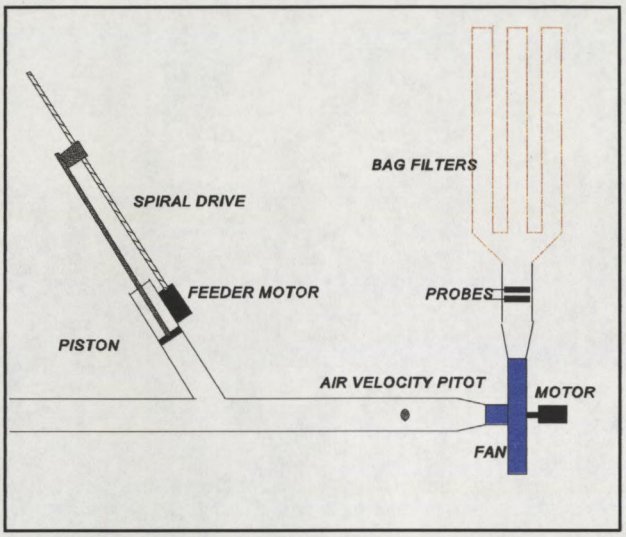

Figure C.3-1 1993 Test rig-Open loop

The test results were not very good mainly due to the inconsistencies in feeder speed. The feeder tended to get stuck and the fly ash (fly ash was used instead of PF due to its easy availability and relative cleanness compared to PF; the theory was still under test and the chemical composition of the material used was irrelevant) fell into the air stream in lumps rather than a steady stream.

This led to the flow rig used in 1994 which is discussed in the main body of the report (Section 3, pp 20).

Appendix D Hendrina Power Station graphs

This appendix shows the remainder of the graphs not given in the main body of the text of Section 4. They show the comparison between the electrostatic mass flow rate and the probe parameters such as current difference.

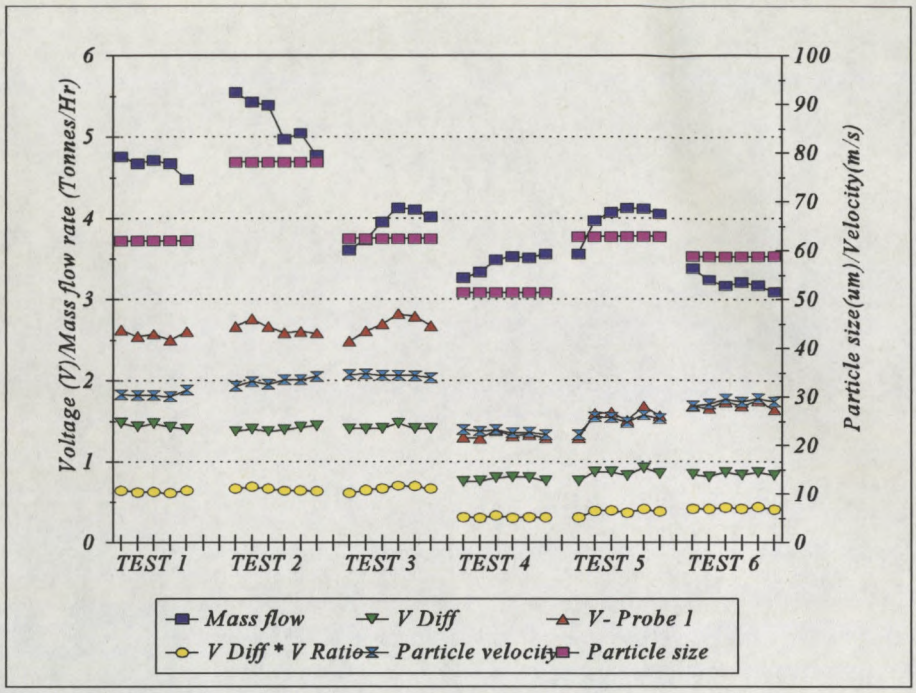

Figure D-1 Pipe 1- Electrostatic mass flow rate, probe voltage parameters and particle size. 3 tests at 22 Tonnes/Hr (1, 2 & 3) and 3 tests at 13 Tonnes/Hr (4, 5 & 6)

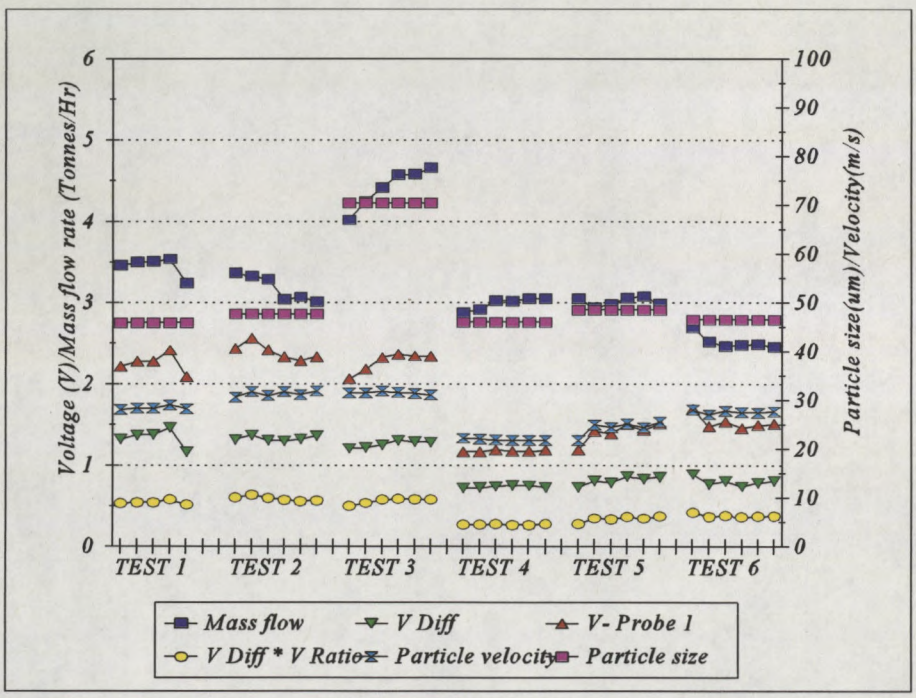

Figure D-2 Pipe 3- Electrostatic mass flow rate, probe voltage parameters and particle size. 3 tests at 22 Tonnes/Hr (1, 2 & 3) and 3 tests at 13 Tonnes/Hr (4, 5 & 6)

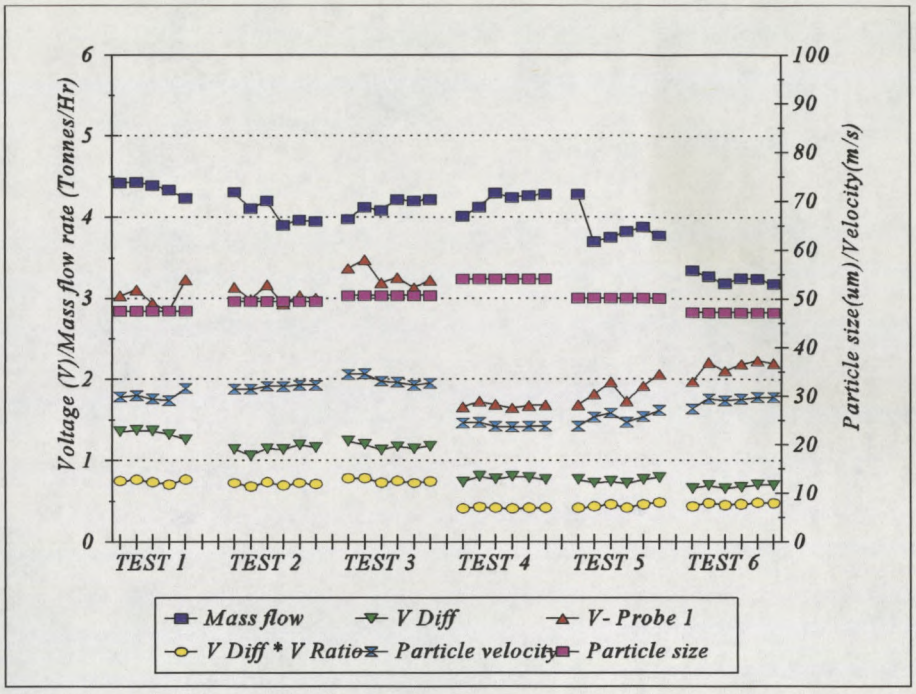

Figure D-3 Pipe 4- Electrostatic mass flow rate, probe voltage parameters and particle size. 3 tests at 22 Tonnes/Hr (1, 2 & 3) and 3 tests at 13 Tonnes/Hr (4, 5 & 6)

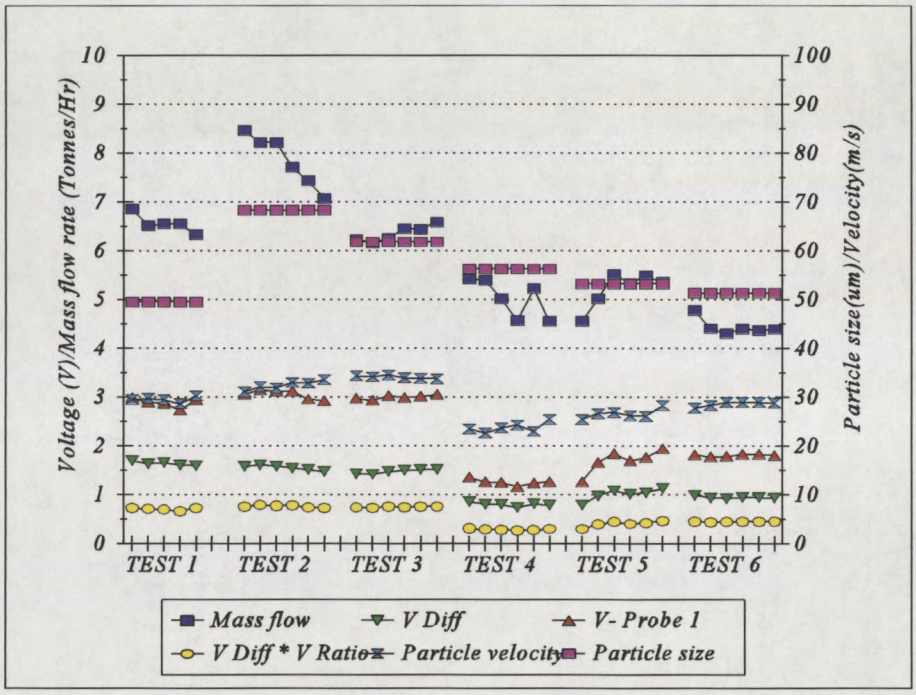

Figure D-4 Pipe 5- Electrostatic mass flow rate, probe voltage parameters and particle size. 3 tests at 22 Tonnes/Hr (1, 2 & 3) and 3 tests at 13 Tonnes/Hr (4, 5 & 6)

Appendix E Particle size analysis graphs

This appendix shows the remainder of the particle size distribution curves referred to in Section 4 (pp38).

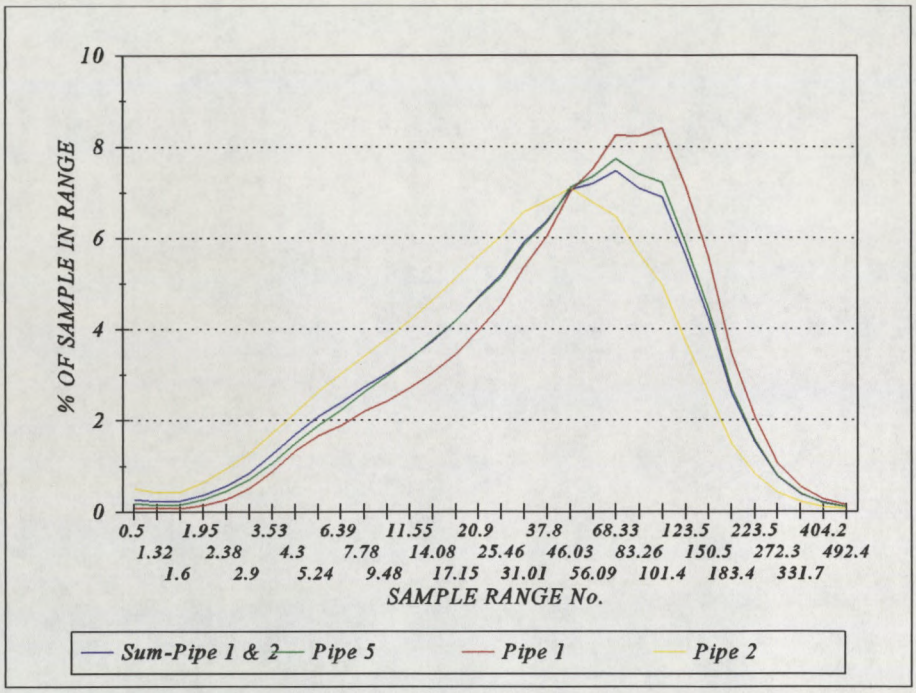

Figure E-1 Test 2 - Particle size distribution.

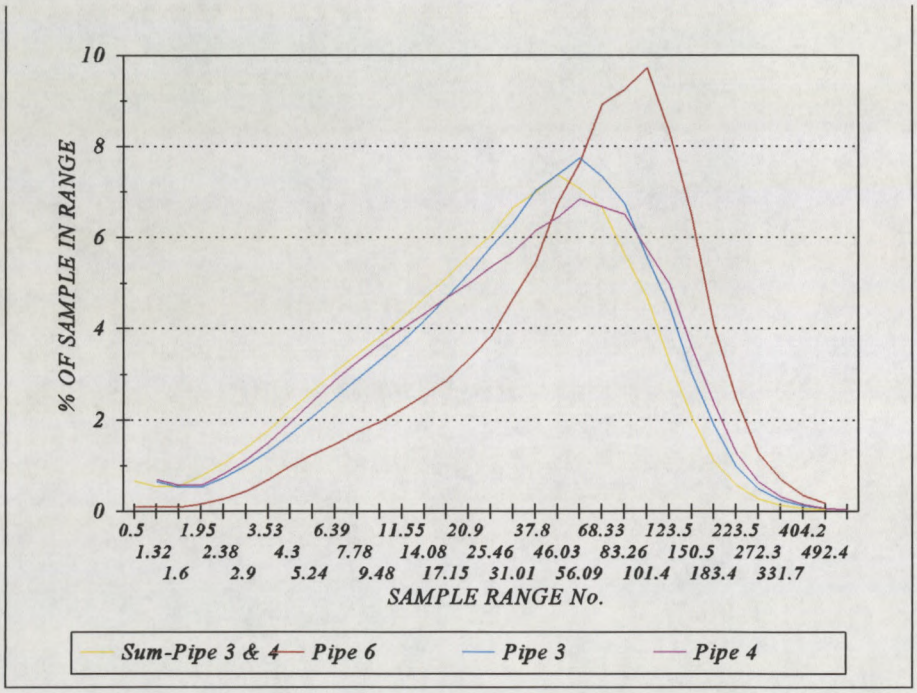

Figure E-2 Test 2 - Particle size distribution.

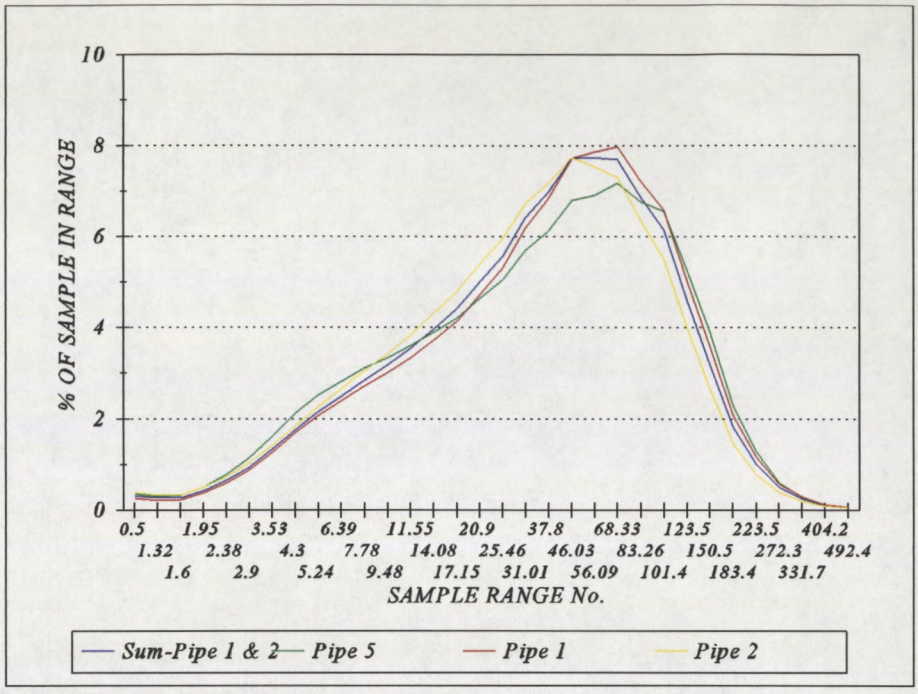

Figure E-3 Test 3 - Particle size distribution.

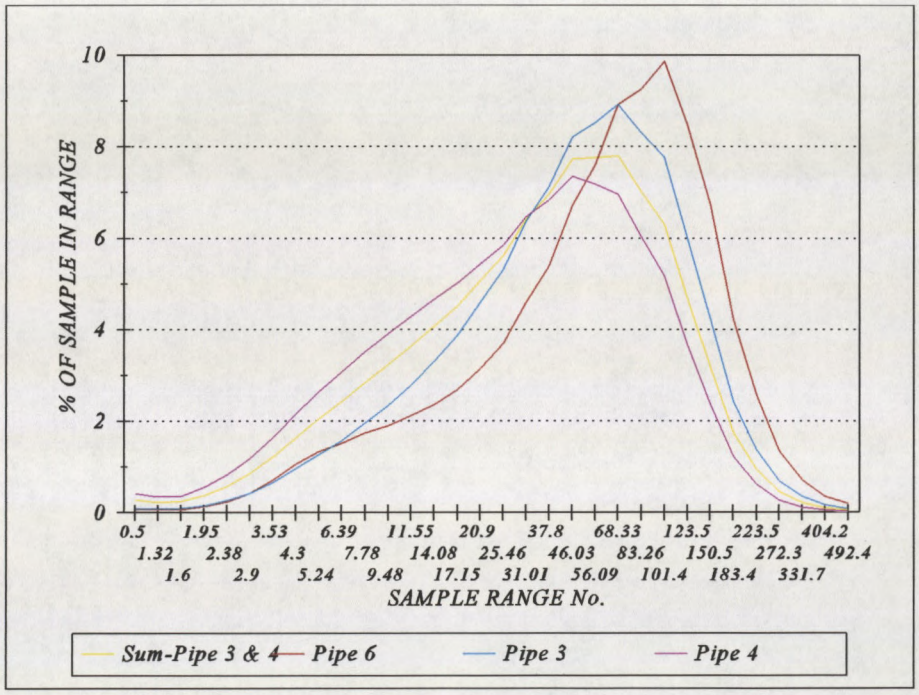

Figure E-4 Test 3 - Particle size distribution.

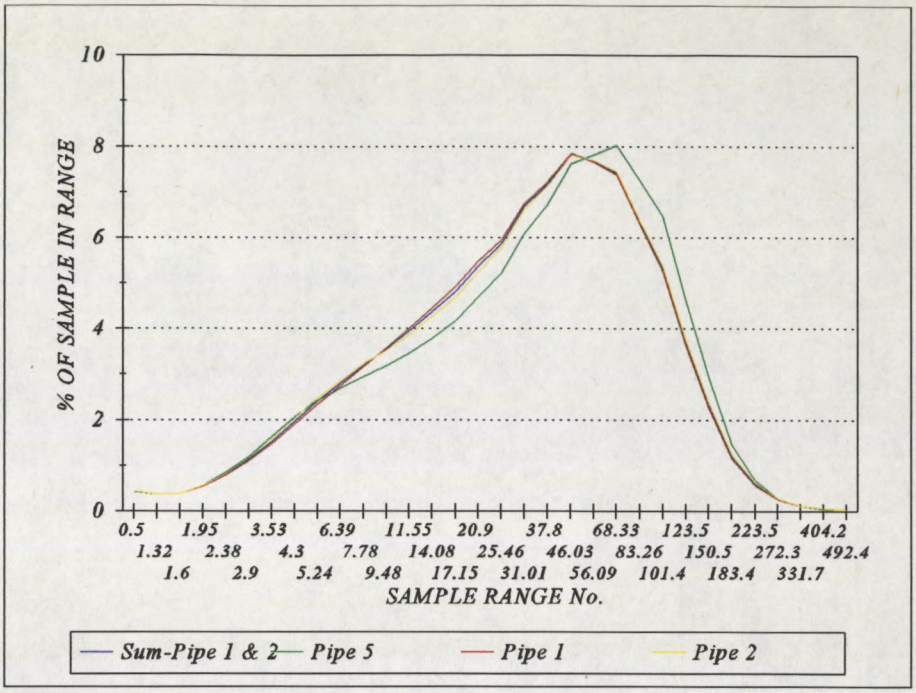

Figure E-5 Test 4 - Particle size distribution.

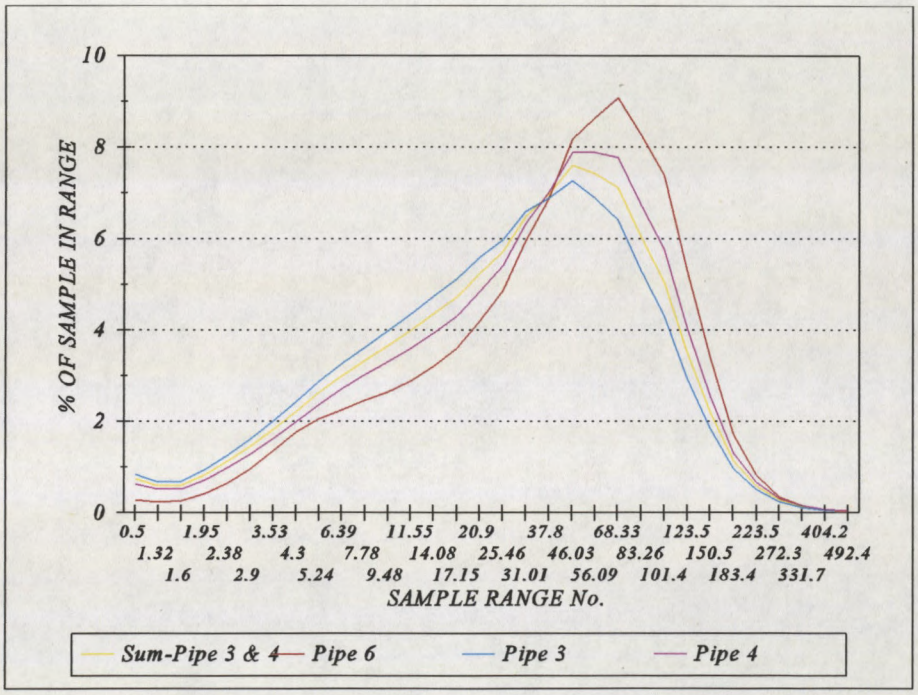

Figure E-6 Test 4 - Particle size distribution.

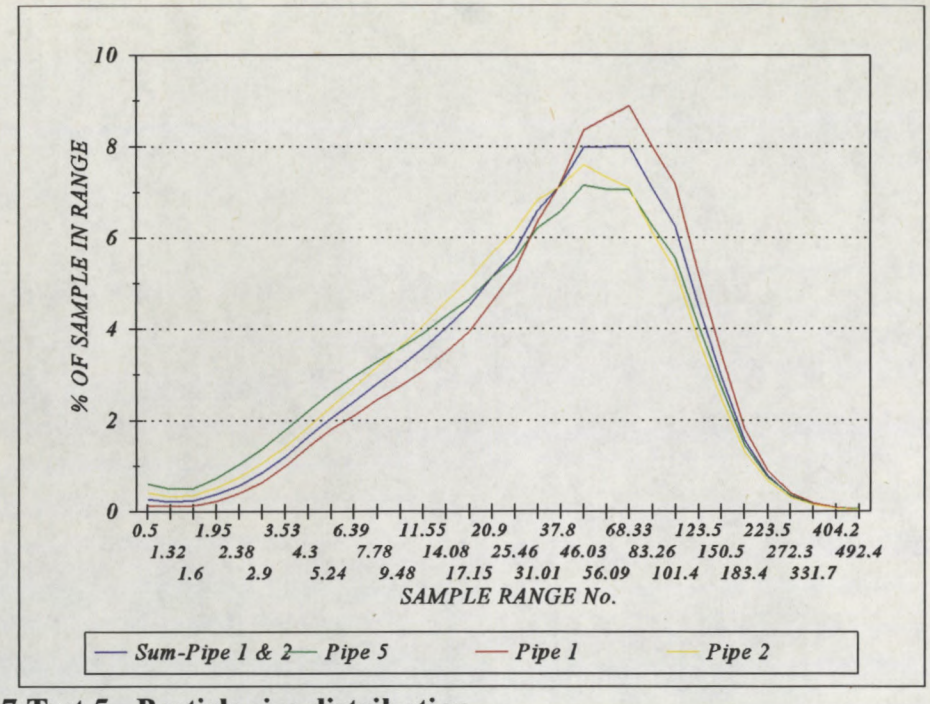

Figure E-7 Test 5 - Particle size distribution.

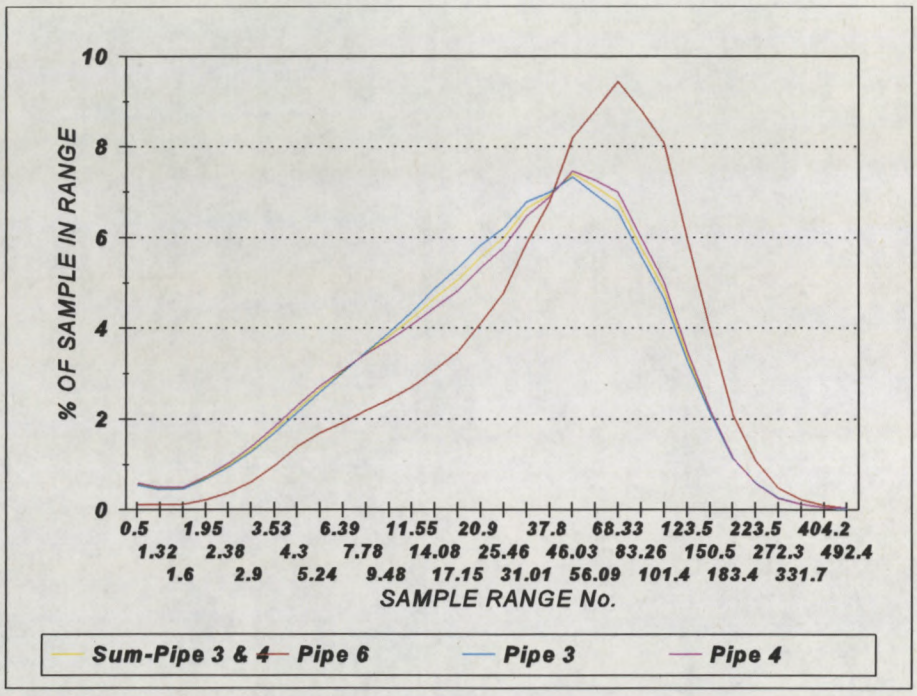

Figure E-8: Test 5 - Particle size distribution.

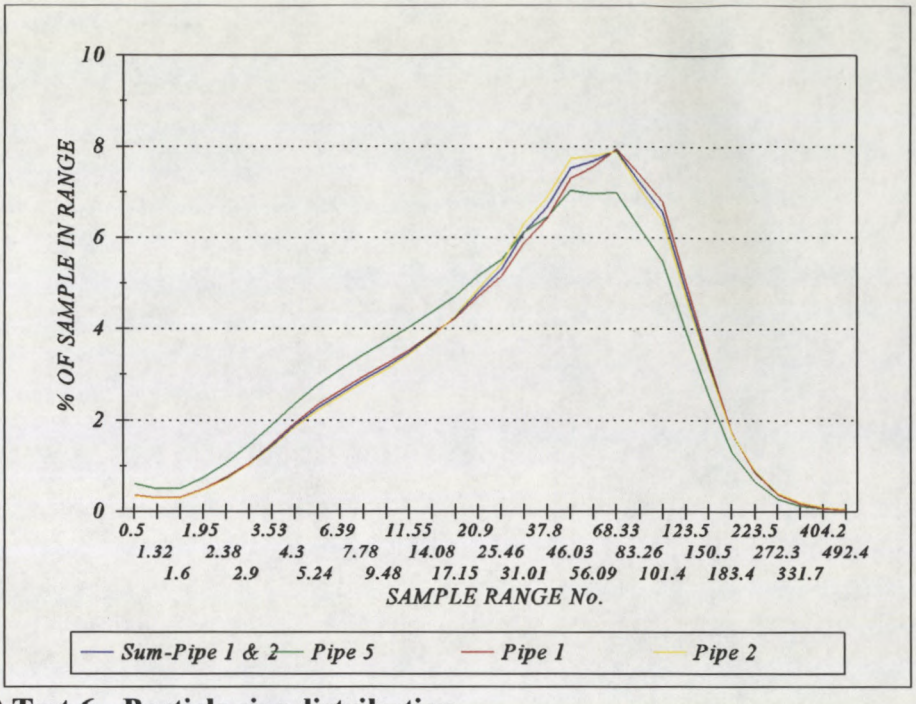

Figure E-9 Test 6 - Particle size distribution.

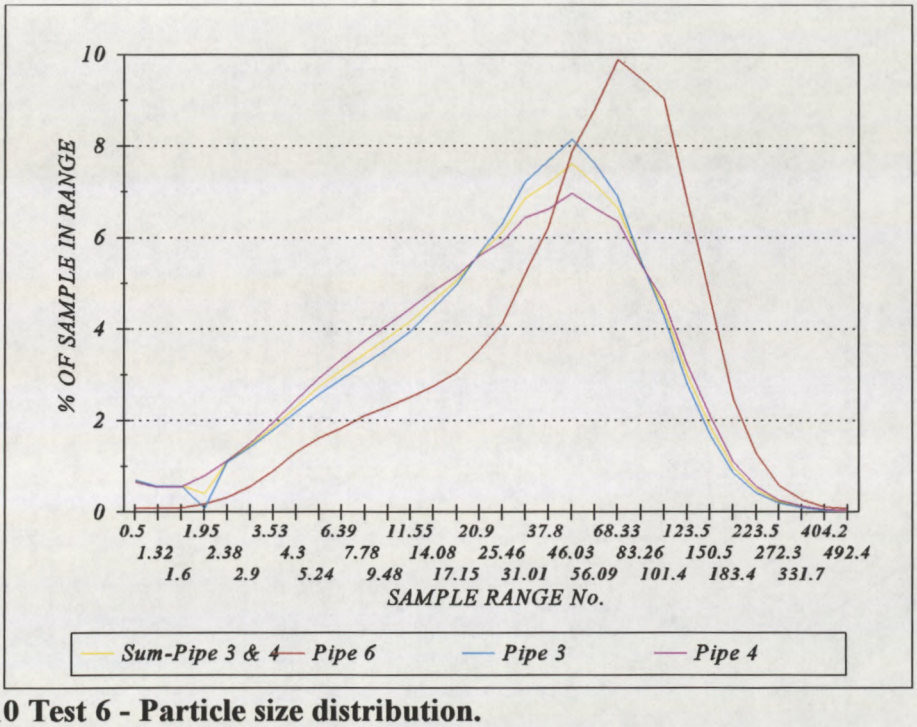

Figure E-10 Test 6 - Particle size distribution.

Appendix F PF sampling results

The appendix shows three tables. Tables F-1 and F-3 give the results for Hendrina power station in 1994 and 1995 respectively. The table shows that in each case 6 tests were done and during each test 4 pipes were sampled. The presented figures give the average particle size (D_p) of the sample extracted from each pipe and the mass flow rate (M) calculated from the mass of the sample extracted.

Table F-2 gives the results for tests done at Kendal power station in 1995. In this case three tests were done but the mill configuration requires that 8 pipes be sampled.

Hendrina - 1994

	Pipe No.	D_p (μm)	M (kg/s)		Pipe No.	D_p (μm)	M (kg/s)
Test 1	1	61.98	1.25	Test 4	1	51.39	0.88
	2	51.54	1.08		2	52.13	0.76
	3	45.86	0.82		3	45.95	0.71
	4	47.42	0.95		4	53.93	0.70
Test 2	1	78.17	1.35	Test 5	1	62.86	0.67
	2	51.90	1.07		2	52.26	0.65
	3	47.74	1.12		3	48.54	0.74
	4	49.42	0.77		4	49.67	
Test 3	1	62.47	1.40	Test 6	1	58.90	1.00
	2	54.52	0.97		2	58.59	1.17
	3	70.41	0.61		3	46.60	0.69
	4	50.64	0.81		4	47.22	0.58

Table F-1: Hendrina PF sampling results 1994

Kendal - 1995

	Pipe No.	D_p (μm)	M (kg/s)		Pipe No.	D_p (μm)	M (kg/s)
Test 1 (70%)	1L	69.2	2.62	Test 2 (55%)	1L	66.3	
	1U	62.4	1.80		1U	60.3	
	2L	66.2	2.42		2L	64.4	
	2U	78.7	2.43		2U	73.5	
	3L	74.0	2.40		3L	70.8	
	3U	68.5	2.41		3U	63.1	
	4L	71.0	3.04		4L	70.9	
	4U	61.0	2.26		4U	62.3	
Test 3 (40%)	1L	61.2	1.27				
	1U	58.0	0.88				
	2L	58.2	1.34				
	2U	65.3	1.16				
	3L	67.8	1.32				
	3U	58.3	1.28				
	4L	66.6	1.59				
	4U	62.6	1.60				

Table F-2: Kendal PF sampling results - 1995

	Pipe No.	D_p (μm)	M (kg/s)		Pipe No.	D_p (μm)	M (kg/s)
Test 1	1	76.64	1.36	Test 4	1	57.22	1.11
	2	62.02	0.63		2	44.06	1.01
	3	57.69	0.91		3	54.17	1.04
	4	34.23	0.47		4	81.90	1.45
Test 2	1	60.86	1.07	Test 5	1	53.91	1.27
	2	72.25	1.06		2	112.64	1.12
	3	64.51	0.97		3	51.05	1.81
	4	49.08	0.58		4	39.83	0.79
Test 3	1	56.80	1.07	Test 6	1	69.63	1.23
	2	56.49	0.68		2	50.84	1.19
	3	74.23	1.42		3	70.97	1.48
	4	103.79	1.06		4	59.17	1.00

Table F-3: Hendrina PF sampling results - 1995

Appendix G Project motivation

There are various groups within the Eskom Technology group, the Eskom power stations and possibly outside companies which would find a permanent on-line method for the mass flow rate measurement of pneumatically conveyed solids very useful. The method, (iso-kinetic sampling) used on the stations at present is cumbersome, time consuming and inaccurate (Section 4, pp 38). Also it is not an on-line technique and thus problems with the PF flow such as a blocked pipe and poor distribution are not detected immediately. A further example is that Lethabo Power Station sometimes has oscillations in flow occurring in the pipes (Marantos 1992). In such a situation iso-kinetic sampling can lead to erroneous results for the following reason. If pipe 1 were to be sampled at the peak of an oscillation and pipe 2 at the trough of an oscillation then pipe 1 would appear to have a high mass flow rate and pipe 2 a low one. In reality the average mass flow rate in each pipe could be the same, and would be found to be so if the iso-kinetic sampling were carried out over the entire period of the oscillation. Such problems can remain undetected for long periods of time (dependant on the frequency of iso-kinetic sampling) leading to uneven and undesirable flame conditions in the boiler. Work began, at a number of institutions, on the measurement of pneumatically conveyed solids as long ago as 1960. Various methods, which are discussed in the body of the report, have been studied and some have proved successful under certain conditions. For example, the capacitive method can be used effectively for pipe diameters of less than 100 mm. However, no solution to the problem of mass flow rate measurement for the application to which this work pertains, i.e. the thermal power station environment, where pipe diameters are greater than 300 mm and factors such as particle size and velocity are not constant, has been identified.

The method selected for investigation is an electrostatic one and up to now, though the accuracy of the technique for actual mass flow rate measurement has not been quantified, the velocity of the solid can be accurately measured and a trend in the distribution of the solid in the different pipes can be seen. Following are the results of enquiries made into the need for an instrument which can measure, on-line such parameters as particle velocity, PF distribution and mass flow rate of pneumatically conveyed solids. The total cost saving to Eskom if these parameters can be measured is in the region of R 28.5 million per annum.

G.1 Energy technology: Izak Potgieter

Izak Potgieter (Potgieter 1994) is presently working on a project to reduce the

excess air to a boiler. This reduction, for one 665 Megawatt boiler running at 97% of full load would lead to the following emission decreases and financial savings

(I) 20% reduction in particulate emissions.
(ii) 15% reduction in NO_x
(iii) 40000 Tonnes/annum reduction in CO_2 emissions.
(iv) An overall decrease in wear and tear on the boiler because of the reduced gas volume flow
(v) 22000 Tonnes/annum reduction in coal consumption, which at R 23 per tonne, amounts to R 0.5 million.

A similar saving from a financial point of view for all the "six packs" operated by Eskom would result in a reduction of 924 000 Tonnes of coal per annum which would result in a saving of R 21 million per annum.

The reduction in excess air is only possible under certain conditions. One of the primary requirements is that the PF distribution be uniform throughout the boiler. This is because poor distribution has the following effects. In an area of high PF concentration some of the PF remains unburnt and in an area of low concentration surging can occur i.e. the flame is continually extinguished and relit. Thus it is of fundamental importance that the distribution be measured so that should there be imbalances corrective action can be taken.

G.2 Mechanical Technology: Felix von Bormann

The following is an extract from a letter from Felix van Bormann (van Bormann 1994) to Stassinos Marantos.

With respect to Eskom, the justification of the Collapsible Grating Probe (Marantos 1993a) will depend on three fields of application: (I) usefulness of the probe to T-R-I and its research and investigation programmes, (ii) applicability to power station continuous monitoring systems, (iii) need in the external market for such a flow transducer.

(I) In the opinion of the staff of Mech Tech, the CGP is useful to T-R-I for a number of reasons. The CGP offers the opportunity of obtaining both the velocity and the mass flow of the product in a conveying line. Mech Tech is developing a small materials handling expertise,

with Henk on belt conveyors, and other pneumatic lines in order to carry out accelerated erosion tests. A working probe of this capability (and low cost) would be a perfect jumping point into the market. It is recommended that Mech Tech become involved in the development of the CGP.

The Cold Accelerated Erosion Rig (CAER) has been developed by Mech Tech, for the investigation of erosion of air heater elements and related spin-off projects (coatings, screens and boiler tubes). This rig emulates the flue gas dust load, which is very light by pneumatic conveying standards. Even high speed dilute phase conveying has a product/air ratio of 10:1 while flue gas load is typically 1:8. At these low loads, lasers and SIC meters can be used for large diameter ducts but, on smaller ducts there is no means of monitoring the flow.

Use of the CGP, in the CAER, is welcomed as the probe gives immediate indication of whether there is ash flow or not. Preliminary check has shown induced voltage of up to 60 V for 50% ash flow. At present the best low cost method is to monitor the air temperature before the feeder and at the test section - the hot ash raises the temperature between these points or, when there is no ash the temperature remains constant. The high speed of the CAER makes other, non-intrusive forms of transducers problematic. They simply do not read fast enough. The turbulence of the flow in the CAER means that there is no problem with obstruction induced variation in flow. Investigation in the CAER will show the relationship between air and dust velocity, and the rig is the perfect tool to validate and complete the CGP.

(ii) For use within the stations, the applications are attractive: PF flow monitoring and control, flame control, flue gas flow monitoring and distribution (through primary and secondary air heaters and the precipitator ducts), and chimney ash mass flow. This kind of information will give a more systematic view of the plant, especially from the fluid flow perspective. Thus changes in one area will be immediately obvious what effect it has on another part of the plant. To be in the state qualified enough to be installed in the control room of a station, a development period of about 5 years should be expected. Slow development of such ground breaking technology can

only be compounded by a few number of qualified people working thereon. A recommended minimum of three systems engineers should be working on this.

(iii) Because of the potential effectiveness of the electrostatic probe, there is the possibility of external customers being interested in the probe. Companies such as Bulher, Bateman, Steinmuller and Bulk Handling would surely be interested for the same reasons as stated above - low cost, dilute conveying. They should be contacted for confirmation in this regard.

Thus referring to the opening paragraph, the CGP will satisfy a need and thus open a market that cannot be ignored, within T-R-I, Eskom and external companies (to be confirmed). Mech Tech believes that T-R-I-M and the research steering committee is justified in authorising work to continue on the CGP.

Cost association to the electrostatic probe:

In order to evaluate the value of the probe to Eskom, a certain cost must be given to the value of having a working probe and system installed in 1994. For the Mech Tech side the air heater CAER research costs have been R 600 000 for 1993 and 1994. For the particular application on this rig with its light ash load and high velocity, the conveyed product detection and ash monitoring methods available will cost around R 50 000 for a laser (before modification for the small duct diameter). Other systems cannot handle the rig specifications.

At Matimba Power Station, PF balancing is predicted to give an appreciable efficiency increase of 0.5%to the boiler. This relates to a saving of millions per year in fuel, power and maintenance costs. Iso-kinetic sampling is being used with its debatable accuracies and roping sensitive results . Just looking at the percentage envisaged by S Marantos, the triboelectric probe should have 10% accuracy which is 50% better than iso-kinetic sampling. For 1993 the maintenance cost of the station were: R 450 000 in materials and R 50 000 in labour for air heater outages. Boiler outages were R 1 300 000 for materials and R 880 000 in labour. Mills resulted in R 1 500 000 in materials and R 640 000 in labour. The average running cost per year is approximately R 840 million. This coupled to the maintenance cost relates to a saving of R 430 000 at Matimba due to the probe accuracy alone. Multiply that by the number of operational stations (reduced for size difference) and the figures close in on R 2 800 000 per year.

Hopefully once the balancing is done the PF lines will not need continuous monitoring, but if needed, a station like Matimba would install several of the probes for approximately R 90 000. There are also other applications such as flue gas monitoring, balancing correlation which would have an intrinsic value of about R 1 000 000 per year, especially for bag filter precipitators. Also, it should be a consideration that Matimba has cancelled a project to install a PF sampling infrastructure: cost R 373 000 in 1994. Considerably more than the cost of the triboelectric probe cost of about R 90 000. A good ROI is 1000%. The probe has the potential to achieve that if R 200 000 is allocated to it per year.

Sincerely

Felix von Bormann

G.3 Eskom Power Station: Performance monitoring

The present method of measuring mass flow rate of PF in the pipes is done using an iso-kinetic sampling technique. An on-line method of mass flow rate measurement would eliminate this need and PF sampling would have to be done only when a problem developed with the on-line system. Typical figures for the cost of the PF sampling process to a station are as follows:

C-upper @ R 95.00/Hr * 20 hrs = R 1900.00
C-lower @ R 85.00/Hr * 20 hrs = R 1700.00
B-lower @ R 54.00/Hr * 20 hrs = R 1080.00

This amounts to a total cost of R 4680.00 each time the procedure is carried out on a single unit. Since the unit should be sampled at two different loads and the process carried out every month the total cost amounts to R 673 920.00 per station per year. This amounts to a saving for all Eskom's "six pack" stations of approximately R 4.7 million per annum. The problem extends further however. When the sampling process is carried out the unit has to be placed on manual control and this can lead to the unit not producing the load required by National Control. A station can be financially penalised by National Control for not load following.

G.4 Materials Technology: Andre de Villiers

Andre de Villiers (de Villiers 1994) of materials technology is planning to carry out an investigation into the erosion and ware of pipe liners sometime during the next two years. For the purposes of their tests it is essential that the particle velocity is known accurately. Using the cross correlation technique with two Collapsible Grating Probes the velocity can be determined.